# Elucidating the mechanisms of kinetochore assembly using a novel assay

Jackie Lang

A dissertation

submitted in partial fulfillment of the

requirements for the degree of

Doctor of Philosophy

University of Washington

2018

Reading Committee:

Susan Biggins, Chair

Charles Asbury

Steven Hahn

Program Authorized to Offer Degree:

Molecular and Cellular Biology

University of Washington

# Abstract

Elucidating the mechanisms of kinetochore assembly using a novel assay

Jackie Lang

Chair of the Supervisory Committee
Dr. Susan Biggins
Department of Biochemistry

Cells rely upon the kinetochore in order to segregate their chromosomes during every cellular division. The kinetochore is a large, complex protein structure that must assemble onto the centromeric region of the chromosome and attach to the spindle microtubules. Therefore, it is imperative that cells accurately establish the centromere and build functional kinetochores in order to ensure proper segregation of the DNA. The centromeric nucleosome is marked by the conserved CENP-A histone. In order to restrict CENP-A$^{Cse4}$ incorporation to the centromere, the cellular levels of CENP-A$^{Cse4}$ in budding yeast are kept low by ubiquitination. I found that CENP-A$^{Cse4}$ is also post-translationally modified with SUMO, a small protein that is similar in many ways to ubiquitin. CENP-A$^{Cse4}$ is sumoylated by the Siz1 and Siz1 E3 SUMO ligases, and the sumoylation peaks during S phase of the cell cycle. I found that sumoylation does not effect CENP-A$^{Cse4}$ stability, but later work from another group suggested that sumoylation targets

CENP-A$^{Cse4}$ for ubiquitination and subsequent degradation. It will be important to resolve these discrepancies and understand how CENP-A$^{Cse4}$ is regulated by this novel post-translational modification. In order to create a biochemical tool that could help address unanswered questions such as this, I developed an assay to assemble kinetochores *in vitro* onto a centromeric template. The cell-free assay I developed has the same fundamental requirements as kinetochore assembly *in vivo*, including a dependency upon the CENP-A$^{Cse4}$ chaperone, suggesting that a centromeric nucleosome forms onto the DNA template. Importantly, this *de novo* assembly method is sensitive to phosphoregulatory events and generates complete kinetochores that are capable of binding to microtubules. I used this assay to address why kinetochores recruit the key microtubule-binding Ndc80 complex through two pathways: the Mis12 complex and CENP-T$^{Cnn1}$. Although budding yeast CENP-T$^{Cnn1}$ is nonessential, I found that it becomes required for Ndc80 complex recruitment and cell viability when the Mis12 complex pathway to assembly is inhibited by phosphoregulation. Thus, CENP-T$^{Cnn1}$ can independently recruit the Ndc80 complex and is required to maintain intact kinetochores throughout the cell cycle. The potential applications for the kinetochore assembly assay are numerous and extend to many fundamental questions about centromere and kinetochore biology.

# Table of Contents

# List of Figures

# List of Tables

# List of Supplemental Figures

# List of Supplemental Tables

# Acknowledgements

I have to start by thanking all the scientific mentors I have had over the years. My eighth grade biology teacher, Clyde Laird, sparked my passion for science and helped me realize that I wanted to pursue biology as a career. At UC Davis, Dr. Sean Burgess gave me the first opportunity to work in a laboratory on my own project. She mentored me through my first fellowship and presentation of my research, and provided me a rewarding introduction to scientific research. I then had the good fortune of working in Susan Strome's lab at UC Santa Cruz. She encouraged me to develop my own hypotheses from modENCODE data and to explore questions I was interested in. She was also an amazing resource as I was applying to and choosing a graduate school.

My thesis advisor, Sue Biggins, is a thoughtful and intentional mentor. She has allowed me to pursue my own interests and lead my own project, while guiding me in the right direction. She is an incredible role model in so many ways, from her passion and excellence in science, to her love for mentoring, to her support of her trainees' careers. I am also grateful to all the members of the Biggins lab, past and present, who were amazing colleagues and provided insightful discussions on my research throughout my time here. Thank you to my entire advisory committee: Chip Asbury, Toshi Tsukiyama, Steve Hahn, and Edith Wang. They have been instrumental in helping me navigating my project and provided useful outside perspectives on my work. I need to thank Matt Miller, a postdoc in the lab who has been my "second PI" and has encouraged me through the toughest times in my thesis. In addition to being a thoughtful and generous person, he can think through difficult scientific questions with amazing clarity and is always happy to get into long conversations about my project. I would also like to acknowledge Alex Chan, a smart and driven summer undergraduate student whom I was fortunate to mentor.

He contributed greatly my project, and to the lab, by helping develop a protocol for quantitative mass spectrometry. I also thank Donna Modrell, our efficient and highly organized administrator who has greatly simplified my life on countless occasions.

Since before even choosing the UW for graduate school, I had heard amazing stories about the Fred Hutch and I held it on a pedestal. It has lived up to my exceedingly high expectations, and I am thankful to have been a part of the Fred Hutch Basic Sciences Division, which provided a collaborative and high-caliber environment in which to receive my doctoral training. Thank you to Pat Heath and Luna Yu, who somehow solve all computer-related issues in minutes. The Ombudsman, Karen Peterson, is not only a kind and compassionate person, but she is exceptionally good at what she does and is an irreplaceable resource for any trainee at the Hutch who is considering a career outside of academia. During my time here, I got involved with Hutch United, a grassroots organization dedicated to promoting the success of underrepresented scientists at the Fred Hutch. Working with Hutch United has provided me with a sense of community, introduced me to incredible people throughout the Center, and allowed me to give back to the Fred Hutch in a meaningful way by putting on programs that I believe are important for improving the environment in academic science. My time with Hutch United was personally and professionally fulfilling and taught me valuable leadership and management skills.

The MCB Program has been a huge support system since day one. I need to thank the various MCB administrators Michele Karantsavelos, MaryEllin Robinson, Maia Low, Andrea Brocato, Marci Burden, Maria Sanders, Nomi Odano, and Diane Darling for streamlining everything from program requirements to health insurance. I am also grateful to the MCB Directors, Michael Emerman, Dave Raible, Katie Peichel, Rich Gardner, and Nina Salama, who helped guide me through important decisions. The MCB Program attracts a lot of excellent

scientists. I am thankful to have gone through graduate school with such supportive, smart colleagues, and I made some wonderful friends in the process. This experience would not have been the same without them.

Most of all, I need to thank my family, who are the real reason I'm here. My wonderful parents raised me to be curious about how the world works and to get outside and really experience it. This fostered my interest in biology, and they have been extremely supportive in so many ways throughout my education. I am so thankful to my sister, who shares my love for science. She has been a great cheerleader and is always interested in hearing about what I do. My partner, Erman, made my life so much easier when I was overwhelmed with school. He has helped me through the hardest and most stressful times, and helped me celebrate the little victories along the way. I couldn't have asked for a better person to help me navigate this journey.

# CHAPTER 1. Introduction

## 1.1 KINETOCHORES AND CENTROMERES

### 1.1.1 The mitotic functions of kinetochores

Chromosomes must be accurately segregated to daughter cells during cell division to avoid aneuploidy, a hallmark of birth defects and cancers [1]. Faithful segregation relies on the attachment of chromosomes to spindle microtubules via the kinetochore, a conserved protein complex that assembles at centromeres [2, 3]. Kinetochores must track dynamically growing and shrinking microtubule tips, monitor for erroneous kinetochore-microtubule attachments, and serve as the platform for the spindle assembly checkpoint [4, 5]. To carry out these many functions, the kinetochore is a highly regulated, megadalton protein structure composed of many subcomplexes (**Figure 1.1**). Although these subcomplexes must faithfully assemble onto the centromere every cell cycle, the underlying mechanisms that regulate kinetochore assembly are still not well understood.

Kinetochores are built on a specialized centromeric chromatin structure, in which canonical histone H3 is replaced with a centromere-specific variant, CENP-A [6, 7]. The constitutive centromere-associated network (CCAN) binds to this centromeric chromatin to form the inner kinetochore, which includes ~15 proteins altogether. In addition to harboring the primary recruitment site for the mitotic kinase, Aurora B, the inner kinetochore also serves as the scaffold for outer kinetochore assembly [8, 9]. Another ~20 proteins comprise the outer kinetochore, which mediates microtubule attachment [10]. Many additional proteins associate

with the outer kinetochore, including microtubule-associated proteins (MAPs), most components of the spindle assembly checkpoint (SAC), and the protein phosphatase PP1 [2, 3].

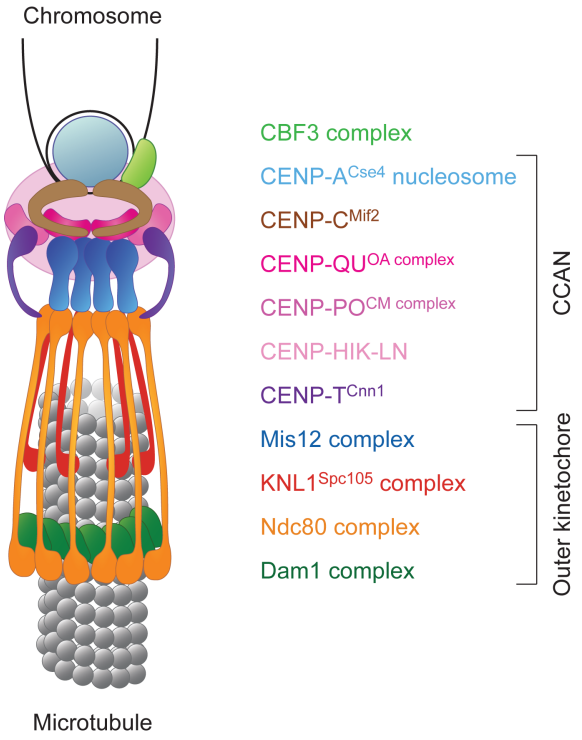


**Figure 1.1. The kinetochore is a conserved protein structure that links centromeres to spindle microtubules**
A schematic of the budding yeast kinetochore with the subcomplexes listed on the right.

These accessory proteins are important for regulating some of the kinetochore's crucial functions. The kinetochore must be able to sense whether or not sister chromatids achieve biorientation, a state in which the sister kinetochores are attached to microtubules from opposite spindle poles [11]. Aurora B and the SAC proteins monitor for unattached or improperly attached kinetochores, which will lack tension from opposing spindle forces. This lack of tension ultimately leads to activation of the checkpoint, preventing progression of the cell cycle until all kinetochores have established proper attachments [12]. PP1 antagonizes Aurora B

phosphorylation of outer kinetochore proteins and, in budding yeast, the SAC proteins in order to stabilize kinetochore-microtubule attachments and silence the checkpoint [13-17]. The kinetochore thus ensures proper chromosome segregation in part through serving as the scaffold for these many regulatory factors.

### 1.1.2 Centromere structure and function

Although the kinetochore is highly conserved, it assembles at one of the fastest evolving regions of the genome, the centromere [18, 19]. There is, however, a defining mark that characterizes functional centromeres in most organisms: the replacement of canonical histone H3 with a centromere-specific histone H3 variant, CENP-A [20]. Most eukaryotes have complex "regional" centromeres composed of repetitive DNA stretches with interspersed CENP-A- and H3-containing nucleosomes [21]. These centromeres recruit repeating subunits of the kinetochore and each chromatid makes 3 to 30 attachments to the microtubules [22] (**Figure 1.2**). Some plants and animals have holocentromeres, where CENP-A nucleosomes span nearly the entire length of the chromosome. In the model nematode *C. elegans*, these massive centromeres are comprised of hundreds of dispersed centromeric sites, wherein individual CENP-A nucleosomes are flanked by canonical nucleosomes [23]. In contrast, budding yeast have a simple "point" centromere defined by a specific DNA sequence, a single CENP-A nucleosome, and a single microtubule attachment site per chromatid [24]. While regional centromeres and holocentromeres are maintained epigenetically, point centromeres are specified by DNA sequence [25]. This great diversity of centromere organization is also reflected in differences in kinetochore composition. For example, the evolution of holocentricity in insects

coincides with a loss of CENP-A, indicating that they have found an alternative way to link centromeres to kinetochores [26].

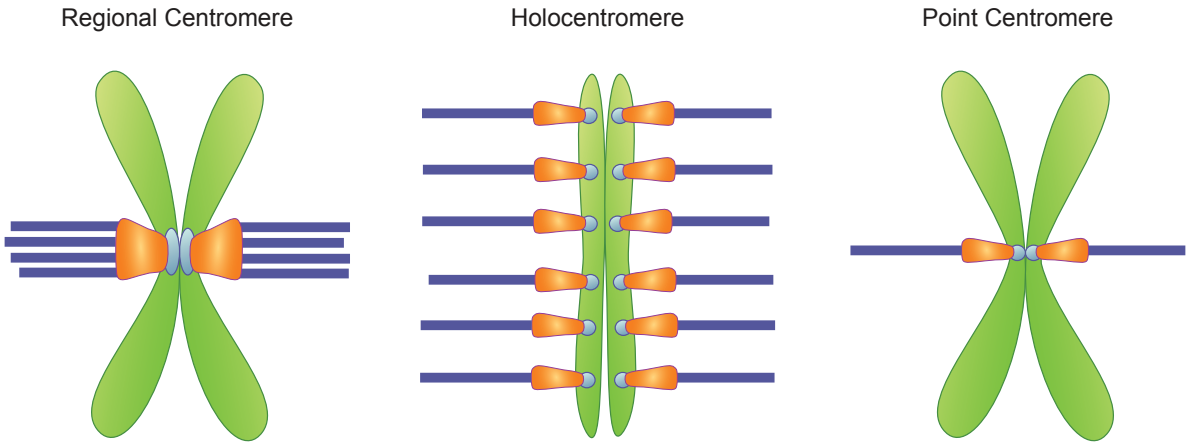


**Figure 1.2. Kinetochores assemble onto a broad array of centromere structures**
Regional centromeres span several megabases of DNA and holocentromeres span entire chromosomes. Each of these assembles numerous kinetochore units and attach to multiple microtubules per chromosome. The point centromeres of budding yeast contain only a single CENP-A nucleosome onto which single kinetochore unit assembles and attaches to one microtubule. Chromosomes are in green, centromeres are in blue, kinetochores are in orange, and microtubules are in dark blue.

The centromeres of most eukaryotes are embedded in heterochromatin, a 'closed' chromatin structure. This type of chromatin is characterized by repressive histone H3 K9 di- or trimethylation, the presence of heterochromatin protein 1 (HP1), and reduced transcription [27]. The dispersed sites of kinetochore nucleation within holocentromeres do not appear to be surrounded by heterochromatin [27]. Instead the individual CENP-A nucleosomes are much like the point centromeres of yeast, which lack the heterochromatic pericentromere found in higher eukaryotes [27].

The pericentromere has been implicated in centromere and kinetochore function in several ways. Heterochromatic pericentromeres have been postulated to serve as a barrier to prevent the spreading of centromeres into active regions of the genome [28]. The well-positioned

H3-containing nucleosomes that flank CENP-A nucleosomes at point centromeres and holocentromeres may be sufficient to fulfill this purpose, hence the lack of heterochromatin at these pericentromeres [29]. The pericentromere is also the site of cohesion enrichment, which promotes sister kinetochore biorientation by resisting pulling forces from the spindle microtubules [30, 31]. In budding yeast, cohesin is recruited to the pericentromere by kinetochore components, and a reduction in pericentromeric cohesin results in increased chromosome loss [30-34]. Another way that pericentromeres contribute to chromosome segregation is through the recruitment of regulators of kinetochore biorientation. Phosphorylation of pericentromeric histone H2A by the mitotic kinase Bub1 recruits Sgo1 [35-37], a conserved protein that regulates kinetochore biorientation and functions as a tension sensor [38-40]. Finally, the pericentromeric region may harbor additional CENP-A molecules, although their function is unclear [41-43]. Whether the pericentromere contributes to the assembly of kinetochores at point centromeres remains unknown.

### 1.1.3 The control of CENP-A localization

Because CENP-A nucleates kinetochore assembly, it is critical that CENP-A nucleosomes are deposited at centromeres and not to ectopic loci. A key region of CENP-A that dictates its centromeric localization and distinguishes it from canonical histone H3 is the CENP-A targeting domain (CATD), which resides within the histone fold domain of CENP-A [44]. In budding yeast, the CATD is recognized by the histone chaperone HJURP$^{Scm3}$, which deposits CENP-A, along with histone H4, to centromeres by recognizing part of the centromeric DNA and other centromere-bound proteins [45-49].

CENP-A localization to chromatin is also controlled through ubiquitin-mediated proteolysis, which prevents CENP-A from incorporating into the chromosome arms [50]. Ubiquitin is a small protein that, when covalently linked to lysine residues, can affect the function or stability of the target protein [51]. Generally, polyubiquitination targets the protein for proteasomal degradation, while monoubiquitination or multiubiquitination can alter the protein's localization or function [51]. Ubiquitination is facilitated by E1, E2, and E3 ligases, which essentially function to activate ubiquitin in an ATP-dependent manner and transfer it to the substrate. Budding yeast have only one E1 enzyme, Uba1, but there are 60-100 E3 enzymes, which confer target specificity [51]. Psh1 was the first E3 ubiquitin ligase reported to target CENP-A$^{Cse4}$ for degradation by the proteasome [52, 53]. It recognizes the CATD of CENP-A$^{Cse4}$ and is important for preventing the ectopic localization of CENP-A$^{Cse4}$ to chromosome arms [52-55]. Other E3 ubiquitin ligases have since been shown to regulate CENP-A$^{Cse4}$ stability: Ubr1, Rcy1, and Slx5 [56-59]. Each of these ligases appear to function independently, and it is unclear whether they target different pools of CENP-A$^{Cse4}$ [59].

### 1.1.4 CENP-A nucleosome structure

In many organisms, CENP-A-containing nucleosomes are the defining mark of centromeres and kinetochore nucleation. However, the structure of this specialized centromeric nucleosome remains controversial [60]. The two most prevalent models are that CENP-A is part of an octameric nucleosome, similar to canonical H3-containing nucleosomes, or that the CENP-A nucleosome is a unique hemisome structure. Both octameric and hemisomal CENP-A$^{Cse4}$ nucleosomes can be reconstituted *in vitro*, but the stiff, AT-rich region of the centromere, where CENP-A$^{Cse4}$ is deposited *in vivo*, can only stably form hemisomes *in vitro* [61]. According to the

hemisome model, a single copy of each H2A, H2B, H4, and CENP-A wrapped by DNA comprise the centromeric nucleosome [60, 62-64]. The CENP-A nucleosome protects a smaller region of DNA from micrococcal nuclease (MNase) digestion than canonical H3-containing octamers, suggesting that this nucleosome may contain fewer histones [65, 66]. In support of this, canonical H3 nucleosomes occupy ~147 bp of DNA, while the region of centromeric DNA available for CENP-$A^{Cse4}$ binding at point centromeres is only 80 bp in length due to DNA-binding proteins creating barriers on either side [66]. However, ectopically incorporated CENP-$A^{Cse4}$ protects a larger ~135 bp of DNA, suggesting that a specialized nucleosome structure at the centromere may be dictated by the available DNA and centromere-specific binding partners that help distinguish the centromere [66]. Furthermore, centromeric nucleosomes have been reported to induce positive supercoils on DNA *in vivo*, in contrast to the negatively supercoiled DNA around H3 octamers [67]. Interestingly, both the positive supercoiling and the short, 80 bp region of occupied DNA are consistent with the properties of canonical tetrameric nucleosomes in archea [68, 69].

The ability of CENP-$A^{Cse4}$ to form an octamer both *in vitro* and *in vivo*, has helped support the CENP-$A^{Cse4}$ octamer model. An octameric nucleosome contains two copies each of histones H2A, H2B, H4, and either H3 or CENP-A wrapped by DNA [6, 70]. This model would predict the localization of two CENP-$A^{Cse4}$ molecules to the point centromere. Fluorescence imaging *in vivo* determined that there is enough CENP-$A^{Cse4}$ signal at kinetochore clusters for each centromere to be occupied by two CENP-$A^{Cse4}$ molecules [43]. However, it is not clear whether all of the CENP-$A^{Cse4}$ is incorporated into the nucleosome or whether some of it is associating with the pericentromere, as discussed above.

## 1.2 THE STRUCTURE AND ASSEMBLY OF KINETOCHORES

### 1.2.1 An introduction to the kinetochore subcomplexes

The kinetochore is composed of conserved subcomplexes that assemble at centromeres (**Figure 1.1**). Here, I introduce the core components in budding yeast, many of which are conserved in humans.

***Centromere (Cbf1, CENP-A$^{Cse4}$, CBF3):*** The simple point centromere of budding yeast is an approximately 125 bp region of DNA containing three centromere determining elements (CDEI, II, and III) [71]. While CDEI is bound by the nonessential Cbf1 protein and is therefore dispensable [72-74], CDEII and III are both required for kinetochore specification. CDEIII binds the yeast-specific CBF3 complex, which recruits the CENP-A$^{Cse4}$ nucleosome by interacting with its histone chaperone, HJURP$^{Scm3}$ [75-77]. The centromere-specific CENP-A histone (Cse4 in *S. cerevisiae*) is part of a well-positioned nucleosome that prefers the AT-rich (~90% AT rich) CDEII [65].

***Inner Kinetochore (CENP-C$^{Mif2}$, -PORQU$^{COMA}$, -HIK, -LN):*** Within the inner kinetochore, CENP-C$^{Mif2}$ is crucial for recruitment of the rest of the constitutive centromere-associated network (CCAN), and is the major linker to the outer kinetochore [78]. It binds to the CENP-A$^{Cse4}$ nucleosome and at least part of the CDEIII DNA, as well as to the COMA subcomplex and the outer kinetochore Mis12 complex [79, 80]. Aside from CENP-C$^{Mif2}$, the only other essential components of the CCAN are the 'OA' members of the COMA complex, which is necessary for maintaining the mitotic checkpoint response [81]. CENP-U$^{Ame1}$ of the OA complex appears to be another linker protein, as it binds directly to the outer Mis12 complex, but

also recruits the inner CENP-LN$^{Chl4\text{-}Iml3}$ complex [82-84]. The precise role of CENP-LN is unclear, but in humans it may help specify the centromere by recognizing CENP-A [85]. The CENP-HIK complex appears to have a conserved role recruiting CENP-T [86-89]. CENP-T$^{Cnn1}$ is a histone fold domain containing protein that can link directly to the outer kinetochore Ndc80 complex [90-93].

***Outer Kinetochore (Mis12, Ndc80, KNL1$^{Spc105}$, Dam1):*** The outer kinetochore is composed primarily of the conserved KMN (KNL1, Mis12, Ndc80) network, which is the core microtubule attachment site of the kinetochore [94]. The Mis12 complex serves as the 'linker' layer that connects the DNA-binding and microtubule-binding subcomplexes. It localizes to kinetochores through both CENP-C$^{Mif2}$ and CENP-U$^{Ame1}$ and also contains binding sites for both the Ndc80 and KNL1$^{Spc105}$ complexes [82, 83, 95, 96]. The Ndc80 and KNL1$^{Spc105}$ complexes each make direct contact with the microtubules [94]. The yeast-specific Dam1 complex displays Ndc80- and microtubule-dependent localization to kinetochores [97]. Dam1 forms a ring around microtubules [98] and is necessary to strengthen kinetochore-microtubule attachments [99].

### 1.2.2 Hierarchical assembly of the kinetochore

Many biochemical studies over the last two decades have identified and characterized the discrete subcomplexes that comprise the kinetochore [2, 100]. By combining these data with the effects of deleting or depleting of proteins *in vivo*, a rough map of protein-protein interactions throughout the kinetochore can be generated [81, 100]. Based on these data, it is thought that the kinetochore builds outward from the centromere and inner kinetochore to the microtubule-binding interface [4]. It is also generally accepted that kinetochore assembly occurs in a

hierarchical manner by the stepwise recruitment of preformed subcomplexes [3, 81]. In support of this, most subcomplexes require the presence of every member in order to form a stable complex *in vitro* and to localize to kinetochores *in vivo*. Furthermore, kinetochore composition is highly regulated based on the cell cycle stage and the state of microtubule attachment. For example, metazoan CCAN and KMN load at different times [101], and attachment to microtubules recruits the Dam1 complex [97]. All of these data point toward stepwise assembly of the kinetochore as a more biologically attractive model than the mere binding of a preassembled or static kinetochore. However, yeast kinetochores cluster, making impossible to visualize individual kinetochores *in vivo* [102]. This has prevented the field from examining the exact order of recruitment to the kinetochore and the precise stoichiometry of the components. For instance, we still do not know whether larger assemblies, such as the KMN network, are preformed before reaching the kinetochore, or whether each subcomplex binds individually through carefully regulated steps. There is also little known about the order of recruitment within the CCAN.

The cell cycle timing of kinetochore assembly differs greatly between yeast and higher eukaryotes. Budding yeast kinetochores assemble almost completely during S phase, within approximately five minutes after the replication fork passes through the centromere [103, 104]. Aside from this short window, yeast kinetochores are fully assembled and bound to microtubules. The CCAN (constitutive centromere-associated network) in metazoans also localizes to the centromere throughout the cell cycle, but the KMN does not localize to kinetochores until mitosis [101]. This difference is caused, in part, by the different mechanisms by which the cells complete mitosis. Yeast undergo a closed mitosis in which the nuclear envelope remains intact throughout the cell cycle [105]. This is in contrast to open mitosis in

metazoans, where the nuclear envelope breaks down at the entry into mitosis. The outer kinetochore Ndc80 complex localizes to the cytoplasm for the majority of the cell cycle, and is thus compartmentally separated from the centromere and inner kinetochore [106]. Its assembly at the kinetochore requires both nuclear envelope breakdown and CDK activity [106]. A better understanding of how the cell regulates kinetochore assembly and composition is necessary for us to dissect the critical functions of the kinetochore.

### 1.2.3 The regulation of centromere and kinetochore assembly by post-translational modifications

The N-terminal tails of CENP-A and the other histones are post-translationally modified as a major form of epigenetic regulation. For example, histone H3 can undergo at least 17 different post-translational modifications (PTMs) and these function to regulate chromatin condensation, gene expression, DNA replication, and cell differentiation [107]. A majority of these modifications are acetylation, methylation, or ubiquitination of lysine or arginine residues. Compared to H3, CENP-A has a decreased lysine content, and its arginine residues do not appear to be modified [108]. CENP-A is therefore post-translationally modified to a far lesser extent than H3. Interestingly, the histone-fold domain of CENP-A is fairly well-conserved across species, while the N-terminus is the most variable region, sharing only 7% identity between human and *S. cerevisiae* [108]. This may be a result of different regulatory needs of epigenetically inherited regional centromeres and sequence-specific point centromeres. Still, yeast CENP-$A^{Cse4}$ undergoes at least five types of modifications: acetylation, methylation, phosphorylation, ubiquitination, and sumoylation [108]. These PTMs regulate the stability, localization, and CCAN recruitment of CENP-$A^{Cse4}$ [108]. CENP-$A^{Cse4}$ is phosphorylated by

Aurora $B^{Ipl1}$ at four sites, and this may function to destabilize kinetochores with defective microtubule attachments [109]. Conversely, methylation of lysine 49 appears to be required for recruiting kinetochore components to the centromere [110]. CENP-$A^{Cse4}$ is also acetylated at arginine 37, although the function of this modification has yet to be identified [109]. As discussed above, deposition of the CENP-$A^{Cse4}$ nucleosome is regulated in part through ubiquitination [52, 54, 55]. Sumoylation of CENP-$A^{Cse4}$ may be involved in this process as well [58, 111], which will be discussed in detail in Chapter 2.

Sumoylation of the centromere and kinetochore proteins appears to have a conserved role in regulating mitotic chromosome segregation [112]. Like ubiquitin, SUMO (small ubiquitin-like modifier) is a small protein that can be conjugated to lysine residues using a series of E1, E2, and E3 SUMO ligases [113, 114]. It can impose diverse effects on its substrates, such as increasing stability, altering binding partners, and marking for ubiquitination and subsequent degradation by the proteasome [113-116]. SUMO was initially discovered in *S. cerevisiae*, when overexpression of SUMO suppressed a temperature sensitive mutant of the inner kinetochore protein, CENP-$C^{Mif2}$ [117]. SUMO has also been identified in a screen for mutants with defects in chromosome segregation [118], and a deletion of the yeast $SUMO^{Smt3}$ leads to an early mitotic arrest [119]. By fluorescence microscopy, SUMO localizes to mitotic centromeres and kinetochores in various organisms, including *Drosophila*, *Xenopus*, and humans [120-122]. Although the cellular localization of sumoylation has not been detected by immunofluorescence in yeast, many SUMO substrates have been identified throughout the kinetochore by mass spectrometry, including Cbf1, Ndc10, CENP-$A^{Cse4}$, $Survivin^{Bir1}$, $INCENP^{Sli15}$, CENP-$O^{Mcm21}$, and Ndc80 [58, 123-125]. The function of sumoylation on most of these proteins is unknown. Preventing sumoylation of the centromere-binding Ndc10 protein causes abnormal anaphase spindles and chromosome

misseggregation [125], but how Ndc10 sumoylation is functioning on a molecular level has not been discovered. It will be important for future studies to focus on the cell cycle regulation of sumoylation and how it affects the assembly and function of kinetochores.

There is also evidence that some phosphorylation events from mitotic kinases can regulate kinetochore assembly. Most phosphorylation sites on kinetochores function to regulate microtubule attachments and the mitotic checkpoint, but several sites have been shown to regulate kinetochore assembly [2, 3]. For example, the binding of the Mis12 complex to CENP-$C^{Mif2}$ is regulated by the conserved phosphorylation of two residues on Dsn1 of the Mis12 complex [82, 83]. Localization of the inner kinetochore CENP-$T^{Cnn1}$ at kinetochores is also phosphoregulated, in this case by the CDK, Mps1, and Aurora B kinases [90, 92, 126, 127]. A better understanding of how these many post-translational modifications work together to regulate the kinetochore will contribute to studies *in vivo* and *in vitro*.

### 1.2.4 Dual pathways to Ndc80 complex recruitment

The Ndc80 complex is a key microtubule-binding component of the kinetochore. It is recruited to centromeres through two receptors: the Mis12 complex and CENP-T [90-92, 96, 127, 128]. The Mis12 complex (Mis12c) pathway is initiated by CENP-$C^{Mif2}$ and CENP-$U^{Ame1}$ of the inner kinetochore and also recruits KNL1c of the outer kinetochore, thus forming the KMN network (KNL1-Mis12-Ndc80) [82, 83], and also recruits CENP-$LN^{Chl4\text{-}Iml3}$ [84, 94]. CENP-T is a histone fold domain (HFD) containing protein with a long, unstructured N-terminus that reaches to the outer kinetochore to bind Ndc80c. CENP-T and the yeast homolog, Cnn1, compete with Mis12c to bind to the same interaction surface of the Ndc80 complex [90-93]. In humans, both CENP-C (which recruits Mis12c) and CENP-T are essential, and in fact, each one

alone is sufficient for outer kinetochore recruitment and microtubule binding when tethered to an ectopic locus [127]. Similarly, the tethering of budding yeast CENP-T$^{Cnn1}$ imparts partial stability on acentric minichromosomes via Ndc80 recruitment [92], indicating that its role as an alternative kinetochore platform is conserved. Although CENP-T$^{Cnn1}$ is nonessential in yeast, CENP-T$^{Cnn1}$ mutants display increased chromosome loss [92, 126]. Why the cells of many organisms use two receptors for the Ndc80 complex has remained unclear.

The mechanism of CENP-T recruitment to the kinetochore is also poorly understood. Initially, CENP-T was thought to be a novel nucleosome at centromeres, since the human protein can interact with other HFD containing proteins to form a heterotetramer with structural similarity to canonical nucleosomes [91, 128]. Together, they have the capability to bind and partially wrap DNA *in vitro* [91, 128]. In addition, both the heterotetramerization and DNA binding capabilities are necessary for assembling a functional kinetochore *in vivo* [128]. However, it was later found that CENP-T requires other CCAN members for it kinetochore localization [86-89, 129-131]. Furthermore, the budding yeast CENP-TW$^{Cnn1\text{-}Wip1}$ do not associate with CENP-S/X$^{Mhf1\text{-}Mhf2}$, and the DNA binding sites of CENP-T$^{Cnn1}$ overlap with those of CENP-A$^{Cse4}$ [88]. These data have called into question whether CENP-T forms a unique nucleosome structure at the centromere *in vivo*, and whether that structure is required for kinetochore function.

In budding yeast, CENP-T$^{Cnn1}$ enriches at kinetochores at the onset of anaphase as a result of phosphoregulation [91, 126]. In order to then bind the Ndc80 complex, CENP-T$^{Cnn1}$ must be dephosphorylated at a residue (serine 74) located in a key position within the binding interface [92]. It is unclear why CENP-T$^{Cnn1}$ recruitment is temporally regulated and whether this affects the Mis12 pathway of Ndc80 recruitment. However, Mis12c remains at kinetochores

when CENP-T$^{Cnn1}$ binds, so it has been postulated that there is an "anaphase switch" in receptor for the Ndc80 complex from Mis12c to CENP-T$^{Cnn1}$ [91]. It has also been speculated that using CENP-T$^{Cnn1}$ as a receptor provides a flexible kinetochore-microtubule attachment that is better suited for transducing force and moving chromosomes.

Interestingly, although Mis12c and CENP-T were initially thought to be distinct, mutually exclusive pathways for connecting the centromere to the outer kinetochore, a link between the two has recently been found in humans. CENP-T recruits its own Ndc80c, but also binds to Mis12c, bringing in an additional Ndc80c as part of the KMN network [132, 133]. It is not yet clear whether the responsible Mis12c binding site is conserved on yeast CENP-T$^{Cnn1}$. It will be interesting to know whether CENP-T$^{Cnn1}$ shares this linkage to the KMN network or whether it is an independent Ndc80c recruitment pathway. These may have important implications for why the yeast CENP-T$^{Cnn1}$ is nonessential. Many questions remain as to why a second pathway for linking centromeres to kinetochores exists, what the precise role of CENP-T is, and how its kinetochore association is regulated.

## 1.3 ASSAYS TO STUDY THE KINETOCHORE *IN VITRO*

### 1.3.1 Biochemical, structural, and functional assays

Numerous techniques *in vitro* have contributed to our understanding of how kinetochores assemble onto centromeres and attach to microtubules [2, 3]. For example, recombinant fragments of the CENP-C$^{Mif2}$ protein were used to reveal that CENP-C$^{Mif2}$ binds to the CDEIII region of budding yeast point centromeres [79]. Structural studies have also illuminated the mechanistic details of some steps of kinetochore assembly. The crystal structure of the Mis12 complex explained how its recruitment to the kinetochore is regulated by Aurora B

phosphorylation [82, 83]. Our lab previously developed a method to purify intact kinetochores from yeast, which have allowed us to analyze kinetochores by electron microscopy (EM) to visualize the outer kinetochore bound to microtubules [134, 135]. By using kinetochores purified from mutant extracts, this study helped identify how the globular microtubule-binding domains of the Ndc80 complex and the ring structure of the Dam1 complex work together to establish kinetochore-microtubule attachments.

Purified kinetochores have also contributed to functional studies *in vitro*. By manipulating kinetochore-bound beads using an optical trap, we can bind kinetochores to microtubules on a glass slide and assay the strength of this attachment under different conditions [135]. These studies have contributed considerably to our understanding of how tension affects kinetochores. We learned that kinetochores exhibit a catch bond-like behavior, where increasing tension, to a point, functions to stabilize kinetochore-microtubule attachments independently of regulation by mitotic kinases [135, 136]. However, these biophysical assays have thus far only tested the effect of putting tension across the outer kinetochore. In future studies, it will be important to characterize how tension across the inner kinetochore, and even across the centromeric nucleosome, impact the biophysical behavior of kinetochores and the catch bond-like attachment. Although numerous additional studies have contributed to our understanding of the kinetochore, we still do not know the structures of most of the subcomplexes, nor do we understand how they all interact to form a functional kinetochore.

### 1.3.2 Kinetochore assembly techniques

It has been difficult to fully elucidate the regulation and requirements for kinetochore assembly due to the difficulty in manipulating and directly assaying this process *in vivo*. Despite

*in vitro* success in other fields, assembling functional replication and transcription machinery [137, 138], no studies thus far have achieved complete assembly of the kinetochore *de novo*. Attempts to assemble the budding yeast kinetochore *in vitro* began over 20 years ago, prior to the discovery of many kinetochore components [139]. Naked centromeric DNA incubated in yeast whole cell extract assembled components that conferred microtubule-binding capability, but none of the outer kinetochore components were known at the time. It was later discovered that the microtubule-binding factors that assembled were not outer kinetochore, but the Chromosomal Passenger Complex, which assembles proximal to the DNA and can also bind microtubules [8]. Many years later, a study investigating the role of transcription in kinetochore assembly used a DNA template of eight tandem repeats of the yeast centromere [138]. After incubation in extract, assembly of the inner kinetochore was achieved, but no outer components bound to the DNA.

In other organisms, progress has been made with partial reconstitution systems *in vitro*. Pre-formed arrays of CENP-A nucleosomes incubated in *Xenopus* egg extracts can assemble particles capable of polymerizing microtubules and eliciting a mitotic checkpoint response when the microtubules are depolymerized [140]. This assay enabled the study of the role of CENP-A domains in centromere and kinetochore assembly, using CENP-A mutants that would be lethal *in vivo*. Recently, the entire linkage between the CENP-A nucleosome and KMN was reconstituted using recombinant proteins [141]. The researchers were able to define proteins that bound specifically to CENP-A nucleosomes and characterize several binding interactions throughout the kinetochore. While both of these methods have contributed greatly to the field, there are some limitations. Both of these kinetochores are assembled onto pre-formed CENP-A-containing octameric nucleosomes, but the structure of the CENP-A nucleosome *in vivo* is still controversial and may have very different properties from those used in these experiments [60]. Also, the

recombinant proteins used in the latter method lack post-translational modifications from the cell that may regulate kinetochore assembly. Furthermore, the CENP-T pathway for Ndc80 assembly is not present in the latter method and may not be present in the former method. Taking all these factors into consideration, it is not clear whether these techniques mimic the assembly process *in vivo*.

## 1.4 RESEARCH QUESTIONS

### 1.4.1 What is the function of CENP-A$^{Cse4}$ sumoylation?

The importance of CENP-A$^{Cse4}$ ubiquitination in regulating CENP-A$^{Cse4}$ levels and chromatin localization has become increasing clear in recent studies [52-55]. In Chapter 2, I demonstrate that CENP-A$^{Cse4}$ is also post-translationally modified with SUMO, a novel modification of the centromeric histone. The prospects of CENP-A$^{Cse4}$ regulation by sumoylation are intriguing, since SUMO can have a wide variety of effects on its substrates, including regulating the substrates stability or binding partners. I find that the Siz1 and Siz2 E3 SUMO ligases are responsible for CENP-A$^{Cse4}$ sumoylation. Furthermore, this modification is cell cycle regulated, peaking during S phase. This coincides with the timing of CENP-A$^{Cse4}$ deposition, yet I found no evidence to suggest that sumoylation alters the ectopic or centromeric localization of CENP-A$^{Cse4}$. It also does not appear to regulate the recruitment of kinetochore proteins to the centromeric nucleosome. I compare my work to recent findings from another group and suggest future work to determine the effect of sumoylation on CENP-A$^{Cse4}$ function.

### 1.4.2 What are the requirements for kinetochore assembly *in vitro*?

The difficulty of manipulating or visualizing assembly of the kinetochore *in vivo* has left the field with many unanswered questions. While kinetochores can assemble on pre-formed nucleosomal arrays in Xenopus egg extracts [140], kinetochores have never been assembled *de novo* on a DNA template. I therefore exploited the sequence-specific budding yeast centromere to develop a DNA-based method to assemble kinetochores *in vitro*. In Chapter 3, I discuss the development of this assay, highlighting the major findings that have the potential to influence other biochemical work. Ultimately, kinetochore assembly *in vitro* by the method I developed has the same fundamental requirements as *in vivo*. The assembly relies upon the CENP-A chaperone, suggesting the formation of a centromeric nucleosome. I also demonstrate that the assembly is a stepwise and cell cycle regulated process. Importantly, the assembled kinetochores span from the DNA to the microtubule-binding interface and are functional for binding microtubules. I can interrupt assembly using various kinetochore mutants or improve it through phosphoregulation, indicating that this is a tunable assembly process that can be used to search for additional regulatory events.

### 1.4.3 Why do cells use two pathways to recruit Ndc80?

I then used the assembly assay developed in Chapter 3 to investigate why kinetochores recruit the microtubule-binding Ndc80 complex via two receptors: the Mis12 complex and CENP-$T^{Cnn1}$. Because this is a DNA-based method, I first address the long-standing question of how CENP-$T^{Cnn1}$ is recruited to kinetochores. I demonstrate that CENP-$T^{Cnn1}$ has no detectable independent DNA-binding capability, but rather it requires all other inner kinetochore subcomplexes for its localization. I also find that the CENP-$T^{Cnn1}$ pathway becomes essential for

Ndc80 recruitment and cell viability when the interaction between Mis12c and CENP-$C^{Mif2}$ is weakened due to a lack of Aurora B phosphorylation. I therefore propose that CENP-$T^{Cnn1}$ recruits Ndc80 independently of the Mis12c pathway and is required to keep kinetochores intact as they undergo phosphoregulation.

# CHAPTER 2. An examination of the function of CENP-A$^{Cse4}$ modification with SUMO

## 2.1 SUMMARY

Kinetochore formation requires centromere recognition, which is accomplished in part through the replacement of canonical histone H3 with a centromere-specific histone H3 variant, CENP-A. To restrict incorporation of the CENP-A$^{Cse4}$ nucleosome to the centromere, the cellular levels of CENP-A$^{Cse4}$ are regulated through ubiquitin-mediated proteolysis. In addition to ubiquitination, I demonstrate that CENP-A$^{Cse4}$ is also sumoylated and identify the responsible E3 SUMO ligases as Siz1 and Siz2. I found that CENP-A$^{Cse4}$ sumoylation peaks during S phase, suggesting that it may be involved in CENP-A$^{Cse4}$ deposition or assembly of the kinetochore onto the CENP-A$^{Cse4}$ nucleosome. However, sumoylation does not alter CENP-A$^{Cse4}$ stability, localization to ectopic chromatin, or interactions with other kinetochore proteins. Another group has since proposed that the sumoylation is recognized by a SUMO-dependent ubiquitin ligase, Slx5. I discuss their findings in relation to our data and propose the most parsimonious model for CENP-A$^{Cse4}$ sumoylation.

## 2.2 INTRODUCTION

Proper establishment of centromeric chromatin is required for kinetochore assembly and the faithful segregation of chromosomes during cellular division. The conserved histone H3 variant, CENP-A, occupies functional centromeres in most eukaryotes and is therefore required for viability [20]. To restrict incorporation of the CENP-A$^{Cse4}$ nucleosome to the centromere,

CENP-A$^{Cse4}$ levels in yeast are kept low through ubiquitin-mediated proteolysis. Although several E3 ubiquitin ligases contribute to CENP-A$^{Cse4}$ ubiquitination, the Psh1 ligase is important for regulating CENP-A$^{Cse4}$ localization to chromatin [52-55]. In the absence of Psh1-mediated ubiquitination, CENP-A$^{Cse4}$ is stabilized and its cellular levels increase [52-55]. Psh1 directly binds the conserved chromatin-modifying FACT (facilitates chromatin transcription/transactions) complex that destabilizes ectopic CENP-A$^{Cse4}$ nucleosomes to facilitate the association of Psh1 with ectopically localized CENP-A$^{Cse4}$ [55]. The overexpression of CENP-A$^{Cse4}$ in *psh1Δ* cells results in ectopic spreading of CENP-A$^{Cse4}$ into euchromatin and is lethal to cells [52-55]. The reasons for lethality have not yet been fully elucidated, but the ectopic incorporation of CENP-A$^{Cse4}$ results in transcriptional misregulation that may contribute to the lethality [54].

The search for other post-translational modifications that regulate CENP-A$^{Cse4}$ stability or function has lead to the discovery of various modifications, including phosphorylation, methylation, and acetylation [108]. I demonstrate here that CENP-A$^{Cse4}$ is also post-translationally modified with SUMO, a small ubiquitin-like modifier. Like ubiquitin, SUMO is covalently linked to lysine residues and has a broad range of functional consequences, such as altering the interaction of its substrates with DNA or other proteins, or altering the proteins stability by either protecting it from ubiquitination or by recruiting a SUMO-targeted ubiquitin ligase [113-116]. Therefore, there are many potential functions of CENP-A$^{Cse4}$ sumoylation, some of which may co-exist. First, sumoylation may tag CENP-A$^{Cse4}$ for ubiquitin-mediated proteolysis, to degrade excess CENP-A$^{Cse4}$. Second, sumoylation may function to stabilize CENP-A$^{Cse4}$ by protecting it from ubiquitination and subsequent proteolysis, perhaps with

specificity toward the centromere-bound pool. Third, sumoylation may alter the binding affinity of CENP-A$^{Cse4}$ toward the DNA or inner kinetochore components.

To investigate these possibilities, I first identified Siz1 and Siz2 as the E3 SUMO ligases responsible for CENP-A$^{Cse4}$ sumoylation. Unlike ubiquitination, CENP-A$^{Cse4}$ sumoylation does not appreciably affect CENP-A$^{Cse4}$ stability. In agreement with this, the loss of Siz1/2-mediated sumoylation is not toxic to cells when CENP-A$^{Cse4}$ is overexpressed. I found that CENP-A$^{Cse4}$ sumoylation increases during S phase when CENP-A$^{Cse4}$ nucleosomes are deposited and kinetochores assemble, suggesting that sumoylation may have a role in these processes. For the sake of concisely outlining the differences between our findings and those that have since been published by another group [58, 111], I will save the comparison of the two studies for the discussion.

## 2.3 RESULTS

### 2.3.1 CENP-A$^{Cse4}$ is sumoylated *in vivo* by the Siz1 and Siz2 SUMO ligases

The cellular levels of CENP-A$^{Cse4}$ are regulated by numerous E3 ubiquitin ligases [56-59]. CENP-A$^{Cse4}$ that has been overexpressed and purified exhibits a ladder of slower-migrating conjugates when analyzed by SDS-PAGE and immunoblotting (**Figure 2.1A, left**). Previous work has identified these bands as ubiquitinated forms CENP-A$^{Cse4}$ [52, 53]. Upon deletion of *PSH1*, a CENP-A$^{Cse4}$-specific E3 ubiquitin ligase, the ubiquitinated forms are replaced by a new ladder of CENP-A$^{Cse4}$ conjugates. SUMO (small ubiquitin-like modifier) is a good candidate protein for this new ladder because, like ubiquitin, SUMO can form chains, and therefore a ladder of upper conjugates. Furthermore, the SUMO protein has a mass of 11 kDa, which is approximately the shift between the unmodified CENP-A$^{Cse4}$ band and the first modified form of

CENP-A$^{Cse4}$. Immunoblotting for the SUMO protein revealed that the slower-migrating forms of CENP-A$^{Cse4}$ observed in *psh1Δ* cells are sumoylated conjugates (**Figure 2.1A, right**). There are also low levels of CENP-A$^{Cse4}$ sumoylation in wildtype (WT) cells, suggesting that sumoylation occurs under normal conditions and also that ubiquitin and SUMO may compete for lysine residues on CENP-A$^{Cse4}$.

Sumoylation of CENP-A$^{Cse4}$ is not an artifact of CENP-A$^{Cse4}$ overexpression. The amount of sumoylated CENP-A$^{Cse4}$ forms relative to the unmodified form is comparable when CENP-A$^{Cse4}$ is expressed under the endogenous promoter (**Supplemental Figure 2.1**). Furthermore, an allele of CENP-A$^{Cse4}$ which has had all 16 of its lysines mutated to arginines (*Flag-cse4-16R*) is unable to be modified with ubiquitin or SUMO, indicating that the Flag-tag is not sumoylated (**Figure 2.1B, lane 7**).

I exploited the enhanced sumoylation in *psh1Δ* cells to identify the E3 SUMO ligase responsible for CENP-A$^{Cse4}$ sumoylation. Budding yeast have only four E3 SUMO ligases: Cst9, which is meiosis specific, Mms21, which has roles in DNA damage repair and is required for viability, and Siz1 and Siz2, which often work together and carry out a majority of the sumoylation in budding yeast [115, 142]. I generated strains with *psh1Δ*, *pGal-Flag-CSE4*, and either a *SIZ1* deletion, a *SIZ2* deletion, or a temperature sensitive allele of *MMS21* (*mms21-CH*). Overexpressed and purified CENP-A$^{Cse4}$ from each strain revealed that no individual E3 SUMO ligase mutant abolished sumoylation of CENP-A$^{Cse4}$ (data not shown), so double E3 SUMO ligase mutants were generated. In the *psh1Δ siz1Δ siz2Δ*, CENP-A$^{Cse4}$ sumoylation was abolished (**Figure 2.1B, lane 4**), indicating that the Siz1 and Siz2 E3 SUMO ligases function together to sumoylate CENP-A$^{Cse4}$.

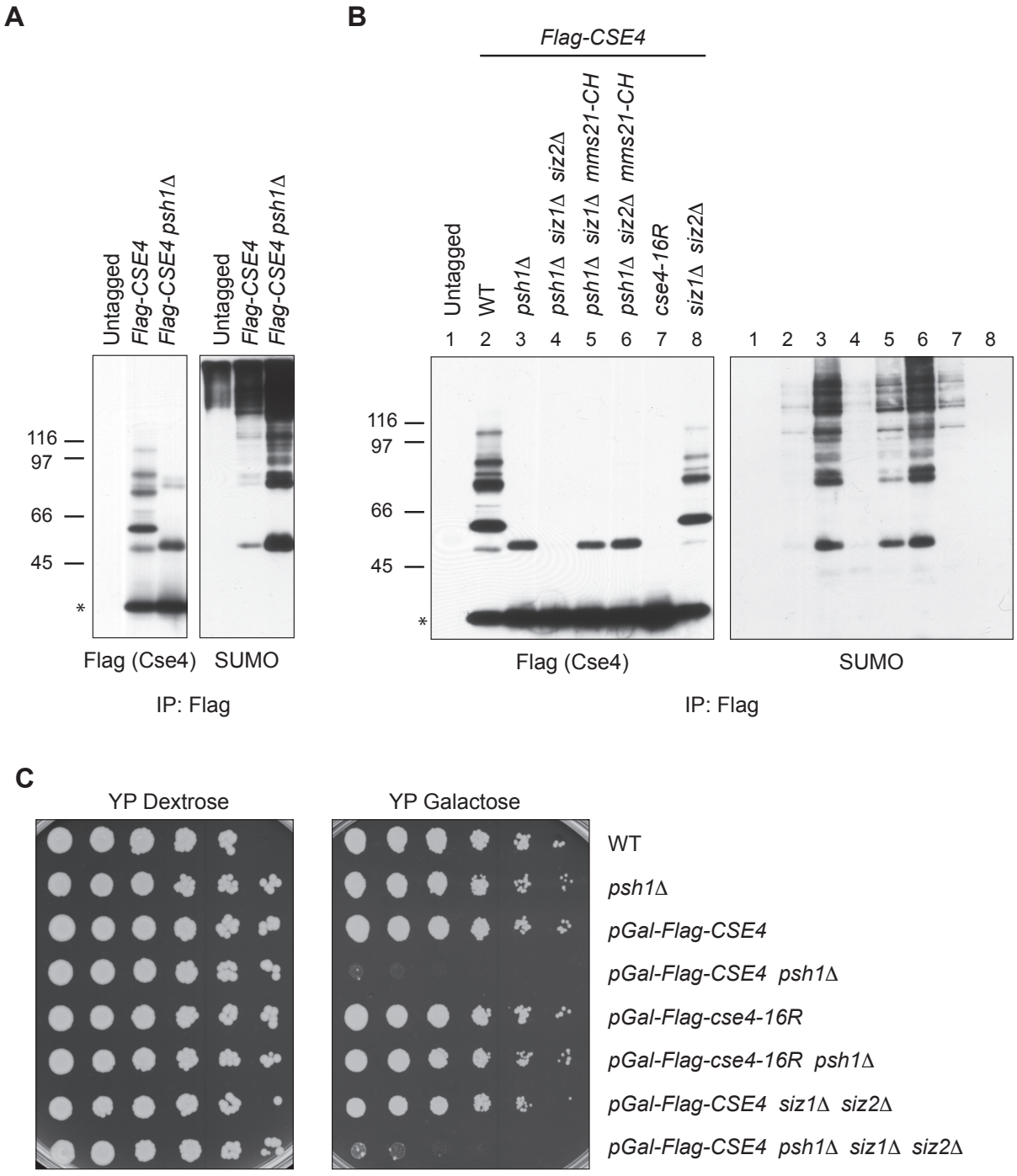


**Figure 2.1. CENP-A$^{Cse4}$ is sumoylated by the Siz1 and Siz2 E3 SUMO ligases**
**(A)** Flag-Cse4 was transiently overexpressed, immunoprecipitated from WT (SBY3), *pGAL-3Flag-CSE4* (SBY8904), and *pGAL-3Flag-CSE4 psh1D* (SBY8903), and analyzed by immunoblotting with the indicated antibodies. **(B)** Overexpressed Flag-Cse4 was immunoprecipitated and analyzed by the indicated immunoblots from strains: WT (SBY3), *pGAL-3Flag-CSE4* (SBY8904), *pGAL-3Flag-CSE4 psh1D* (SBY8903), *pGAL-3Flag-CSE4 psh1D siz1D siz2D cir0* (SBY11038), *pGAL-3Flag-CSE4 psh1D siz1D mms21-CH* (SBY10082), *pGAL-3Flag-CSE4 psh1D siz2D mms21-CH* (SBY11008), *pGAL-Flag-*

*cse4-16R* (SBY11009), and *pGAL-3Flag-CSE4 siz1D siz2D cir0* (SBY11040). **(C)** Yeast cultures were serial diluted and plated on the indicated media for a growth assay using strains: WT (SBY3), *psh1D* (SBY8336), *pGAL-3Flag-CSE4* (SBY8904), and *pGAL-3Flag-CSE4 psh1D* (SBY8903), *pGAL-Flag-cse4-16R* (SBY11009), *pGAL-3Flag-CSE4-16R psh1D* (SBY11010), *pGAL-3Flag-CSE4 siz1D siz2D cir0* (SBY11040), and *pGAL-3Flag-CSE4 psh1D siz1D siz2D cir0* (SBY11038).

I first asked whether removing Siz1/2-mediated sumoylation has a synthetic phenotype with CENP-A$^{Cse4}$ overexpression. Overexpression of CENP-A$^{Cse4}$ in the absence of Psh1-mediated ubiquitination results in increased cellular levels of CENP-A$^{Cse4}$, ectopic localization to non-centromeric chromatin, and subsequent cell death [52-55]. Surprisingly, the lysine-free *cse4-16R* allele is viable when overexpressed and can rescue the *psh1Δ* mutant, even through *cse4-16R* is unable to be ubiquitinated and is stabilized relative to WT CENP-A$^{Cse4}$ [50, 52] (**Figure 2.1C**). This suggests that the lysine residues are leading to the observed lethality, so I asked whether sumoylation of the lysines is responsible. Deletion of *SIZ1/2* did not rescue the *psh1Δ* phenotype, indicating that CENP-A$^{Cse4}$ sumoylation may not be the cause of inviability. However, since Siz1/2 are responsible for most of the sumoylation in budding yeast [142], deleting them may cause pleiotropic effects that prevent cells from coping with excess CENP-A$^{Cse4}$.

### 2.3.2 CENP-A$^{Cse4}$ does not have a primary site of sumoylation

As the mediator of centromeric chromatin and kinetochore assembly, CENP-A$^{Cse4}$ has many binding partners, including other histones, the DNA, and various components in the inner kinetochore [3]. Identifying the sumoylated residue(s) could indicate which binding interactions may be affected by CENP-A$^{Cse4}$ sumoylation as well as allow us to generate a separation of function mutant that lacks only CENP-A$^{Cse4}$ sumoylation. Therefore, I overexpressed and purified Flag-CENP-A$^{Cse4}$ from WT and *psh1Δ* mutants and analyzed the samples by mass

spectrometry. This analysis revealed lysine 49 (K49), in the N-terminus of CENP-A$^{Cse4}$, to be the primary site of sumoylation (personal communication with Judit Villen). I therefore generated a CENP-A$^{Cse4}$ allele with this residue mutated to arginine to prevent sumoylation (*Flag-cse4-K49R*) and an allele with this residue as the sole lysine (*Flag-cse4-15R(K49$^{WT}$)*). Purification of these CENP-A$^{Cse4}$ variants in a *psh1Δ* background showed that K49 is neither necessary nor sufficient for CENP-A$^{Cse4}$ sumoylation (**Figure 2.2A**).

I also looked for potential sites of sumoylation by searching for the consensus motif that is frequently found in substrates ("Ψ-K-*X*-E", where Ψ is a hydrophobic residue, *X* is any amino acid, and K is the sumoylated lysine) [143-145]. A lysine residue at the C-terminus of CENP-A$^{Cse4}$ (K215) fits the consensus motif. As with K49, I mutated and restored this residue, and the adjacent K216, in a *psh1Δ* background. The *Flag-cse4-K215/216R* mutant showed a modest reduction of the sumoylated form, but restoring these two sites (*Flag-cse4-14R(K215/216$^{WT}$)*) was not sufficient to detect sumoylation on CENP-A$^{Cse4}$ (**Figure 2.2B**). These data suggest that K215 and K216 may contribute to the observed CENP-A$^{Cse4}$ sumoylation, but are not sufficient to cause the highly elevated levels of sumoylation in a *psh1Δ* mutant. Siz1/2 may have a preferred target site on CENP-A$^{Cse4}$ that I have not identified, and the overall levels of sumoylation in the *psh1Δ* mutant may require a threshold number of lysine residues.

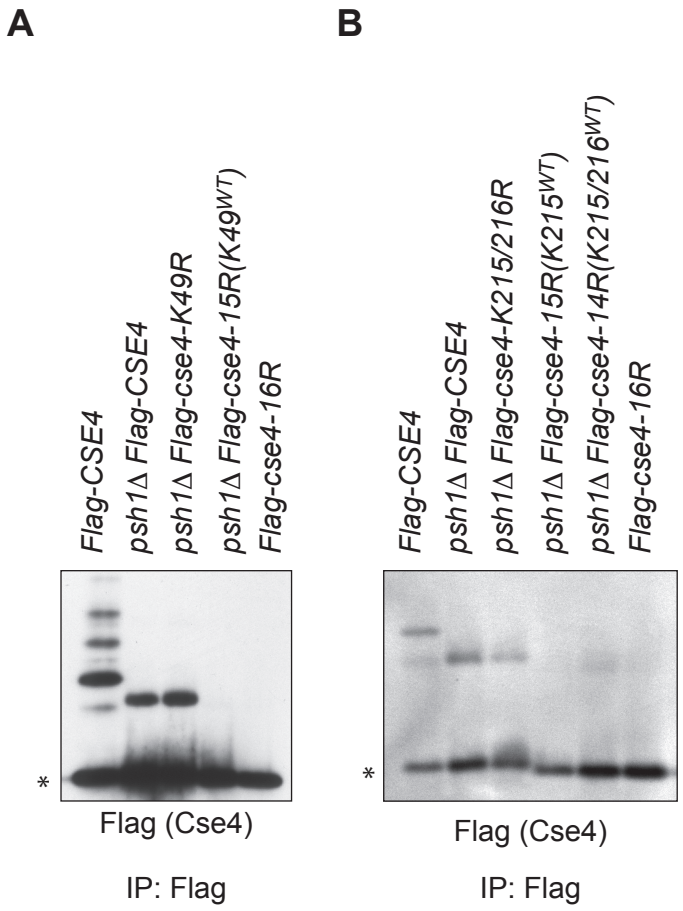


**Figure 2.2. CENP-A$^{Cse4}$ residues K215/216 contribute to total sumoylation levels**
Overexpressed Flag-Cse4 was immunoprecipitated and analyzed by the indicated immunoblots from the following strains: **(A)** *pGAL-3Flag-CSE4 cir0* (SBY11029), *pGAL-3Flag-CSE4 psh1D cir0* (SBY11025), *pGAL-3Flag-cse4-K49R psh1D cir0* (SBY11774), *pGAL-3Flag-cse4-15R(K49$^{WT}$) psh1D cir0* (SBY11776), and *pGAL-3Flag-cse4-16R cir0* (SBY11212)**. (B)** *pGAL-3Flag-CSE4* (SBY8904), and *pGAL-3Flag-CSE4 psh1D* (SBY8903), *pGAL-3Flag-cse4-K215/215R psh1D* (SBY11023), *pGAL-3Flag-cse4-15R(K215$^{WT}$) psh1D* (SBY11020), *pGAL-3Flag-cse4-14R(K215/216$^{WT}$) psh1D* (SBY11021), and *pGAL-Flag-cse4-16R* (SBY11009).

### 2.3.3 CENP-A$^{Cse4}$ sumoylation is cell cycle regulated

In order to help identify the role of sumoylation of CENP-A$^{Cse4}$, I asked whether this modification is cell cycle regulated. I overexpressed and purified Flag-CENP-A$^{Cse4}$ from WT and *psh1Δ* cells that were grown asynchronously or arrested in G1, S phase, or mitosis (using α-factor, HU, or nocodazole, respectively). In WT cells, the level of ubiquitinated CENP-A$^{Cse4}$

remains unchanged throughout the cell cycle, consistent with the finding that CENP-A$^{Cse4}$ has a short half-life at all cell cycle stages [52] (**Figure 2.3**). By comparing the amount of sumoylated forms relative to unmodified Flag-CENP-A$^{Cse4}$ (marked with an asterisk) in the *psh1Δ* mutant, CENP-A$^{Cse4}$ sumoylation is lowest during G1 and highest during S phase. In budding yeast, CENP-A$^{Cse4}$ nucleosomes are deposited to the chromatin and kinetochores assemble during S phase after the replication fork passes through the centromere [103, 104]. The S phase enrichment of CENP-A$^{Cse4}$ sumoylation suggests that it may function to regulate CENP-A$^{Cse4}$ deposition or its recruitment of the inner kinetochore.

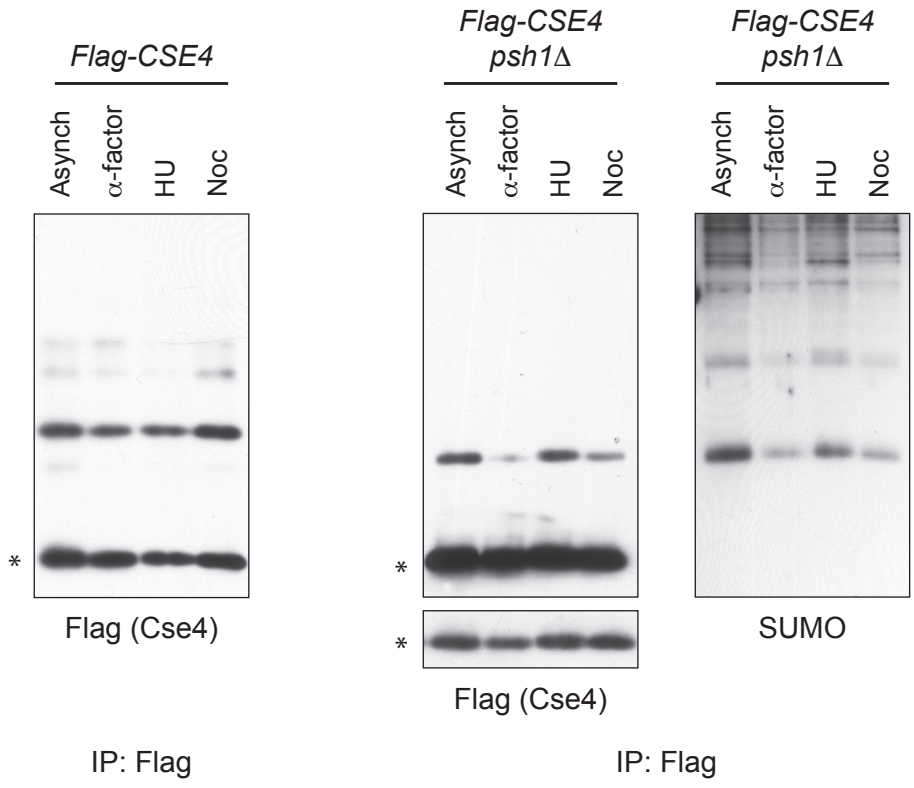


**Figure 2.3. Sumoylation of CENP-A$^{Cse4}$ is cell cycle regulated**
Cells were grown asynchronously or arrested at various stages of the cell cycle with alpha-factor (G1 arrest), HU (S phase), and nocodazole (M). Flag-Cse4 was overexpressed, immunoprecipitated from *pGAL-3Flag-CSE4 cir0* (SBY11029) and *pGAL-3Flag-CSE4 psh1D cir0* (SBY11025), and analyzed by the indicated immunoblots.

### 2.3.4 Sumoylation does not affect CENP-A$^{Cse4}$ stability

Like polyubiquitination, polysumoylation of proteins can ultimately target them for proteasomal degradation [51, 116], so I reasoned that sumoylation may function as another pathway to degrade CENP-A$^{Cse4}$. Conversely, sumoylation can also function to stabilize proteins [113, 114], in which case SUMO and ubiquitin may have opposing effects on the stability of CENP-A$^{Cse4}$. To assay CENP-A$^{Cse4}$ stability, I briefly overexpressed Flag-CENP-A$^{Cse4}$, inhibited translation with cycloheximide, and analyzed the abundance of Flag-CENP-A$^{Cse4}$ over time. As has been reported, CENP-A$^{Cse4}$ was stabilized by the deletion of the E3 ubiquitin ligase, *PSH1* [52-55]. (**Figure 2.4A** and **2.4B**). Deletion of *SIZ1/2* had only a subtle effect on CENP-A$^{Cse4}$ stability that was variable across experiments. Generally, *SIZ1/2* deletion in a WT background either had no effect or slightly destabilized CENP-A$^{Cse4}$. Because results were inconsistent over many stability assays, I show two representative experiments, one in which CENP-A$^{Cse4}$ is destabilized in the *siz1/2Δ*, and one in which it is unchanged (**Figure 2.4A**). In a *psh1Δ* background, *SIZ1/*2 deletion typically had no effect, but sometimes stabilized CENP-A$^{Cse4}$ (**Figure 2.4B**). I postulated that the observed variability could result from analyzing asynchronous cultures. Because sumoylation is highest in S phase, I performed the stability assay from S phase arrested cells, when loss of sumoylation would have the largest effect. Again, there was no significant change in the half-life of CENP-A$^{Cse4}$ in the absence of Siz1/2 (**Figure 2.4C**). I concluded that Siz1/2-dependent sumoylation does not have a significant effect on the degradation kinetics of CENP-A$^{Cse4}$.

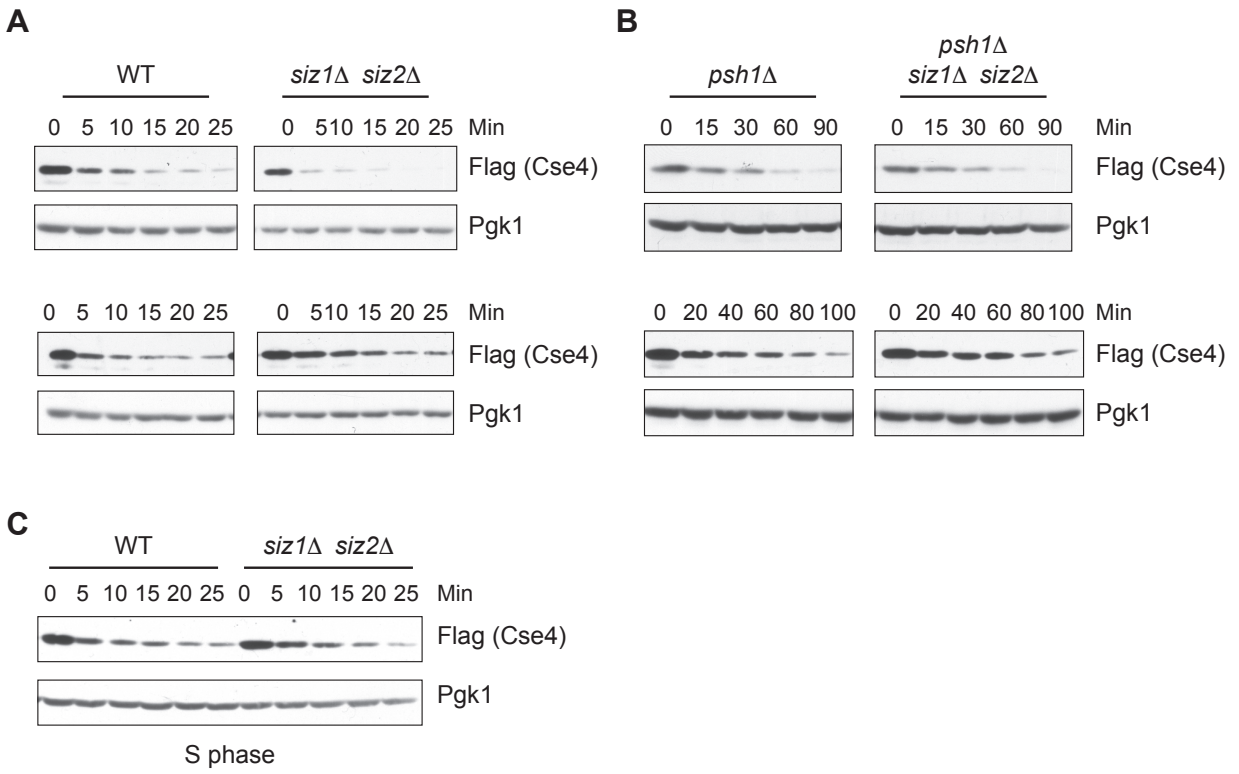


**Figure 2.4. Sumoylation does not significantly affect the stability of CENP-A$^{Cse4}$**
**(A)** Flag-Cse4 was overexpressed for one hour before the addition of glucose and cycloheximide at time 0 minutes. Samples were collected at the indicated time points and cell lysates were analyzed by immunoblotting for Flag and Pgk1 as a loading control. Two experiments are shown (top and bottom). The strains used were *pGAL-3Flag-CSE4 cir0* (SBY11029) and *pGAL-3Flag-CSE4 siz1D siz2D cir0* (SBY11040). **(B)** Cse4 stability assays were performed the same as in (A), except Flag-Cse4 was overexpressed for 30 minutes. The strains used were *pGAL-3Flag-CSE4 psh1D cir0* (SBY11025) and *pGAL-3Flag-CSE4 psh1D siz1D siz2D cir0* (SBY11038). **(C)** Cse4 stability assays were performed as in (A), except that cells were treated with hydroxyurea (HU) for two hours before the one hour galactose induction. The strains used were *pGAL-3Flag-CSE4 cir0* (SBY11029) and *pGAL-3Flag-CSE4 siz1D siz2D cir0* (SBY11040).

### 2.3.5 Protein interactions within the kinetochore are unaffected by Siz1/2-mediated sumoylation

In yeast, SUMO was initially discovered by its genetic interaction with CENP-C$^{Mif2}$, one of the first kinetochore proteins to assemble at the centromere [117]. Furthermore, modification with SUMO can function to alter the binding partners of its substrates, so I asked whether sumoylation regulates interactions between CENP-A$^{Cse4}$ and inner kinetochore proteins. I first

looked for gross differences in kinetochore composition upon *SIZ1/2* deletion, since these ligases may target the other kinetochore proteins that are sumoylated [58, 123-125]. I purified kinetochores from WT and *siz1/2Δ* strains by immunoprecipitating Dsn1-Flag, a middle kinetochore protein. Weakened interactions within the inner kinetochore would confer a decrease of CENP-$A^{Cse4}$ and inner kinetochore proteins. However, by silver stain analysis the overall stoichiometry of the purified kinetochores remained unchanged (**Figure 2.5A, left**), and immunoblotting against CENP-$A^{Cse4}$ and CENP-$C^{Mif2}$ showed no significant difference between the strains (**Figure 2.5A, right**). Sumoylation of the centromere-binding protein, Ndc10, has been postulated to destabilize kinetochores [125]. However, low levels of Ndc10 co-purify with kinetochores [135], so I were unable to assay for this effect. By this method, there appears to be no large-scale effect of sumoylation on kinetochore composition.

I then sought to directly test the interaction of CENP-$A^{Cse4}$ with various inner kinetochore proteins by purifying overexpressed Flag-CENP-$A^{Cse4}$ and looking for the co-purification of CENP-$C^{Mif2}$ or CENP-$N^{Chl4}$. In both WT and *psh1Δ* mutant backgrounds, the deletion of *SIZ1/2* appeared to promote the co-purification of CENP-$C^{Mif2}$ (**Figure 2.5B**), suggesting that level of CENP-$A^{Cse4}$ sumoylation does not regulate the stability of inner kinetochore interactions. However, I noticed that CENP-$C^{Mif2}$ has upper conjugates that are abolished upon deletion of Siz1/2, indicating that CENP-$C^{Mif2}$ may be sumoylated. This is particularly interesting since SUMO was discovered in budding yeast as a suppressor of a CENP-$C^{Mif2}$ temperature sensitive mutant, and CENP-$C^{Mif2}$ can be sumoylated *in vitro* [117, 146]. However, I could not detect these slower-migrating forms when I purified CENP-$C^{Mif2}$-myc itself (data not shown), but the possibility of CENP-$C^{Mif2}$ sumoylation should be further explored. These data suggest that either CENP-$C^{Mif2}$ is not sumoylated, or that only the CENP-$A^{Cse4}$-bound pool of CENP-$C^{Mif2}$ is

sumoylated. Because CENP-A$^{Cse4}$ and CENP-C$^{Mif2}$ still interact strongly in *siz1/2Δ* mutants, sumoylation does not appear to regulate this interaction.

Removal of *SIZ1/2* also does not regulate the interaction between CENP-C$^{Mif2}$ and CENP-N$^{Chl4}$. Surprisingly, *PSH1* deletion enhanced the association between CENP-N$^{Chl4}$ and CENP-A$^{Cse4}$, regardless of whether *SIZ1/2* were deleted (**Figure 2.4C**). This suggests that Psh1 negatively regulates the interaction between CENP-A$^{Cse4}$ and CENP-N$^{Chl4}$ through a sumoylation-independent mechanism.

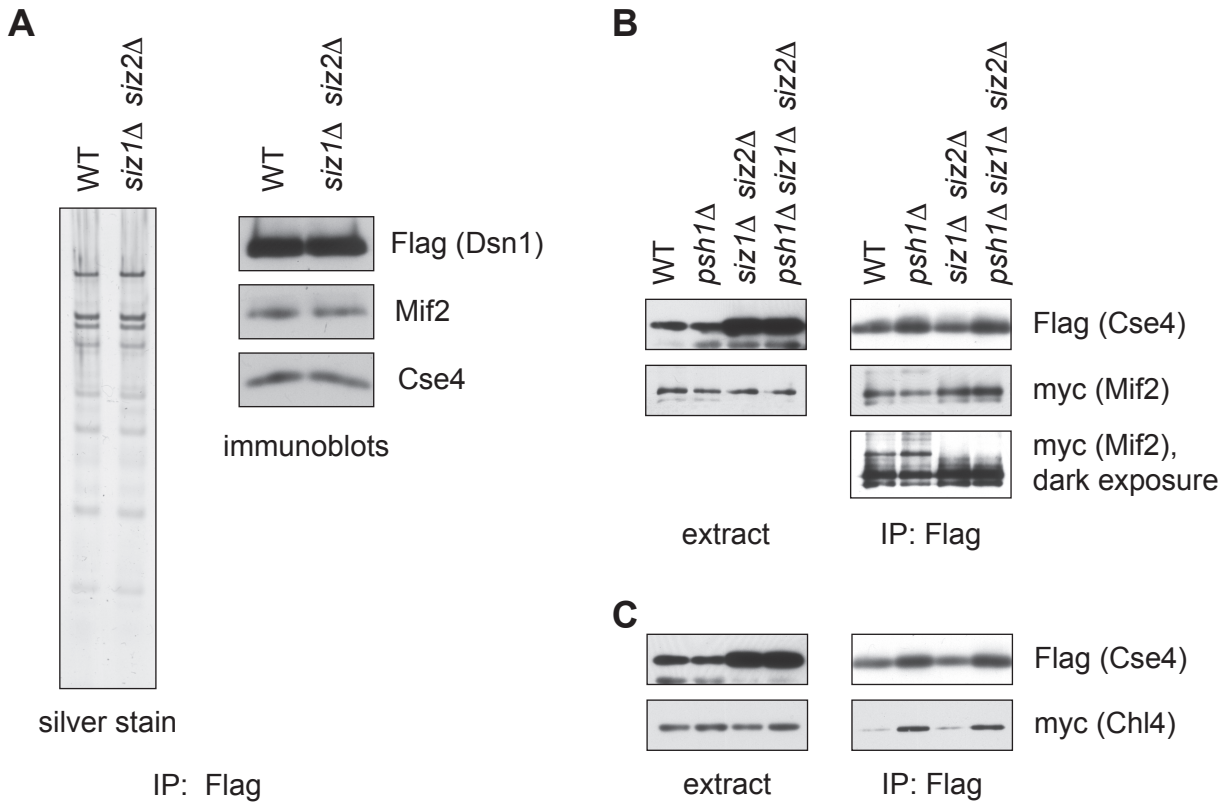


**Figure 2.5. CENP-A$^{Cse4}$ sumoylation does not alter inner kinetochore interactions**
**(A)** Dsn1-Flag was immunoprecipitated from *DSN1-6His-3Flag cir0* (SBY11323) and *DSN1-6His-3Flag siz1D siz2D cir0* (SBY11290) and analyzed by silver stain (left) and immunoblotting (right). **(B, C)** Overexpressed Flag-Cse4 was immunoprecipitated and co-purifying proteins were analyzed by the indicated immunoblots. The strains used were **(B)** *pGAL-3Flag-CSE4 MIF2-13myc cir0* (SBY11156), *pGAL-3Flag-CSE4 MIF2-13myc psh1D cir0* (SBY11157), *pGAL-3Flag-CSE4 MIF2-13myc siz1D siz2D cir0* (SBY11158), and *pGAL-3Flag-CSE4 MIF2-13myc psh1D siz1D siz2D cir0* (SBY11130). **(C)** *pGAL-3Flag-CSE4 CHL4-13myc cir0* (SBY11159), *pGAL-3Flag-CSE4 CHL4-13myc psh1D cir0* (SBY11160),

*pGAL-3Flag-CSE4 CHL4-13myc siz1D siz2D cir0* (SBY11161), *pGAL-3Flag-CSE4 CHL4-13myc psh1D siz1D siz2D cir0* (SBY11131).

## 2.4 DISCUSSION

### 2.4.1 Relating our findings to recent studies

Since the time that I was investigating CENP-A$^{Cse4}$ sumoylation, another group published related work, and I will outline the similarities and differences here [58, 111]. In agreement with our findings, Ohkuni, et al. identified Siz1/2 as the E3 SUMO ligases for CENP-A$^{Cse4}$. Although I was unable to identify a key sumoylated residue, they identified K65 on CENP-A$^{Cse4}$ as the primary target of sumoylation. They reported that overexpressed *cse4-K65R* had a reduction, but not complete abolition, of sumoylated conjugates. I note that their studies were performed with WT *PSH1*, where sumoylation levels are low. Because I found that CENP-A$^{Cse4}$ sumoylation levels are highly elevated in a *psh1Δ*, I speculate that SUMO and ubiquitin compete for lysines. Under WT conditions, sumoylation may be restricted to key residues, potentially from competition with Psh1. In the absence of Psh1 ubiquitination, more residues become available and Siz1/2 may target additional sites for sumoylation. The high levels of CENP-A$^{Cse4}$ sumoylation in a *psh1Δ* mutant could therefore have masked differences in our site mutants that I may have seen in WT yeast. Given that the *cse4-K215/216R* that I tested showed a slight reduction in sumoylation even in a *psh1Δ* background, these residues may also serve as important sumoylation sites under WT conditions. All potential candidate sites for sumoylation should be tested in both WT and *psh1Δ* mutant backgrounds to address whether they are primary sites of sumoylation or only sumoylated opportunistically in the absence of ubiquitination.

Ohkuni et al. then postulate that Slx5, a SUMO-dependent E3 ubiquitin ligase, recognizes the sumoylation and ubiquitinates CENP-A$^{Cse4}$ independently of Psh1. They found

that Slx5 interacts with CENP-A$^{Cse4}$ *in vivo* via co-immunoprecipitation, but do not demonstrate whether this interaction depends on Siz1/2. Some *cse4-K65R* transformants had reduced binding to Slx5, suggesting that sumoylation of this residue may promote the CENP-A$^{Cse4}$-Slx5 interaction. However, the results were highly variable. To carefully examine whether Slx5 recognizes sumoylated CENP-A$^{Cse4}$, this interaction should be tested in a *siz1/2Δ* that completely lacks CENP-A$^{Cse4}$ sumoylation, a *psh1Δ* that has highly elevated levels of CENP-A$^{Cse4}$ sumoylation, and *cse4-16R* that has neither ubiquitination nor sumoylation.

They found that the *slx5Δ* and *siz1/2Δ* mutants have inhibited growth when CENP-A$^{Cse4}$ is overexpressed, much like the *psh1Δ* mutant, suggesting that they contribute to CENP-A$^{Cse4}$ degradation. These data are in direct contrast to our findings that *siz1/2Δ* has no growth defects upon CENP-A$^{Cse4}$ overexpression. This discrepancy is caused by their strains containing the 2-micron plasmid that is parasitic in most lab strains of budding yeast. The 2-micron plasmid encodes its own regulatory proteins to maintain itself at around 50 copies per cell, and this maintenance mechanism is SUMO-regulated [147]. In *siz1/2Δ* mutants, 2-micron accumulates at up to 40-fold higher copy number than in WT cells, which is hypothesized to sequester replication or segregation machinery [147]. Unless *siz1/2Δ* cells are cured of the 2-micron plasmid, they are sick, displaying cold sensitivity and irregular colony shapes. Ohkuni et al. saw a growth defect with *siz1/2Δ* because they were overexpressing CENP-A$^{Cse4}$ from a 2-micron plasmid. In addition, another group reported that the *slx5Δ* mutant had no growth defect upon CENP-A$^{Cse4}$ overexpression [59].

Their work then exclusively utilizes the *slx5Δ* mutant as opposed to the *siz1/2Δ* mutant that I studied. If Slx5 acts as a SUMO-dependent ubiquitin ligase for CENP-A$^{Cse4}$, these two mutants should have similar effects on CENP-A$^{Cse4}$. Our analysis of the effect of sumoylation on

CENP-A$^{Cse4}$ stability in both a WT and *psh1Δ* background yielded subtle and inconsistent results. I concluded that sumoylation does not significantly affect the stability of CENP-A$^{Cse4}$. Ohkuni et al. reported that *SLX5* deletion caused CENP-A$^{Cse4}$ to be stabilized. Although the differences they published are also subtle, they concluded significance by quantifying the results using only two replicates. Given the high variability I saw, many replicates would be required for an accurate representation of the results. Another potential explanation for the difference in findings is that Slx5 activity toward CENP-A$^{Cse4}$ is not SUMO-mediated, as there is evidence that it can ubiquitinate non-sumoylated substrates [148]. Because the sumoylation of CENP-A$^{Cse4}$ is cell cycle regulated, and because the effect on stability is subtle, stability assays in *siz1/2Δ* and *slx5Δ* mutants should be performed in S phase arrested cells and quantified over many experiments. Understanding whether sumoylation protects CENP-A$^{Cse4}$ or leads to its degradation is crucial for defining its cellular function.

### 2.4.2 Considering additional findings

In characterizing the sumoylation of CENP-A$^{Cse4}$, I found that this modification is cell cycle regulated, peaking during S phase. Comparatively, Psh1-mediated ubiquitination does not fluctuate throughout the cell cycle, suggesting that this proteolysis pathway is constitutively active to remove CENP-A$^{Cse4}$ that has mislocalized to chromosome arms [55]. Because the timing of CENP-A$^{Cse4}$ sumoylation is markedly different, it seems unlikely that sumoylation serves as a secondary pathway to degrade the same pool of CENP-A$^{Cse4}$ that Psh1 does. Sumoylation of CENP-A$^{Cse4}$ is highest during S phase, when CENP-A$^{Cse4}$ nucleosomes are deposited. Siz1/2 may target excess CENP-A$^{Cse4}$ in the vicinity of the centromere or may target centromere-bound CENP-A$^{Cse4}$. Either of these pools of CENP-A$^{Cse4}$ would likely be smaller

than that in chromosome arms, meaning far less sumoylation is required than Psh1-mediated ubiquitination. This agrees with the relative levels of these two modifications on CENP-A$^{Cse4}$ in WT cells (**Figure 2.1A**). It will be important for future studies to define which pool of CENP-A$^{Cse4}$ is sumoylated using better-suited methods, such as a mini-chromosome purification or a DNA-based kinetochore assembly assay that will be described in the next chapter.

Whether sumoylation more broadly affects CENP-A$^{Cse4}$ deposition or stability in chromatin should also be examined. I attempted to assay for the chromatin enrichment of sumoylated CENP-A$^{Cse4}$ through various methods. First, I tried to visualize its DNA-localization by performing chromatin spreads, whereby the non-soluble components of the nucleus are fixed and stained by immunofluorescence. CENP-A$^{Cse4}$ is normally present as clear foci in WT, but localizes throughout the DAPI when overexpressed in a *psh1Δ* mutant. I also attempted to compare the levels of CENP-A$^{Cse4}$ in the soluble and chromatin fractions of cell lysates. For a more detailed analysis of CENP-A$^{Cse4}$ localization, I performed chromatin immunoprepcipitations (ChIP) on Flag-CENP-A$^{Cse4}$ and analyzed its abundance at several euchromatic loci that exhibit consistent Flag-CENP-A$^{Cse4}$ ectopic localization by quantitative PCR [54]. Generally, deletion of *SIZ1/2* had no widespread effect on the ectopic localization of CENP-A$^{Cse4}$ (data not shown), but all of these experiments were preliminary and should be repeated in the future. These experiments will help answer whether sumoylation plays a role in CENP-A$^{Cse4}$ localization to the euchromatin, or whether it is a result of CENP-A$^{Cse4}$ mislocalization.

### 2.4.3 A model for CENP-A$^{Cse4}$ regulation by ubiquitin and SUMO

Under WT conditions, Psh1 appears to be the prominent ubiquitin ligase for CENP-A$^{Cse4}$. I found that in a *psh1Δ* mutant, ubiquitinated conjugates are not detectable and are replaced by high levels of sumoylated CENP-A$^{Cse4}$. Siz1 and Siz2 are weak competitors for lysine modification, but can sumoylate CENP-A$^{Cse4}$ at low levels, perhaps at a precise, available residue(s). Slx5 may recognize this sumoylation to ubiquitinate CENP-A$^{Cse4}$ independently of Psh1. Slx5 appears to ubiquitinate CENP-A$^{Cse4}$ to a much lesser extent than Psh1 does, because in an *slx5Δ* the upper ubiquitinated forms of CENP-A$^{Cse4}$ are reduced but still detectable [58]. Whether Slx5 interacts only with sumoylated CENP-A$^{Cse4}$ should be carefully tested as outlined above. However, I note that there are slightly reduced levels of ubiquitinated CENP-A$^{Cse4}$ forms in the *siz1/2Δ* mutant (**Figure 2.1A, right**), which may be due to a loss Slx5 ubiquitination.

Upon *PSH1* deletion, the bulk of CENP-A$^{Cse4}$ ubiquitination is abolished. Siz1 and Siz2 may have increased access to lysine residues and sumoylate CENP-A$^{Cse4}$ to very high levels, likely with diminished site-specificity. However, this disagrees with their data that show similar, low levels of CENP-A$^{Cse4}$ sumoylation in WT and a *psh1Δ* mutant. The reason for such a striking difference is unclear, since I see significantly enhanced CENP-A$^{Cse4}$ sumoylation in a *psh1Δ* mutant. Regardless, Slx5 should ubiquitinate the sumoylated CENP-A$^{Cse4}$ to target it for degradation. However, I detect an abundance of sumoylated CENP-A$^{Cse4}$ in a *psh1Δ* mutant. Slx5 may be a limiting factor, or may only recognize sumoylation of a specific CENP-A$^{Cse4}$ residue, perhaps K65 as identified by Ohkuni et al. If so, any effect of sumoylation on CENP-A$^{Cse4}$ stability or function would only be distinguishable in WT cells and would be masked in the *psh1Δ* mutant.

Psh1 and Slx5 may target different pools of CENP-A$^{Cse4}$. Psh1 ubiquitinates mislocalized CENP-A$^{Cse4}$ throughout the cell cycle, and its activity is required for viability when CENP-A$^{Cse4}$ is overexpressed. Slx5 may also ubiquitinate CENP-A$^{Cse4}$ throughout the cell cycle, but the sumoylated forms are enriched during S phase indicating that at least Siz1/2 activity toward CENP-A$^{Cse4}$ is cell cycle regulated. Sumoylation may target a centromere proximal pool, ensuring that multiple CENP-A$^{Cse4}$ nucleosomes do not get deposited in the wake of the replication fork. Alternatively, sumoylation may target centromere-bound CENP-A$^{Cse4}$ and either protect it from ubiquitination or promote its binding affinity to the inner kinetochore. Carefully determining whether sumoylation leads to CENP-A$^{Cse4}$ stability or degradation is pivotal to distinguishing between these hypotheses.

## 2.5 Materials And Methods

### 2.5.1 Yeast strain construction and microbial techniques

The *Saccharomyces cerevisiae* strains used in this study are listed in Supplementary Table 2.1, and integrated plasmids are listed in Supplementary Table 2.2. Standard genetic crosses and media were used to generate and grow yeast [149]. Gene deletions and epitope tagged alleles (3Flag, 9myc) were constructed by standard PCR-based integration as described in [150] and confirmed by PCR. Point mutants were made using site-directed mutagenesis and confirmed by sequencing. The E3 SUMO ligase mutants were gifts from Xiaolan Zhao.

For all experiments with transiently overexpressed 3Flag-Cse4, cells were grown at 30 °C in lactic acid media to log phase and induced with 2% galactose for 1.5 hours. For experiments with *mms21-CH* mutants, cultures were shifted to 37 °C for the final two hours of growth. For stability assays, 3Flag-Cse4 was overexpressed with 4% galactose for one hour in a WT

background, or 30 minutes in the *psh1Δ* background. 50 μg/mL cycloheximide and 2% glucose were added to the cultures at time = 0 minutes. All other liquid cultures were grown in yeast peptone dextrose rich (YPD) media at room temperature to log phase. Cells were arrested in G1, S phase, or mitosis by adding drug (10 μg/mL α-factor in DMSO, 0.2 M hydroxyurea, or 10 μg/mL Nocodazole in DMSO, respectively) to log phase cells in liquid culture for three hours until at least 90% of the cells were shmoos (α-factor) or large-budded (hydroxyurea and Nocodazole).

Growth assays were performed by diluting saturated cultures 1:20 and from that making a 1:5 serial dilution series. This series was plated on yeast extract-peptone-dextrose (YPD) and yeast extract-peptone-galactose (YPG) plates that were incubated at 23 °C.

### 2.5.2 Protein techniques

Whole cell extracts from stability assay samples were made by freezing cells in liquid nitrogen and resuspending in SDS buffer. Cells were lysed using glass beads and a beadbeater (Biospec Products), then clarified by centrifugation at 16,100 g for 5 minutes at 4 °C.

### 2.5.4 Protein biochemistry

Immunoprecipitation of Flag-tagged CENP-A$^{Cse4}$ or Dsn1 were performed as described in [135]. For all 3Flag-Cse4 immunoprecipitations, 5 mM N-Ethylmaleimide (NEM) was also included in the lysis and washing buffers. Silver stains were performed by run running the samples on NuPAGE 4-12% Bis-Tris protein gels (Invitrogen) and silver staining using SilverQuest (Invitrogen).

### 2.5.5 Immunological methods

Whole cell extract or samples were prepared as described above and separated by SDS-PAGE. Proteins were transferred to a nitrocellulose membrane (BioRad) and standard immunoblotting was performed. Primary and secondary antibodies were used as described in [136]. Primary antibodies were used as follows: α-Flag M2 (Sigma-Aldrich Catalog #F3165) 1:3,000; α-myc (9E10, Covance Catalog #MMS-150R) 1:10,000; α-Pgk1 (Invitrogen Catalog #459250) 1:10,000; α-Smt3 1:3,000; α-Mif2 (OD2) 1:6,000; and α-Cse4 (9536) 1:500 [151]. The α-Mif2 antibody was a gift from Arshad Desai and the α-Smt3 antibody was a gift from Pamela Meluh. HRP conjugated secondary antibodies were detected with Pierce enhanced chemiluminescent (ECL) substrate and SuperSignal West Dura and Femto ECL (ThermoFisher Scientific).

## 2.6 ACKNOWLEDGEMENTS

I am grateful to Xiaolan Zhao for providing the E3 SUMO ligase mutant strains. The α-Mif2 antibody was a gift from Arshad Desai and the α-Smt3 antibody was a gift from Pamela Meluh. I would also like to thank all members of the Biggins lab for strains and insightful discussions, particularly Prerana Ranjitkar who first identified that CENP-$A^{Cse4}$ is sumoylated.

## 2.7 SUPPLEMENTAL FIGURES

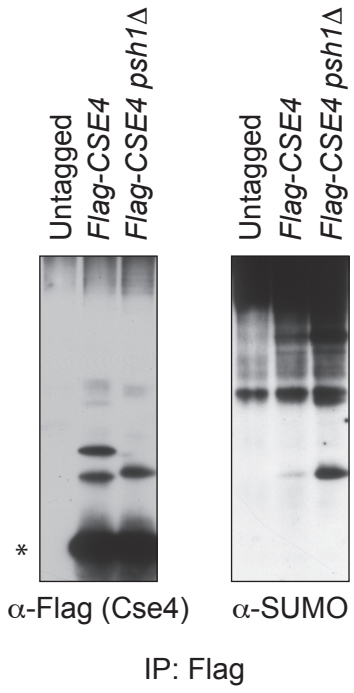


**Supplemental Figure 2.1. Endogenously expressed CENP-A$^{Cse4}$ is sumoylated**
Flag-Cse4 expressed from the endogenous promoter was immunoprecipitated from WT (SBY3), *3Flag-CSE4 cse4D* (SBY10111), and *3Flag-CSE4 cse4D psh1D* (SBY10424) and analyzed by the indicated immunoblots.

## 2.8 SUPPLEMENTAL TABLES

**Supplemental Table 2.1. Yeast strains used in this chapter**
Complete genotypes of the *Saccharomyces cerevisiae* strains used are listed along with the strain number to reference. All strains are isogenic with W303.

| Strain | Genotype | Integrated plasmids |
|---|---|---|
| SBY3 | *MAT***a** *ura3-1 leu2,3-112 his3-11 trp1-1 ade2-1 LYS2 can1-100 bar1-1* | |
| SBY8336 | *MAT***a** *ura3-1 leu2,3-112 his3-11 trp1-1 ade2-1 LYS2 can1-100 bar1-1 psh1Δ* | |
| SBY8903 | *MAT***a** *ura3-1::pGAL-3Flag-CSE4:URA3 leu2,3-112 his3-11 trp1-1 ade2-1 LYS2 can1-100 bar1-1 psh1Δ::KanMX* | pSB1665 |
| SBY8904 | *MAT***a** *ura3-1::pGAL-3Flag-CSE4:URA3 leu2,3-112 his3-11 trp1-1 ade2-1 LYS2 can1-100 bar1-1* | pSB1665 |
| SBY10082 | *MAT***a** *ura3-1::pGAL-3Flag-CSE4:URA3 leu2,3-112 his3-11 trp1-1 ade2-1 LYS2 can1-100 bar1-1 psh1Δ::KanMX siz1Δ::KanMX mms21-CH:HIS3* | pSB1665 |
| SBY10111 | *MAT***a** *ura3-1::3Flag-CSE4:URA3 leu2,3-112 his3-11 trp1-1 ade2-1 lys2- can1-100 bar1-1 cse4Δ::KanMX* | pSB1067 |
| SBY10424 | *MAT***a** *ura3-1::3Flag-CSE4:URA3 leu2,3-112 his3-11 trp1-1 ade2-1 lys2- can1-100 bar1-1 cse4Δ::KanMX psh1Δ::KanMX* | pSB1067 |
| SBY11008 | *MAT***a** *ura3-1::pGAL-3Flag-CSE4:URA3 leu2,3-112 his3-11 trp1-1 ade2-1 LYS2 can1-100 bar1-1 psh1Δ::KanMX siz2Δ::URA3 mms21-CH:HIS3* | pSB1665 |
| SBY11009 | *MAT***a** *ura3-1::pGAL-3Flag-cse4-16R:URA3 leu2,3-112 his3-11 trp1-1 ade2-1 LYS2 can1-100 bar1-1* | pSB1685 |
| SBY11010 | *MAT***a** *ura3-1::pGAL-3Flag-cse4-16R:URA3 leu2,3-112 his3-11 trp1-1 ade2-1 LYS2 can1-100 bar1-1 psh1Δ* | pSB1685 |
| SBY11020 | *MAT***a** *ura3-1::pGAL-3Flag-cse4-15R(K215$^{WT}$):URA3 leu2,3-112 his3-11 trp1-1 ade2-1 LYS2 can1-100 bar1-1 psh1Δ::KanMX* | pSB1960 |
| SBY11021 | *MAT***a** *ura3-1::pGAL-3Flag-cse4-14R(K215/216$^{WT}$):URA3 leu2,3-112 his3-11 trp1-1 ade2-1 LYS2 can1-100 bar1-1 psh1Δ::KanMX* | pSB1961 |
| SBY11023 | *MAT***a** *ura3-1::pGAL-3Flag-cse4-K215/216R:URA3 leu2,3-112 his3-11 trp1-1 ade2-1 LYS2 can1-100 bar1-1 psh1Δ::KanMX* | pSB1781 |
| SBY11025 | *MAT***a** *ura3-1::pGAL-3Flag-CSE4:URA3 leu2,3-112 his3-11 trp1-1 ade2-1 LYS2 can1-100 bar1-1 psh1Δ::KanMX cir0* | pSB1665 |
| SBY11029 | *MAT***a** *ura3-1::pGAL-3Flag-CSE4:URA3 leu2,3-112 his3-11 trp1-1 ade2-1 LYS2 can1-100 bar1-1 cir0* | pSB1665 |

| | | |
|---|---|---|
| SBY11038 | *MAT***a** *ura3-1::pGAL-3Flag-CSE4:URA3 leu2,3-112 his3-11 trp1-1 ade2-1 LYS2 can1-100 bar1-1 psh1Δ::KanMX siz1Δ::KanMX siz2Δ::URA3 cir0* | pSB1665 |
| SBY11040 | *MAT***a** *ura3-1::pGAL-3Flag-CSE4:URA3 leu2,3-112 his3-11 trp1-1 ade2-1 LYS2 can1-100 bar1-1 siz1Δ::KanMX siz2Δ::URA3 cir0* | pSB1665 |
| SBY11130 | *MAT***a** *ura3-1::pGAL-3Flag-CSE4:URA3 leu2,3-112 his3-11 trp1-1 ade2-1 LYS2 can1-100 bar1-1 MIF2-13myc:HIS3 psh1Δ::KanMX siz1Δ::KanMX siz2Δ::URA3 cir0* | pSB1665 |
| SBY11131 | *MAT***a** *ura3-1::pGAL-3Flag-CSE4:URA3 leu2,3-112 his3-11 trp1-1 ade2-1 LYS2 can1-100 bar1-1 CHL4-13myc:HIS3 psh1Δ::KanMX siz1Δ::KanMX siz2Δ::URA3 cir0* | pSB1665 |
| SBY11156 | *MAT***a** *ura3-1::pGAL-3Flag-CSE4:URA3 leu2,3-112 his3-11 trp1-1 ade2-1 LYS2 can1-100 bar1-1 MIF2-13myc:HIS3 cir0* | pSB1665 |
| SBY11157 | *MAT***a** *ura3-1::pGAL-3Flag-CSE4:URA3 leu2,3-112 his3-11 trp1-1 ade2-1 LYS2 can1-100 bar1-1 MIF2-13myc:HIS3 psh1Δ::KanMX cir0* | pSB1665 |
| SBY11158 | *MAT***a** *ura3-1::pGAL-3Flag-CSE4:URA3 leu2,3-112 his3-11 trp1-1 ade2-1 LYS2 can1-100 bar1-1 MIF2-13myc:HIS3 siz1Δ::KanMX siz2Δ::URA3 cir0* | pSB1665 |
| SBY11159 | *MAT***a** *ura3-1::pGAL-3Flag-CSE4:URA3 leu2,3-112 his3-11 trp1-1 ade2-1 LYS2 can1-100 bar1-1 CHL4-13myc:HIS3 cir0* | pSB1665 |
| SBY11160 | *MAT***a** *ura3-1::pGAL-3Flag-CSE4:URA3 leu2,3-112 his3-11 trp1-1 ade2-1 LYS2 can1-100 bar1-1 CHL4-13myc:HIS3 psh1Δ::KanMX cir0* | pSB1665 |
| SBY11161 | *MAT***a** *ura3-1::pGAL-3Flag-CSE4:URA3 leu2,3-112 his3-11 trp1-1 ade2-1 LYS2 can1-100 bar1-1 CHL4-13myc:HIS3 siz1Δ::KanMX siz2Δ::URA3 cir0* | pSB1665 |
| SBY11212 | *MAT***a** *ura3-1::pGAL-3Flag-cse4-16R:URA3 leu2,3-112 his3-11 trp1-1 ade2-1 LYS2 can1-100 bar1-1cir0* | pSB1685 |
| SBY11290 | *MAT***a** *ura3-1 leu2,3-112 his3-11 trp1-1 ade2-1 LYS2 can1-100 bar1-1 DSN1-6His-3Flag:URA3 siz1Δ::KanMX siz2Δ::URA3 cir0* | |
| SBY11323 | *MAT***a** *ura3-1 leu2,3-112 his3-11 trp1-1 ade2-1 LYS2 can1-100 bar1-1 DSN1-6His-3Flag:URA3 cir0* | |
| SBY11774 | *MAT***a** *ura3-1::pGAL-3Flag-cse4-K49R:URA3 leu2,3-112 his3-11 trp1-1 ade2-1 LYS2 can1-100 bar1-1 psh1Δ::KanMX cir0* | pSB2052 |
| SBY11776 | *MAT***a** *ura3-1::pGAL-3Flag-cse4-15R(K49$^{WT}$):URA3 leu2,3-112 his3-11 trp1-1 ade2-1 LYS2 can1-100 bar1-1 psh1Δ::KanMX cir0* | pSB2053 |

**Supplemental Table 2.2. Plasmids used in this chapter**
The relevant genes and markers on each plasmid used are listed.

| Plasmids | Description |
|---|---|
| pSB1067 | *3Flag-CSE4, URA3* |
| pSB1665 | *pGal-3Flag-CSE4, URA3* |
| pSB1685 | *pGal-3Flag-cse4-16R, URA3* |
| pSB1781 | *pGAL-3Flag-cse4-K215/216R, URA3* |
| pSB1960 | *pGAL-3Flag-cse4-15R(K215$^{WT}$)* |
| pSB1961 | *pGAL-3Flag-cse4-14R(K215/216$^{WT}$)* |
| pSB2052 | *pGAL-3Flag-cse4-K49R* |
| pSB2053 | *pGAL-3Flag-cse4-15R(K49$^{WT}$)* |

# CHAPTER 3. An assay to assemble kinetochores *de novo* reflects the fundamental properties of assembly *in vivo*

## 3.1 SUMMARY

The kinetochore is a megadalton-sized assembly of proteins. To elucidate the underlying mechanisms of how such a large complex is formed, I developed an assay to assemble kinetochores *de novo* using centromeric DNA and budding yeast extracts. Assembly *in vitro* has the same basic requirements as assembly *in vivo*, including the need for the CENP-A$^{Cse4}$ chaperone, HJURP$^{Scm3}$, suggesting the formation of a centromeric nucleosome. This method generates kinetochores that contain components of all kinetochore subcomplexes and exhibit microtubule-binding activity. Furthermore, assembly is cell cycle regulated and is enhanced by mitotic phosphorylation of the Dsn1 kinetochore protein. Assembling kinetochores *de novo* in yeast extracts provides a powerful and genetically tractable method to elucidate critical regulatory events in the future.

## 3.2 INTRODUCTION

Chromosome segregation depends on the kinetochore, the machine that establishes force-bearing attachments between DNA and spindle microtubules. Kinetochores are formed every cell cycle via a highly regulated process that requires coordinated assembly of multiple subcomplexes on specialized chromatin. The complexity of regional centromeres, the difficulty in visualizing kinetochore assembly *in vivo*, and the inability to fully replicate the process *in vitro* has rendered many questions about kinetochore assembly inaccessible. First, it is unclear

whether DNA replication is required for kinetochore assembly [103, 104]. Second, while many protein-protein interactions within the kinetochore have been identified, the hierarchy of subcomplex assembly, protein-protein requirements, and regulatory processes remain poorly understood. Third, because centromeres *in vivo* are in the context of pericentromere, and because extra CENP-A molecules have been detected near the centromere [41-43], it remains controversial whether a single centromeric nucleosome is sufficient for assembly, or whether the pericentromere is also required. A cell-free assay to assemble kinetochores *de novo* would allow us to begin addressing these fundamental questions.

Substantial progress in understanding kinetochore assembly has been made using partial reconstitution systems *in vitro*. For example, pre-formed nucleosomal arrays incubated in *Xenopus* egg extracts assemble microtubule-binding elements that allowed the identification of events required to initiate kinetochore assembly [140]. Furthermore, the binding selectivity of some kinetochore proteins for CENP-A nucleosomes (over H3 nucleosomes) was recently determined by reconstituting the entire linkage between the CENP-A nucleosome and KMN [141]. To identify additional events that regulate kinetochore assembly, I set out to develop a reconstitution system that combines the strengths of these previously developed methods with the added ability to genetically manipulate the system and maintain post-translational modifications. To do this, I used budding yeast because they have a simple "point" centromere that is defined by a ~125 bp specific DNA sequence and a single microtubule attachment site per chromosome [4, 24]. The kinetochore subcomplexes and functions are largely conserved, including the specialized chromatin structure containing CENP-A$^{Cse4}$ that serves as the platform for kinetochore assembly (**Figure 3.1A**).

I therefore developed a method to assemble the kinetochore onto centromeric DNA *in vitro*. Ultimately, the assembly assay has the same fundamental features as kinetochore assembly *in vivo* and can be improved or inhibited by using mutant extracts. Strikingly, the entire kinetochore can assemble on a single centromeric nucleosome without any surrounding pericentromeric chromatin, consistent with recent work showing that KMN can link to a single centromeric nucleosome [141]. The efficiency of assembly is sensitive to phosphoregulation and is highest in extracts from cells arrested in S-phase and mitosis, consistent with the timing of assembly *in vivo*. The assay utilizes the two conserved pathways for Ndc80 recruitment, and the assembled kinetochores are competent to attach to microtubules *in vitro*. In summary, this is the first method for complete assembly of the kinetochore *de novo*, and it can be used to address many questions about centromere and kinetochore biology.

## 3.3 RESULTS

### 3.3.1 Defining conditions for kinetochore assembly *in vitro*

Previous studies showed that tandem arrays of the yeast centromere can assemble a portion of the inner kinetochore, but the outer kinetochore was not present [138]. I instead utilized a minimal DNA template of a single centromere sequence in order to better replicate kinetochore assembly *in vivo*. Because our lab had previously determined conditions to purify intact kinetochores from cells [135], I reasoned that these extract conditions may be permissive for kinetochore assembly *de novo*. I therefore prepared yeast whole cell extracts by our established method and incubated it with various naked DNA templates. The centromeric template contains the chromosome III centromere (117 bp) and ~70 bp of pericentromeric DNA on each side (referred to as "*CEN3*"; **Figure 3.1B**). As negative controls, I used a template

(*CEN3*$^{mut}$) with mutations in the centromere-determining element III (CDEIII) region of DNA that abolishes kinetochore assembly *in vivo* by preventing the CBF3 complex from binding [75, 152]. Additionally, I used a 500 bp DNA template from within the *E. coli ampC* gene that encodes for the enzyme β-lactamase.

Because intact kinetochores have been measured to be ~126 nm [134], I reasoned that kinetochore assembly might be sterically hindered by saturating large, 2.8 μm diameter Dynabeads with the ~84 nm DNA template. To test this, I conjugated the DNA templates to beads either before or after incubation in extract and analyzed the DNA-binding protein Ndc10 by immunoblotting. Far less Ndc10 was detected when conjugating DNA to the beads after the assembly reaction, suggesting that proteins may be binding the DNA and blocking its ability to successfully conjugate to the beads (**Figure 3.1C**).

I therefore established the following general protocol for the kinetochore assembly assay: whole cell extracts are pre-incubated with excess non-specific competitive DNA to sequester DNA-binding proteins, centromeric DNA on beads is added and incubated to allow for assembly, the beads are washed, and bound proteins are eluted and analyzed (**Figure 3.1D**). Numerous parameters were tested to optimize the reaction conditions for assembly *in vitro*, with the measurements for success being improved assembly on the *CEN3* template and reduced binding on the *CEN3*$^{mut}$ template. The results of a subset of the optimized conditions are summarized in **Table 3.1**. Factors that led to the most significant improvements in assembly will be discussed below, as they have the potential to also contribute to other cell-free biochemical assays. Optimized conditions that are specific to the assembly assay will not be discussed in detail, but include the type and concentration of competitive DNA, the ratio of beads to extract,

the temperature and duration of the assembly reaction, and the length of the centromeric DNA templates.

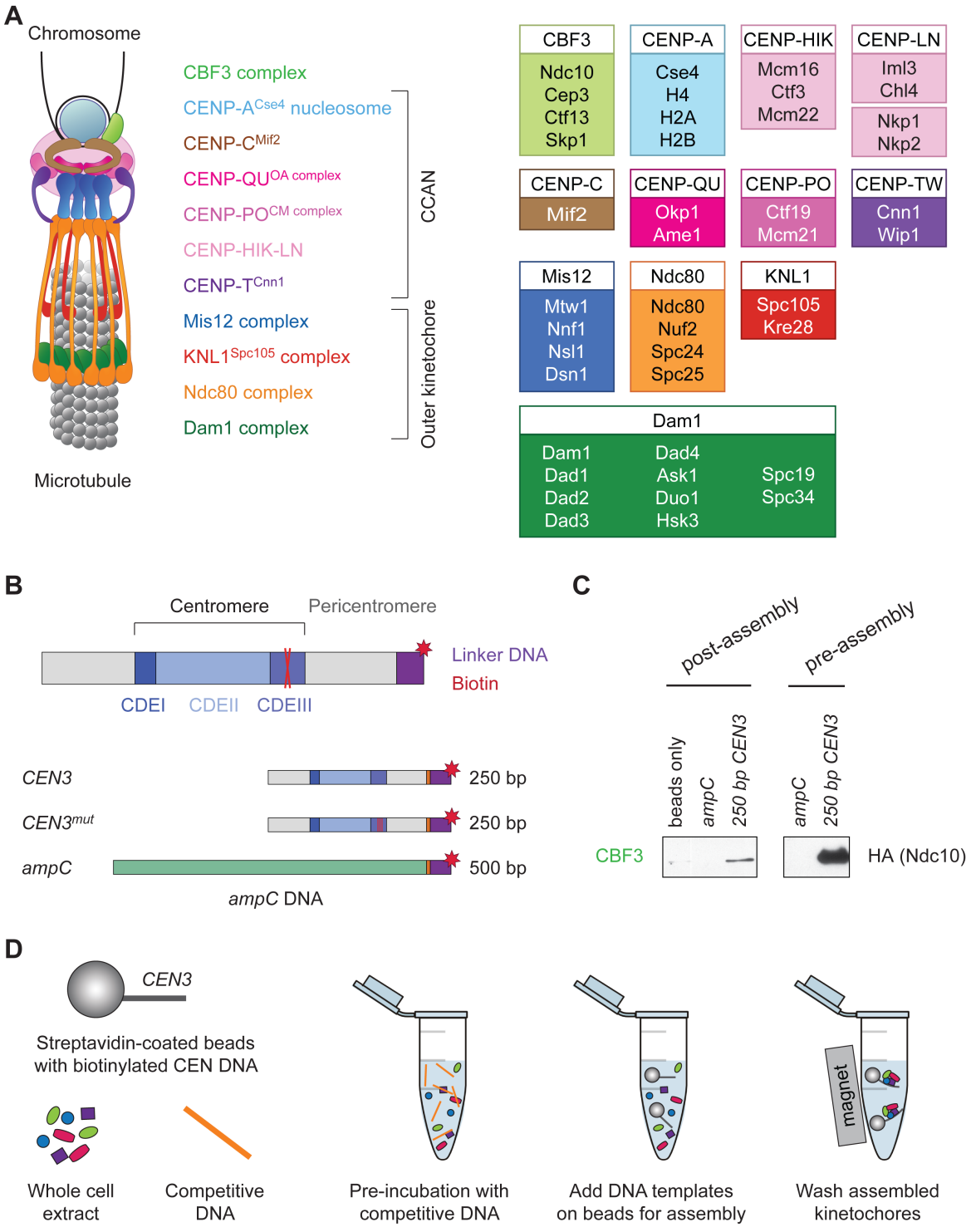


**Figure 3.1. Establishing a protocol to assemble kinetochores *in vitro***

**(A)** A schematic of the budding yeast kinetochore. The listed subcomplexes are ordered based on physical interactions from DNA-proximal to microtubule-proximal components, and the yeast proteins in each kinetochore subcomplex are shown on the right. **(B)** DNA templates for the assembly assay include 500bp from the *E. coli ampC* gene that encodes for b-lactamase (green) as a negative control, the 117 bp chromosome III centromere (*CEN3*), or a mutant *CEN3* (*CEN3*$^{mut}$) containing three point mutations in the

CBF3 binding site (red 'X'). The three centromere-determining elements (CDEs) are indicated and ~70 bp of flanking pericentromeric DNA on either side is shown (grey). The DNA templates also contain linker DNA (purple) before the biotinylation (red star) at the 3' end of the centromere. **(C)** Whole cell extract from *NDC10-3HA CSE4-3FLAG cse4D CHL4-13myc* (SBY11618) was incubated with the indicated templates. DNA templates were bound to beads either before or after the assembly reaction. Ndc10 was analyzed by immunoblotting with an a-HA antibody. **(D)** To assemble kinetochores *in vitro*, yeast whole cell extract is first pre-incubated with competitive DNA. Then, DNA templates conjugated to beads are added to the extract and incubated at room temperature for assembly. The beads are then washed and bound proteins are eluted and analyzed.

**Table 3.1. Conditions tested to optimize the kinetochore assembly assay**

Results from various assembly or extract conditions were given a rating of one to four ('+') relative to one another. Optimal conditions currently used in the assembly assay are highlighted in blue.

| Condition | Details | Assembly on *CEN3* | Cleanliness on *CEN3$^{mut}$* |
|---|---|---|---|
| Order of CEN conjugation to beads | DNA on beads pre-assembly | + | N/A |
| | DNA on beads post-assembly | ++++ | N/A |
| DNA template length | 250 bp | +++ | ++++ |
| | 500 bp (extra room on 3') | +++ | +++ |
| | 500 bp (extra room on 5') | +++ | +++ |
| | 750 bp | ++++ | ++ |
| Competitive DNA | poly dI-dC | ++++ | ++ |
| | sonicated salmon sperm DNA | ++++ | ++++ |
| CEN DNA:competitive DNA ratio | 1:1 | ++++ | ++ |
| | 1:10 | ++++ | +++ |
| | 1:30 | ++++ | ++++ |
| | 1:100 | +++ | ++++ |
| Bead:extract ratio | 1:3 | +++ | ++++ |
| | 1:10 | +++ | ++++ |
| | 1:25 | ++++ | ++++ |
| Assembly temperature | 4 °C | +++ | N/A |
| | 23 °C | ++++ | N/A |
| | 30 °C | +++ | N/A |
| Assembly duration | 30 min | ++ | N/A |
| | 60 min | ++++ | N/A |
| | 120 min | ++++ | N/A |
| Lysing method | bead beating | ++ | + |
| | freezer mill | ++++ | +++ |
| Salt of the buffer | KCl and $MgCl_2$ | + | ++++ |
| | KGlutamate and $Mg(OAc)_2$ | ++++ | ++ |
| Salt concentration | 125 mM | ++++ | ++ |
| | 175 mM | ++++ | +++ |
| | 225 mM | +++ | ++++ |
| $Mg(OAc)_2$ concentration | 4 mM | +++ | ++++ |
| | 6 mM | ++++ | +++ |
| | 9 mM | +++ | +++ |
| pH | 7.6 | ++++ | ++++ |
| | 8 | +++ | +++ |
| Phosphatase inhibitors | + | +++ | ++++ |
| | - | ++++ | ++++ |
| ATP regenerating system | + | +++ | ++++ |
| | - | ++++ | ++++ |

### 3.3.2 Improving the biochemical activity of cell extracts

Our group had previously found that the commonly used salt concentration of 300 mM would not support the purification of intact kinetochores from cells [135]. In developing the assembly assay, not only did I lower the salt concentration, but I also exchanged potassium chloride for potassium glutamate, a more gentle salt utilized in other *in vitro* assays [137, 153]. Changing this parameter resulted in the largest improvement in our assay (**Figure 3.2A**). Additionally, lowering the pH of the buffer to a more physiological level helped prevent binding to the *CEN3*$^{mut}$ template. To further improve our extract conditions, I also compared various cell lysing methods. Bead beating involves adding glass beads to cells resuspended in lysis buffer and essentially vortexing them in a 4 °C room. This method can allow extracts to warm to high temperatures, which can lead to protein denaturation. Freezer mills keep samples submerged in liquid nitrogen throughout the lysing procedure and therefore generate high quality extracts particularly suited for biochemical work. Pulverizing cells using a freezer mill resulted in far better assembly *in vitro* than when lysing using a bead beater (**Figure 3.2B**). Not only was there increased binding of several kinetochore proteins to the *CEN3* template, but there was less background binding to the negative control template.

Although yeast CENP-A$^{Cse4}$ deposition by its chaperone does not require ATP, some protein-protein interactions throughout the kinetochore are regulated by phosphorylation [82, 83, 90, 92, 126, 127, 154-156]. To ask whether ATP promotes assembly *in vitro*, I supplemented the extracts with ATP and an ATP regenerating system of creatine phosphatase and creatine phosphokinase. Kinetochore assembly was largely unaffected, even slightly reduced, by addition of the ATP regenerating system (**Figure 3.2C**). By incubating our extracts with radiolabeled ATP, [ $\gamma$-$^{32}$P] and looking for phosphorylated proteins by autoradiography, I found that our

extracts have substantial kinase activity even in the absence of the ATP regenerating system (**Supplemental Figure 3.1**). These data suggest that the additional ATP is not required for efficient assembly, so I did not include ATP and the regenerating system in subsequent assembly assays.

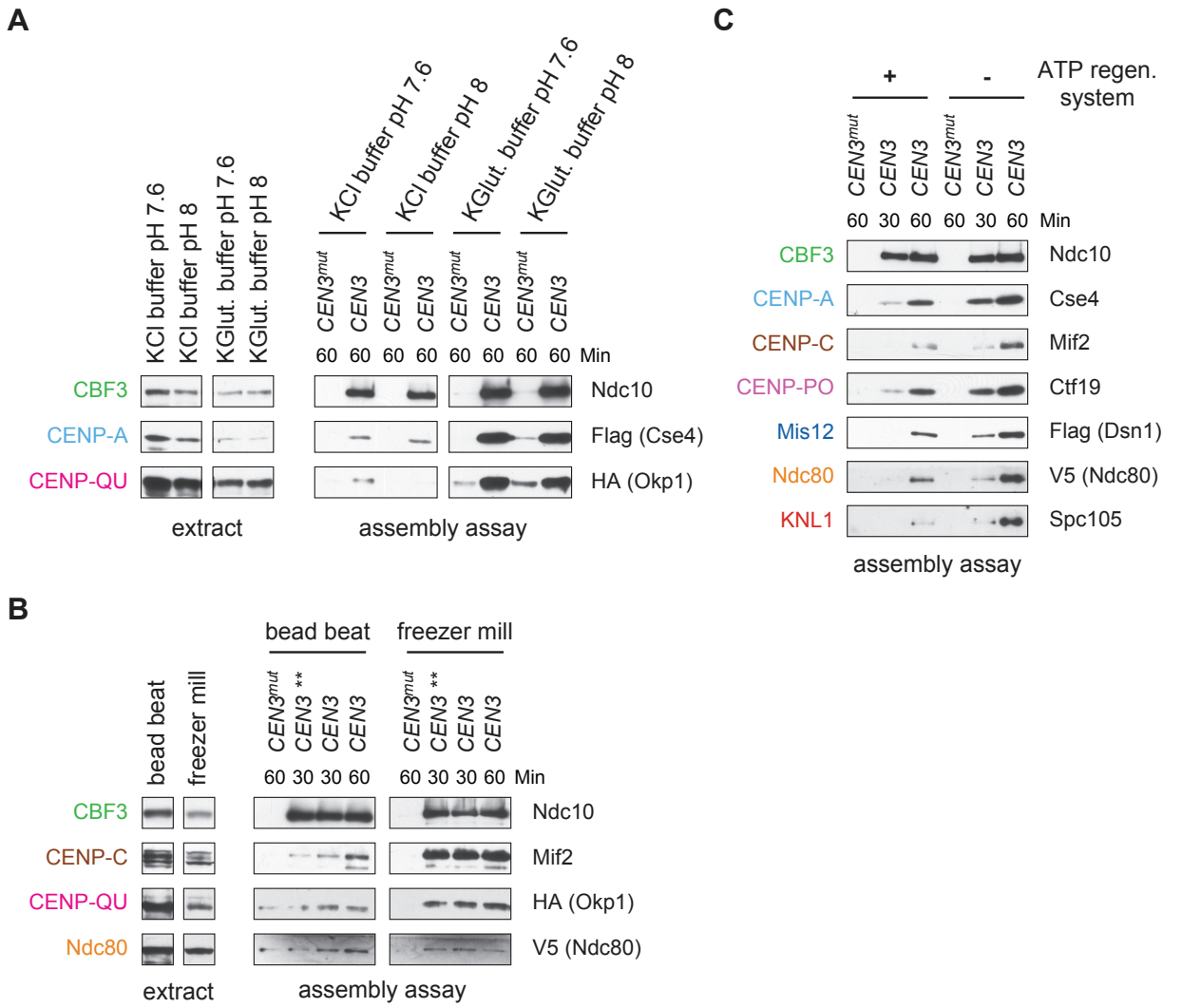


**Figure 3.2. Improving extract conditions through lysis method and buffer**
**(A)** Whole cell extract from *CSE4-3FLAG cse4D OKP1-3HA NDC80-3V5* (SBY12036) was prepared using a buffer containing either potassium chloride and magnesium chloride or potassium glutamate and magnesium acetate, each at a pH of 7.6 or 8. The extracts were used for kinetochore assembly assays for the indicated duration (in minutes). Diluted whole cell extract (left) and DNA-bound proteins (right) were analyzed by immunoblotting with the indicated antibodies. **(B)** Extract from *CSE4-3FLAG cse4D OKP1-3HA NDC80-3V5* (SBY12036) was prepared by lysing cells using a beat beater or a freezer mill. Assembly assays were performed on the indicated DNA templates and analyzed by immunoblotting. The

double asterisks next to some *CEN3* templates indicate assembly reactions that were performed using freeze-thawed extracts rather than fresh extracts. (**C**) Kinetochores were assembled from *dsn1-S240/250D-3Flag dsn1D NDC80-3V5 DAM1-9myc* (SBY12178) extracts in the presence or absence of ATP and an ATP regenerating system. Bound proteins were analyzed by the indicated immunoblots.

Finally, I attempted to improve assembly by compensating for limiting proteins. In order to achieve DNA replication *in vitro*, the pre-replication complex members Cdc6 and the Mcm2-7 replicative helicase must be purified, activated and supplemented into the reaction [137]. I wondered whether similar measures had to be taken to achieve kinetochore assembly *in vitro*. The Mis12 complex (Mis12c) is a lowly abundant in cells and was initially undetectable in the assembled kinetochores, suggesting that limiting amounts of Mis12c may inhibit outer kinetochore assembly. I used several approaches to increase Mis12c abundance, but none were able to improve the efficiency of *in vitro* assembly; I supplemented extracts with either recombinant Mis12c or native Mis12c purified from yeast, overexpressed the entire Mis12 complex in yeast, and also attempted two-step reactions, following the assembly with an incubation with purified yeast kinetochores, which are purified via a Mis12c component and are enriched for outer kinetochore (data not shown).

### 3.3.3 Assembled kinetochores span the kinetochore

With the conditions optimized and kinetochore assembly assay functioning efficiently, I first performed a detailed compositional analysis of the assembled kinetochores. An assembly reaction was performed using an extract prepared from asynchronously growing wildtype (WT) cells and analyzed by immunoblotting against representative components of most kinetochore subcomplexes. Within 30 minutes of assembly, every protein assayed bound specifically to centromeric DNA (**Figure 3.3**). Inner kinetochore components are generally saturated within 30 minutes, while outer kinetochore proteins require longer to reach saturation. To compare the

efficiency of assembly in various mutants and conditions, I analyzed assembly on *CEN3* DNA at two time points hereafter.

To further analyze the composition of the assembled particles, I performed mass spectrometry. I detected 39 out of 49 core kinetochore proteins at higher coverage levels on *CEN3* DNA relative to either *ampC* DNA or *CEN3*$^{mut}$ DNA (**Table 3.2**). In support of centromeric nucleosome assembly, CENP-A$^{Cse4}$ was specifically enriched on *CEN3* DNA. Importantly, I detected components from all known kinetochore subcomplexes on *CEN3* DNA, including the CENP-T$^{Cnn1}$ protein, indicating that both pathways to Ndc80 recruitment are present. The only proteins that were not detected are small proteins that are components of subcomplexes that were otherwise detected in the MS (for example, Dad2 in the Dam1 complex). Together, these data suggest that all kinetochore complexes assemble on centromeric DNA under the conditions I developed.

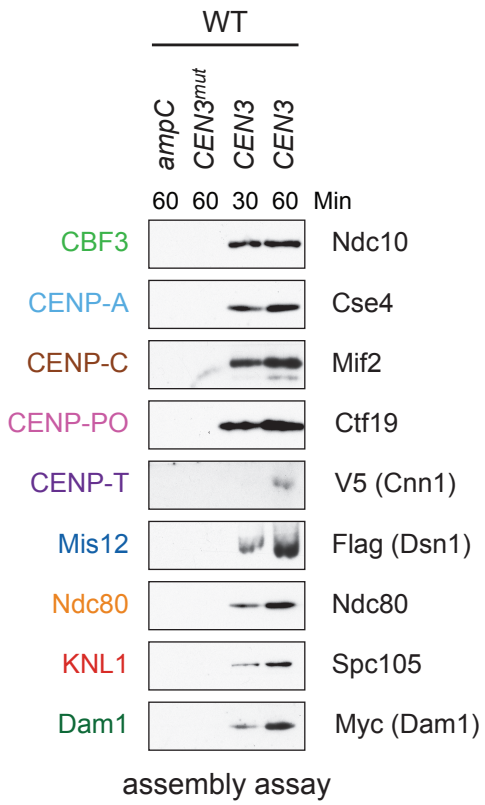


**Figure 3.3. Assembled kinetochores are centromere specific and span the entire kinetochore**
The optimized assembly assay was performed using WT whole cell extracts prepared from a *CNN1-3V5 DSN1-3Flag DAM1-9myc* strain (SBY17228) and DNA-bound proteins were analyzed by the indicated immunoblots.

**Table 3.2. Components from each of the core subcomplexes are detected on assembled kinetochores**

Kinetochores were assembled on *ampC, CEN3$^{mut}$, or CEN3* DNA from an asynchronous WT *DSN1-3Flag* (SBY14441) extract and analyzed by LC/MS/MS mass spectrometry. The table indicates the human ortholog (if applicable) of each yeast protein, the percent coverage, and the number of unique and total peptides detected from each assembly. I included the only detected microtubule-associated protein.

| | | | | *ampC* | | | *CEN3$^{mut}$* | | | *CEN3* | | |
|---|---|---|---|---|---|---|---|---|---|---|---|---|
| | **Subcomplex** | **Yeast Protein** | **Human Protein** | **% Coverage** | **Unique Peptides** | **Total Peptides** | **% Coverage** | **Unique Peptides** | **Total Peptides** | **% Coverage** | **Unique Peptides** | **Total Peptides** |
| CCAN | Cbf1 | Cbf1 | | Not present | | | 62.7 | 30 | 77 | 59.3 | 29 | 60 |
| | Cbf3 | Ndc10 | | 11.4 | 7 | 8 | 32.9 | 23 | 26 | 63.2 | 78 | 194 |
| | | Cep3 | | 3.5 | 1 | 2 | 15.3 | 8 | 9 | 34.2 | 25 | 76 |
| | | Ctf13 | | 2.7 | 1 | 1 | 18.4 | 5 | 5 | 46 | 22 | 38 |
| | | Skp1 | | 28.4 | 3 | 3 | 19.6 | 2 | 2 | 41.8 | 12 | 24 |
| | Nucleosome | Cse4 | CENP-A | 13.1 | 3 | 3 | 24.5 | 6 | 8 | 49.8 | 10 | 31 |
| | | Hta2 | H2A | 35.6 | 7 | 20 | 35.6 | 5 | 13 | 35.6 | 6 | 19 |
| | | Htb2 | H2B | 45 | 8 | 18 | 39.7 | 7 | 29 | 39.7 | 7 | 29 |
| | | Hht1 | H3 | 5.1 | 1 | 1 | 5.1 | 1 | 1 | Not present | | |
| | | Hhf1 | H4 | 45.6 | 7 | 11 | 56.3 | 8 | 19 | 46.6 | 8 | 13 |
| | Nucleosome | Psh1 | | 3.9 | 1 | 1 | Not present | | | Not present | | |
| | Associated | Scm3 | HJURP | Not present | | | 6.3 | 1 | 1 | 28.3 | 8 | 10 |
| | CPC | Ipl1 | Aurora B | Not present | | | Not present | | | 23.7 | 8 | 10 |
| | | Sli15 | INCENP | 7 | 2 | 2 | 14.8 | 6 | 7 | 64.3 | 54 | 113 |
| | | Bir1 | Survivin | 15.1 | 10 | 11 | 22.6 | 14 | 17 | 59.2 | 70 | 177 |
| | | Nbl1 | Borealin | Not present | | | Not present | | | 76.7 | 6 | 11 |
| | Mif2 | Mif2 | CENP-C | Not present | | | 9.7 | 4 | 4 | 58.7 | 29 | 39 |
| | OA | Okp1 | CENP-Q | Not present | | | 20.9 | 7 | 9 | 42.6 | 21 | 34 |
| | | Ame1 | CENP-U | Not present | | | 20.4 | 5 | 6 | 61.4 | 22 | 41 |
| | CM | Ctf19 | CENP-P | Not present | | | 6.8 | 2 | 2 | 44.7 | 21 | 31 |
| | | Mcm21 | CENP-O | Not present | | | 10.3 | 3 | 4 | 65.8 | 26 | 39 |
| | Iml3 | Iml3 | CENP-L | Not present | | | Not present | | | 60.8 | 13 | 19 |
| | | Chl4 | CENP-N | Not present | | | 7.9 | 3 | 3 | 37.1 | 16 | 19 |
| | | Nkp1 | | Not present | | | 26.9 | 4 | 6 | 57.6 | 17 | 28 |
| | | Nkp2 | | Not present | | | 15 | 2 | 4 | 55.6 | 7 | 10 |
| | Ctf3 | Mcm16 | CENP-H | Not present | | | 22.7 | 2 | 3 | 48.6 | 7 | 11 |
| | | Ctf3 | CENP-I | Not present | | | 5.3 | 3 | 3 | 23.7 | 17 | 27 |
| | | Mcm22 | CENP-K | Not present | | | 25.5 | 3 | 4 | 81.6 | 18 | 27 |
| | Cnn1 | Cnn1 | CENP-T | Not present | | | Not present | | | 45.7 | 13 | 18 |
| | | Wip1 | CENP-W | Not present | | | Not present | | | 39.3 | 2 | 2 |
| | | Mhf1 | CENP-S | 48.9 | 4 | 4 | 48.9 | 3 | 7 | 40 | 2 | 5 |
| | | Mhf2 | CENP-X | 43.8 | 4 | 8 | 47.5 | 4 | 6 | 28.8 | 3 | 4 |
| Outer Kinetochore | Mtw1 | Mtw1 | Mis12 | Not present | | | Not present | | | 22.8 | 4 | 4 |
| | | Nnf1 | PMF1 | Not present | | | Not present | | | 13.9 | 2 | 2 |
| | | Nsl1 | Nsl1 | Not present | | | Not present | | | 24.1 | 3 | 3 |
| | | Dsn1 | Dsn1 | Not present | | | Not present | | | 7.3 | 2 | 2 |
| | Ndc80 | Ndc80 | HEC1 | Not present | | | Not present | | | 28.4 | 15 | 16 |
| | | Nuf2 | NUF2 | Not present | | | Not present | | | 32.8 | 12 | 13 |
| | | Spc24 | SPC24 | Not present | | | Not present | | | 57.3 | 8 | 8 |
| | | Spc25 | SPC25 | Not present | | | Not present | | | 27.1 | 5 | 5 |
| | Spc105 | Spc105 | KNL1 | Not present | | | Not present | | | 5 | 3 | 3 |
| | | Kre28 | Zwint1 | Not present | | | Not present | | | Not present | | |
| | Dam1 | Dam1 | | Not present | | | Not present | | | 10.8 | 2 | 2 |
| | | Dad1 | | 26.6 | 1 | 1 | 26.6 | 1 | 2 | 26.6 | 1 | 1 |
| | | Dad3 | | Not present | | | Not present | | | Not present | | |
| | | Ask1 | | Not present | | | Not present | | | 8.2 | 1 | 1 |
| | | Duo1 | | Not present | | | Not present | | | 7.3 | 1 | 1 |
| | | Hsk3 | | 15.9 | 1 | 1 | 15.9 | 1 | 1 | 15.9 | 1 | 1 |
| | | Spc19 | | Not present | | | Not present | | | 8.5 | 1 | 1 |
| | | Spc34 | | Not present | | | Not present | | | 4.7 | 1 | 2 |
| | | Dad2 | | Not present | | | Not present | | | Not present | | |
| | | Dad4 | | Not present | | | Not present | | | Not present | | |
| Microtubule-Associated Proteins | MAPs | Stu2 | CHTOG | 3.5 | 2 | 2 | Not present | | | Not present | | |

### 3.3.4 Kinetochore assembly *in vitro* is a hierarchical process that depends upon CBF3

I next asked whether the assembly assay reflected requirements *in vivo*. Kinetochore assembly is initiated by the binding of the CBF3 complex to CDEIII, which facilitates the deposition of CENP-A$^{Cse4}$ [46, 76]. All kinetochore proteins except Cbf1, which binds directly to CDEI [72, 73], require the Ndc10 component of the CBF3 complex for their localization *in vivo* [157]. I therefore tested the requirement for CBF3 by performing the assembly assay with extracts prepared from WT cells and an *ndc10-1* temperature sensitive mutant. Similar to the negative controls, the assembly reaction was completely inhibited on the *CEN3* DNA in the *ndc10-1* extracts (**Figure 3.4A**). Together, these data indicate that the assembly reaction is initiated by CBF3, consistent with the requirements for assembly *in vivo*.

Kinetochore assembly is a hierarchical process wherein inner kinetochore subcomplexes recognize and bind the centromere and recruit outer kinetochore subcomplexes [3, 158]. Because intact kinetochores can be purified from similar extracts, I reasoned that assembly *in vitro* may not be a stepwise process, but instead a simultaneous binding event of a pre-assembled, soluble kinetochore. To test this, I performed a time course of assembly and assayed components spanning from inner to outer kinetochore. Generally, outer kinetochore proteins took far longer to bind the DNA and reach maximal levels than the DNA-proximal proteins (**Figure 3.4B**). For example, the DNA-binding protein Ndc10 bound at nearly saturated levels within 10 minutes, but the microtubule-binding KNL1$^{Spc105}$ protein was not detectable until 30 minutes and requires 60 minutes to reach saturation. These data suggest that assembly *in vitro* and *in vivo* share the same fundamental feature of assembling in a stepwise manner.

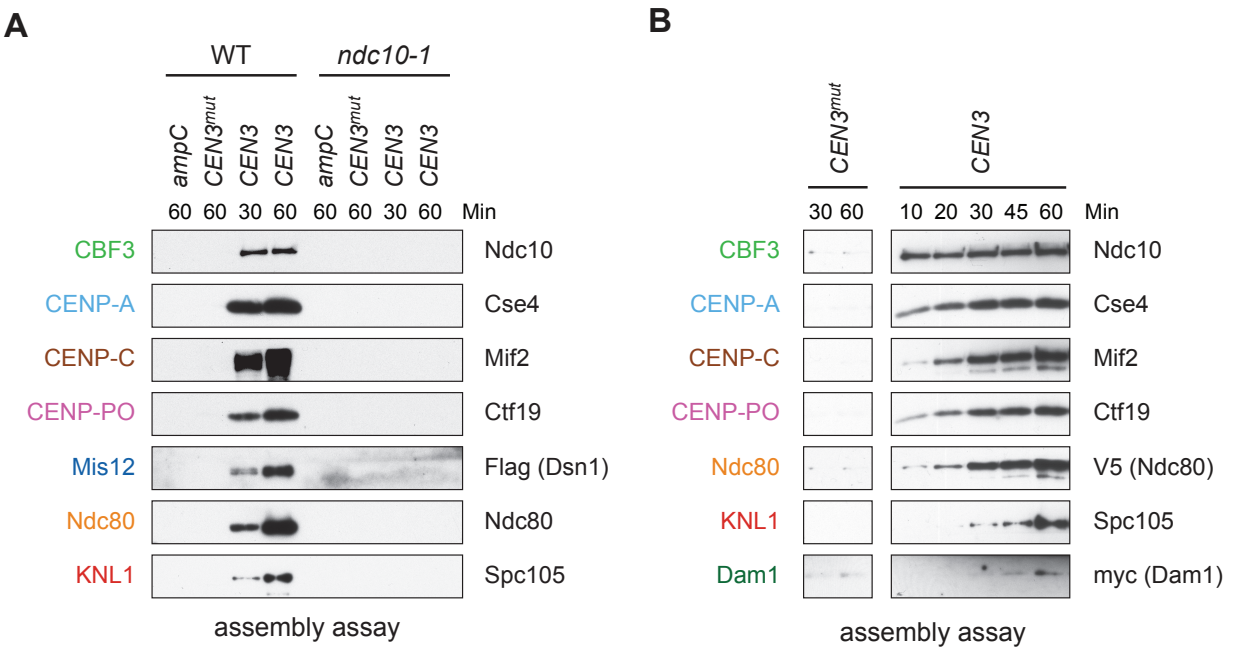


**Figure 3.4. Kinetochore assembly *in vitro* is a CBF3-dependent, stepwise process**
**(A)** Extracts from a *DSN1-6His-3Flag* strain (SBY8253) or a *DSN1-6His-3Flag ndc10-1* strain (SBY8361) shifted to the non-permissive temperature were used for assembly assays. DNA-bound proteins were analyzed by immunoblotting with the indicated antibodies. Extracts in Supplemental Figure 3.2A. **(B)** Kinetochore assembly assays were performed for the indicated durations using extract from *dsn1-S240/250D-3Flag dsn1D NDC80-3V5 DAM1-9myc* (SBY12178) and analyzed by the indicated immunoblots.

### 3.3.5 Kinetochores assemble on a single CENP-A nucleosome

Kinetochore assembly *in vivo* requires a CENP-A nucleosome, so I tested whether CENP-A$^{Cse4}$ requires its chaperone HJURP$^{Scm3}$ for deposition [46, 47, 159]. To do this, I generated cells containing an auxin-inducible degron (AID) allele of *SCM3*, *scm3-AID,* which targets the protein for proteasomal degradation when the TIR1 F-box protein and the hormone auxin are present [160]. Although I could not detect HJURP$^{Scm3}$ protein in extracts due to low intracellular levels, I concluded that the protein was degraded because the cells were inviable when plated on auxin (**Supplemental Figure 3.3**). I prepared extracts from *scm3-AID* strains (with or without *TIR1*) treated with auxin and performed the assembly assay. As expected for the

most upstream protein in the assembly pathway, Ndc10 associated with *CEN3* DNA in the presence or absence of HJURP$^{Scm3}$ (**Figure 3.5A**). However, CENP-A$^{Cse4}$ and all other CCAN components assayed no longer associated with *CEN3* when HJURP$^{Scm3}$ was depleted. This strict requirement for CENP-A$^{Cse4}$ recruitment by its chaperone suggests that CENP-A$^{Cse4}$ is forming a functional nucleosome *in vitro*.

Centromeric nucleosomes can be detected in the surrounding pericentromeric region *in vivo* [41-43], leading to debate about whether a single CENP-A$^{Cse4}$ nucleosome is sufficient for kinetochore assembly [43, 161, 162]. I therefore performed the assembly assay using a shorter 180 bp template that contains ~30 bp of DNA on either side of the centromere. CENP-A$^{Cse4}$ levels were similar on both templates, and the entire kinetochore formed in both cases (**Figure 3.5B**). Together, these data suggest that a single, well-positioned centromeric nucleosome is sufficient for kinetochore assembly in the absence of surrounding pericentromeric DNA.

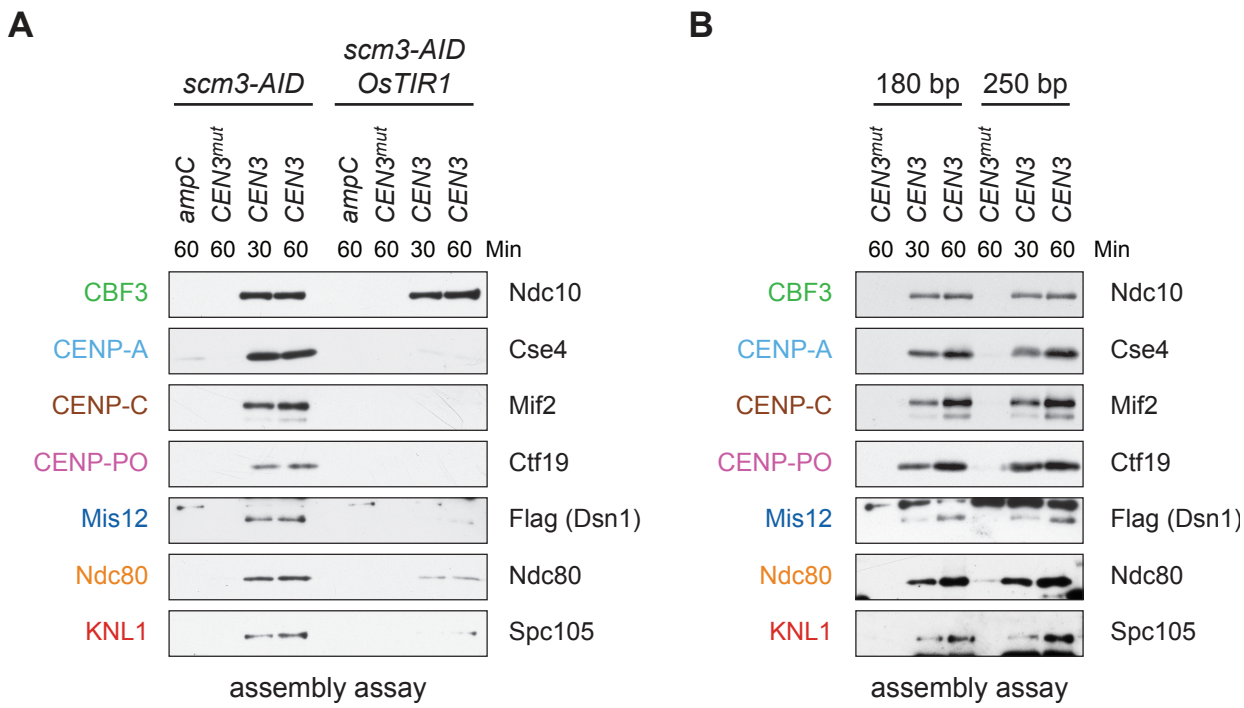


**Figure 3.5. Assembled kinetochore particles contain a single, chaperone-dependent CENP-A$^{Cse4}$ nucleosome**

**(A)** A *DSN1-3Flag scm3-EGFP-AID* strain (SBY16440) and a *DSN1-3Flag scm3-EGFP-AID OsTIR1-myc* strain (SBY16438) were treated with auxin and the extracts were used for assembly assays. DNA-bound proteins were analyzed by immunoblotting for the indicated proteins. Extracts in Supplemental Figure 3.2B. **(B)** Extract from a *DSN1-3Flag CNN1-3V5 DAM1-9myc* (SBY17228) strain was used for assembly assays with 180 bp or 250 bp centromeric DNA templates and DNA-bound proteins were analyzed by the indicated immunoblots.

### 3.3.6 Assembly *in vitro* is regulated by the cell cycle and phosphorylation

Kinetochore assembly is regulated during the cell cycle and occurs during S phase in budding yeast [103, 104], although it isn't clear whether this reflects a requirement for active DNA replication or another S phase event. During mitosis, CENP-T$^{Cnn1}$ levels peak at kinetochores due to phosphoregulation [91, 126]. To test whether the assembly assay is subject to cell cycle regulation, WT cells were grown asynchronously or arrested in G1, S phase, or mitosis, and the extracts were used for *in vitro* assembly assays. Assembly is least efficient in extracts from cells arrested in G1 and most efficient in S phase and mitosis (**Figure 3.6A**),

consistent with cell cycle regulation that occurs *in vivo*. As expected, the CENP-$T^{Cnn1}$ pathway is noticeably enhanced in kinetochores assembled from mitotic extracts. I also note that there appears to be a preference for the assembly of slower-migrating forms of CENP-$C^{Mif2}$ during S phase and mitosis, which may reflect post-translational modifications.

A conserved mitotic phosphorylation event that promotes kinetochore assembly is Aurora B-mediated phosphorylation of Dsn1, which promotes the interaction between Mis12c and the inner kinetochore protein CENP-$C^{Mif2}$ [82, 83, 154-156]. To test the effects of this phosphorylation on kinetochore assembly *in vitro*, I made extracts made from a *dsn1-S240D, S250D* (*dsn1-2D*) phosphomimetic mutant [154]. While the innermost CCAN proteins were present at equivalent levels, the *dsn1*-2D assembled kinetochores showed a strong enrichment for outer kinetochore proteins beginning with the Mis12 complex itself when assayed by immunoblotting and mass spectrometry (**Figure 3.6B** and **Table 2**). To directly quantify the difference between WT and *dsn1-2D* assembly reactions, I performed quantitative mass spectrometry (qMS) using tandem mass tag labeling [163]. Although the qMS data does not allow us to analyze the stoichiometry of components within one sample, I was able to compare relative protein levels between WT and *dsn1-2D* assembled kinetochores. Similar to the immunoblot analysis, there was a strong enrichment of outer kinetochore proteins (3- to 7-fold enrichment) in the *dsn1-2D* assembled kinetochores while the CCAN levels were similar to WT assembled kinetochores (**Figure 3.6C**). Together, these data indicate that our assembly assay *in vitro* reflects requirements known for assembly *in vivo* and is sensitive to critical post-translational modifications.

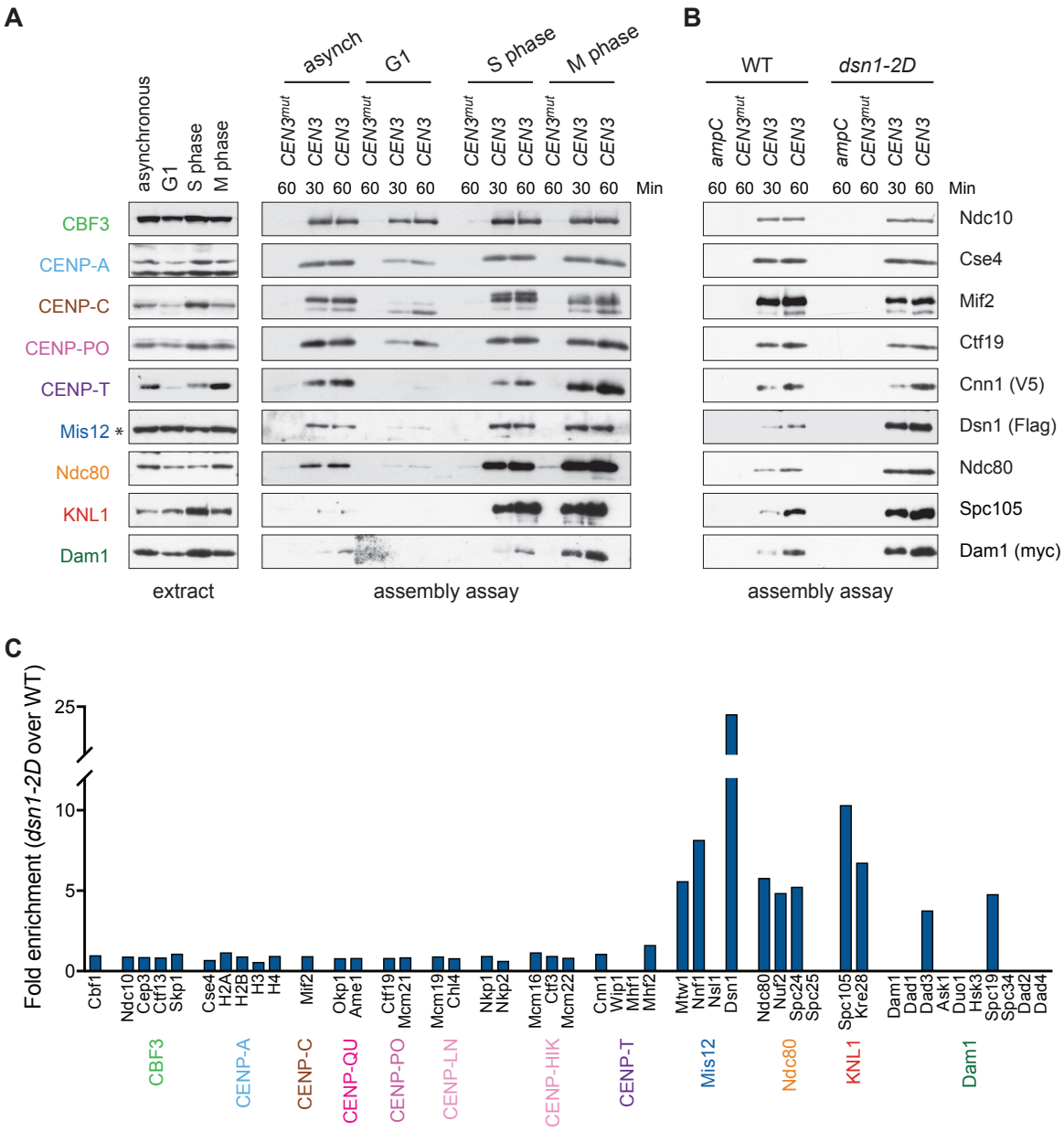


**Figure 3.6. Kinetochore assembly *in vitro* is regulated by the cell cycle and phosphorylation**
**(A)** Kinetochores were assembled using extract from WT cells (*DSN1-3Flag CNN1-3V5 DAM1-9myc* (SBY17227)) that were either asynchronously growing or arrested in G1 (with alpha factor), S phase (with hydroxyurea), or early mitosis (with benomyl). Diluted whole cell extracts and DNA-bound proteins were analyzed by immunoblotting with the indicated antibodies. **(B)** Assembly assays were performed using extracts prepared from benomyl-arrested *DSN1-3Flag CNN1-3V5 DAM1-9myc* (SBY17228) and *dsn1-2D-3Flag CNN1-3V5 DAM1-9myc* (SBY17234) strains on the indicated DNA templates and analyzed by immunoblotting with the indicated antibodies. Extracts in Supplemental Figure 3.2C. **(C)** Assembly assays were performed using extracts from *DSN1-3Flag* (SBY14441) and *dsn1-2D-3Flag* (SBY14151) on *CEN3* DNA. Assembled proteins were labeled with tandem mass tags and analyzed by quantitative mass spectrometry. For each protein, the relative abundance in *dsn1-2D* assembled kinetochores was divided by the relative abundance in WT to calculate the fold enrichment in the *dsn1-2D* assembled kinetochores.

**Table 3.3. Outer kinetochore assembly is enhanced by Dsn1 phosphorylation**

Kinetochores were assembled on the indicated DNA templates from an asynchronous *dsn1-2D-3Flag* (SBY14151) extract and analyzed by mass spectrometry as in Table 3.2. I included the detected microtubule-associated proteins.

| | | | | *ampC* | | | *CEN3$^{mut}$* | | | *CEN3* | | |
|---|---|---|---|---|---|---|---|---|---|---|---|---|
| | **Subcomplex** | **Yeast Protein** | **Human Protein** | **% Coverage** | **Unique Peptides** | **Total Peptides** | **% Coverage** | **Unique Peptides** | **Total Peptides** | **% Coverage** | **Unique Peptides** | **Total Peptides** |
| CCAN | Cbf1 | Cbf1 | | Not present | | | 65 | 27 | 53 | 59.3 | 30 | 92 |
| | Cbf3 | Ndc10 | | 21.2 | 2 | 14 | 24.5 | 19 | 22 | 58.9 | 68 | 563 |
| | | Cep3 | | 20.6 | 8 | 9 | 15.3 | 8 | 10 | 34.5 | 21 | 111 |
| | | Ctf13 | | 2.7 | 1 | 1 | 12.3 | 5 | 5 | 40.6 | 21 | 71 |
| | | Skp1 | | 8.8 | 1 | 2 | 22.2 | 3 | 3 | 44.3 | 11 | 32 |
| | Nucleosome | Cse4 | CENP-A | 20.5 | 5 | 5 | 14 | 4 | 6 | 49.3 | 10 | 34 |
| | | Hta2 | H2A | 35.6 | 5 | 13 | 35.6 | 7 | 20 | 35.6 | 5 | 34 |
| | | Htb2 | H2B | 39.7 | 7 | 18 | 39.7 | 7 | 31 | 31.3 | 6 | 29 |
| | | Hht1 | H3 | Not present | | | 5.1 | 1 | 1 | Not present | | |
| | | Hhf1 | H4 | 56.3 | 9 | 11 | 56.3 | 8 | 16 | 55.3 | 8 | 22 |
| | Nucleosome | Psh1 | | 7.4 | 2 | 2 | Not present | | | Not present | | |
| | Associated | Scm3 | HJURP | Not present | | | Not present | | | 30.5 | 8 | 17 |
| | CPC | Ipl1 | Aurora B | Not present | | | Not present | | | 24.5 | 9 | 15 |
| | | Sli15 | INCENP | 11 | 4 | 5 | 21.9 | 10 | 11 | 62.6 | 61 | 221 |
| | | Bir1 | Survivin | 20.2 | 13 | 15 | 25.5 | 17 | 20 | 64.3 | 71 | 257 |
| | | Nbl1 | Borealin | 23.3 | 1 | 1 | 21.9 | 1 | 1 | 61.6 | 7 | 19 |
| | Mif2 | Mif2 | CENP-C | Not present | | | 13.7 | 5 | 5 | 55.7 | 27 | 54 |
| | OA | Okp1 | CENP-Q | Not present | | | 22.7 | 8 | 9 | 43.6 | 21 | 50 |
| | | Ame1 | CENP-U | Not present | | | 28.7 | 5 | 5 | 54.9 | 19 | 43 |
| | CM | Ctf19 | CENP-P | Not present | | | 9.8 | 3 | 3 | 42.3 | 17 | 41 |
| | | Mcm21 | CENP-O | Not present | | | 25.8 | 7 | 8 | 48.6 | 23 | 42 |
| | Iml3 | Iml3 | CENP-L | Not present | | | 15.5 | 3 | 3 | 60.8 | 13 | 28 |
| | | Chl4 | CENP-N | Not present | | | 7.2 | 3 | 3 | 29 | 12 | 21 |
| | | Nkp1 | | Not present | | | 26.5 | 4 | 6 | 58 | 18 | 35 |
| | | Nkp2 | | Not present | | | 15 | 2 | 3 | 35.9 | 5 | 14 |
| | Ctf3 | Mcm16 | CENP-H | 14.9 | 1 | 1 | 19.9 | 2 | 2 | 44.8 | 6 | 12 |
| | | Ctf3 | CENP-I | Not present | | | 4 | 2 | 2 | 13.9 | 12 | 19 |
| | | Mcm22 | CENP-K | Not present | | | 14.6 | 2 | 2 | 74.9 | 17 | 34 |
| | Cnn1 | Cnn1 | CENP-T | Not present | | | Not present | | | 27.1 | 8 | 11 |
| | | Wip1 | CENP-W | Not present | | | Not present | | | 21.1 | 2 | 2 |
| | | Mhf1 | CENP-S | 48.9 | 3 | 4 | 48.9 | 4 | 9 | 21.1 | 2 | 2 |
| | | Mhf2 | CENP-X | 62.5 | 7 | 8 | 47.5 | 4 | 4 | 28.8 | 2 | 3 |
| Outer Kinetochore | Mtw1 | Mtw1 | Mis12 | Not present | | | 18.7 | 4 | 4 | 48.1 | 13 | 21 |
| | | Nnf1 | PMF1 | Not present | | | 16.9 | 2 | 2 | 30.3 | 10 | 13 |
| | | Nsl1 | Nsl1 | Not present | | | 15.3 | 2 | 2 | 69 | 15 | 21 |
| | | Dsn1 | Dsn1 | Not present | | | 13.4 | 4 | 4 | 39.2 | 21 | 31 |
| | Ndc80 | Ndc80 | HEC1 | Not present | | | 18.5 | 8 | 9 | 56.4 | 37 | 63 |
| | | Nuf2 | NUF2 | Not present | | | 15.7 | 6 | 6 | 51 | 27 | 42 |
| | | Spc24 | SPC24 | Not present | | | 38.5 | 4 | 5 | 63.4 | 12 | 26 |
| | | Spc25 | SPC25 | Not present | | | 8.1 | 1 | 1 | 37.6 | 8 | 10 |
| | Spc105 | Spc105 | KNL1 | Not present | | | 3.1 | 2 | 2 | 45.9 | 41 | 60 |
| | | Kre28 | Zwint1 | Not present | | | 8.3 | 2 | 3 | 29.4 | 7 | 11 |
| | Dam1 | Dam1 | | Not present | | | Not present | | | 21.6 | 5 | 6 |
| | | Dad1 | | 26.6 | 1 | 1 | 26.6 | 1 | 1 | 37.2 | 2 | 4 |
| | | Dad3 | | Not present | | | Not present | | | 29.8 | 2 | 3 |
| | | Ask1 | | Not present | | | Not present | | | 21.2 | 3 | 4 |
| | | Duo1 | | Not present | | | Not present | | | 18.2 | 4 | 4 |
| | | Hsk3 | | 15.9 | 1 | 1 | 15.9 | 1 | 1 | 15.9 | 1 | 1 |
| | | Spc19 | | Not present | | | Not present | | | 30.3 | 4 | 6 |
| | | Spc34 | | Not present | | | Not present | | | 31.5 | 6 | 11 |
| | | Dad2 | | Not present | | | Not present | | | Not present | | |
| | | Dad4 | | Not present | | | Not present | | | Not present | | |
| Microtubule-Associated Proteins | MAPs | Stu2 | CHTOG | Not present | | | Not present | | | 33.6 | 23 | 31 |
| | | Bim1 | | Not present | | | Not present | | | 17.7 | 4 | 5 |
| | | Slk19 | | Not present | | | Not present | | | 1.6 | 1 | 1 |
| | | Bik1 | | Not present | | | Not present | | | 10 | 3 | 4 |

### 3.3.7 Phosphoregulation of kinetochore assembly

Because the *dsn1-2D* mutant had such a striking impact on outer kinetochore assembly, I sought to identify additional, novel phosphoregulated binding events throughout the kinetochore that I could exploit to further improve assembly. To globally test the role of phosphorylation in kinetochore assembly, I treated *dsn1-2D* extracts with lambda phosphatase to remove phosphorylation prior to assembly. I also treated assembled *dsn1-2D* kinetochores with lambda phosphatase post-assembly to analyze the effect on kinetochore stability. Strikingly, only the DNA-binding Ndc10 protein is able to assemble when extracts have been dephosphorylated (**Figure 3.7A**). *Dsn1-2D* assembled kinetochores are also highly destabilized when treated with lambda phosphatase, but are stable when incubated with phosphatase inhibitors. Unlike with the pre-treated extracts, this destabilization begins with CENP-C$^{Mif2}$, while CENP-A$^{Cse4}$ remains stably bound to the centromere. This suggests that CENP-A$^{Cse4}$ may require phosphorylation for its deposition, but not to remain at the centromere once bound. These data also suggest that there may be phosphorylation throughout the kinetochore that promotes its assembly and/or stability. Certainly, the binding of CENP-A$^{Cse4}$ and CENP-C$^{Mif2}$ appears to be phosphoregulated.

Aurora B$^{Ipl1}$ is responsible for the Dsn1 phosphorylation that promotes assembly, but numerous mitotic kinases could contribute to the observed kinetochore stability. To test the contributions of various kinases to kinetochore assembly, I performed the assay using extracts from temperature sensitive mutants of Aurora B$^{Ipl1}$, the SAC protein Mps1, and the cell cycle regulator Cdk1$^{Cdc28}$ (*ipl1-1*, *mps1-1*, and *cdc28-3*). Inactivating Mps1 or Cdk1$^{Cdc28}$ had little impact on assembly, each showing slightly increased or decreased assembly efficiency, respectively (**Figure 3.7B**). Preventing Aurora B$^{Ipl1}$ phosphorylation resulted in the strongest defect in kinetochore assembly *in vitro*, particularly of the CENP-C$^{Mif2}$ and CENP-A$^{Cse4}$ proteins,

which are reported substrates of Aurora $B^{Ipl1}$ phosphorylation *in vivo* [109, 164, 165]. The assembly of $KNL1^{Spc105}$ is also reduced, which could be a result of direct phosphoregulation, or indirect regulation through reduced assembly of the more DNA-proximal components. The *ipl1-1* mutant does not inhibit assembly to the same extent as lambda phosphatase treatment, suggesting that other kinases contribute to assembly or that there was residual Aurora $B^{Ipl1}$ activity. However, inactivating Aurora $B^{Ipl1}$ had a significant impact on assembly, so I turned my attention to the Aurora $B^{Ipl1}$ kinase.

Upon improper kinetochore-microtubule attachments, Aurora B senses the lack of tension across kinetochores through a mechanism that remains controversial [166]. It phosphorylates numerous sites in the outer kinetochore, many of which have been shown to directly destabilize attachment by introducing a negative charge near the microtubule attachment interfaces [94, 167, 168]. Aurora B phosphorylation of Dsn1 is the first and only known example of Aurora B phosphorylation that functions to promote kinetochore assembly rather than destabilize microtubule attachments. Because Dsn1 assembly should be reduced in the absence of Aurora $B^{Ipl1}$ phosphorylation, inner kinetochore proteins at the centromere may be destabilized. This could explain the observed decrease of CENP-$A^{Cse4}$ and CENP-$C^{Mif2}$ in the assembled *ipl1-1* kinetochores. To determine whether Dsn1 is the only Aurora B target important for kinetochore assembly, I assembled WT and *dsn1-2D* kinetochores with and without degraded Aurora $B^{Ipl1}$-AID and analyzed the bound proteins by quantitative mass spectrometry. Outer kinetochore assembly is enhanced in *dsn1-2D* extract, as I have seen, and degrading Aurora $B^{Ipl1}$ in these cells significantly reduces outer kinetochore assembly (**Figure 3.7C**). These data indicate that Dsn1 is not the only Aurora $B^{Ipl1}$ target whose phosphorylation contributes to kinetochore assembly.

This and other mass spectrometry experiments did not provide useful phosphorylation data with which to narrow our search for key Aurora $B^{Ipl1}$ targets. However, Aurora B has a conserved consensus motif of [RK]X[**ST**][ILVST], so I employed a targeted approach to identify candidate residues [169]. I was particularly interested in inner kinetochore proteins, which do not contact the microtubules and are therefore better candidates for Aurora B substrates whose phosphorylation enhance assembly rather than destabilize kinetochore-microtubule attachment. I searched for Aurora B sites in the essential, conserved components of the CCAN. The sites I tested in CENP-$A^{Cse4}$, CENP-$C^{Mif2}$, and CENP-$U^{Ame1}$ are summarized in schematics in **Supplemental Figure 3.4**.

CENP-$A^{Cse4}$: CENP-$A^{Cse4}$ has four Aurora $B^{Ipl1}$ consensus sites (S22, S33, S40, and S105) that are phosphorylated *in vivo* [109]. Most of these sites are in its N-terminal tail, where histones are heavily regulated by post-translationally modification. Phosphorylation of these sites has been postulated to destabilize kinetochores, because the phosphomimetic mutant, *CENP-$A^{cse4}$-4D*, has a synthetic phenotype with temperature sensitive inner kinetochore mutants [109]. I found that both the phosphomimetic mutant and phosphonull mutant (to prevent phosphorylation) impaired assembly to the same extent, indicating that one or both of the mutants were hypomorphic (data not shown).

CENP-$C^{Mif2}$: CENP-$C^{Mif2}$ contains five potential sites of Aurora $B^{Ipl1}$ phosphorylation. S10 and S13 are in the Mis12 binding domain, but no phosphorylation has been reported at these sites. S54, S98, and S154 are all in an uncharacterized region. S54 and S154 are phosphorylated *in vivo* [164, 165], and there are no reports of S98 phosphorylation. I generated alleles with various combinations of the five sites mutated to mimic or block phosphorylation. Because some of these mutants were reported to be lethal or sick [165], I expressed them from an ectopic locus

and replaced the endogenous *CENP-C$^{Mif2}$* with a degron (*CENP-C$^{Mif2}$-AID*) or a temperature sensitive allele (*mif2-3*). In both cases, the low levels of non-degraded endogenous CENP-C$^{Mif2}$ somewhat confounded our results, but I found no evidence for an effect on kinetochore assembly. I also did not see a sick phenotype in any of the mutants, so integrated some of the mutants at the endogenous locus, but still did not see an effect on assembly or viability. Finally, I combined some of the mutants with a *CENP-T$^{CNN1}$* deletion to inhibit the second pathway to outer kinetochore assembly, thereby sensitizing the genetic background to defects in kinetochore assembly. The *CENP-C$^{mif2}$-S54/98A* may have impaired assembly in *cnn1Δ*, but this was difficult to interpret due to poor degradation of CENP-C$^{Mif2}$-AID (data not shown). Additionally, the *CENP-C$^{mif2}$-S54A* mutants exhibited slight temperature and benomyl sensitivity, however this was also covering the *CENP-C$^{mif2}$-AID* allele and should be tested more carefully (data not shown).

CENP-U$^{Ame1}$: CENP-U$^{Ame1}$ has one potential, unreported Aurora B$^{Ipl1}$ site, T5, which is located within the Mis12 binding domain. I assayed kinetochore assembly in the phosphomimetic and phosphonull mutants at the endogenous locus in numerous genetic backgrounds (WT, *dsn1-2D*, and *cnn1Δ*) and in mitotic arrests. However, I did not find a strong or consistent effect on assembly (data not shown).

Taken together, Aurora B contributes to kinetochore assembly, primarily through Dsn1 phosphorylation. Additional phosphorylated proteins may contribute, but these require further testing to confirm their role in kinetochore assembly.

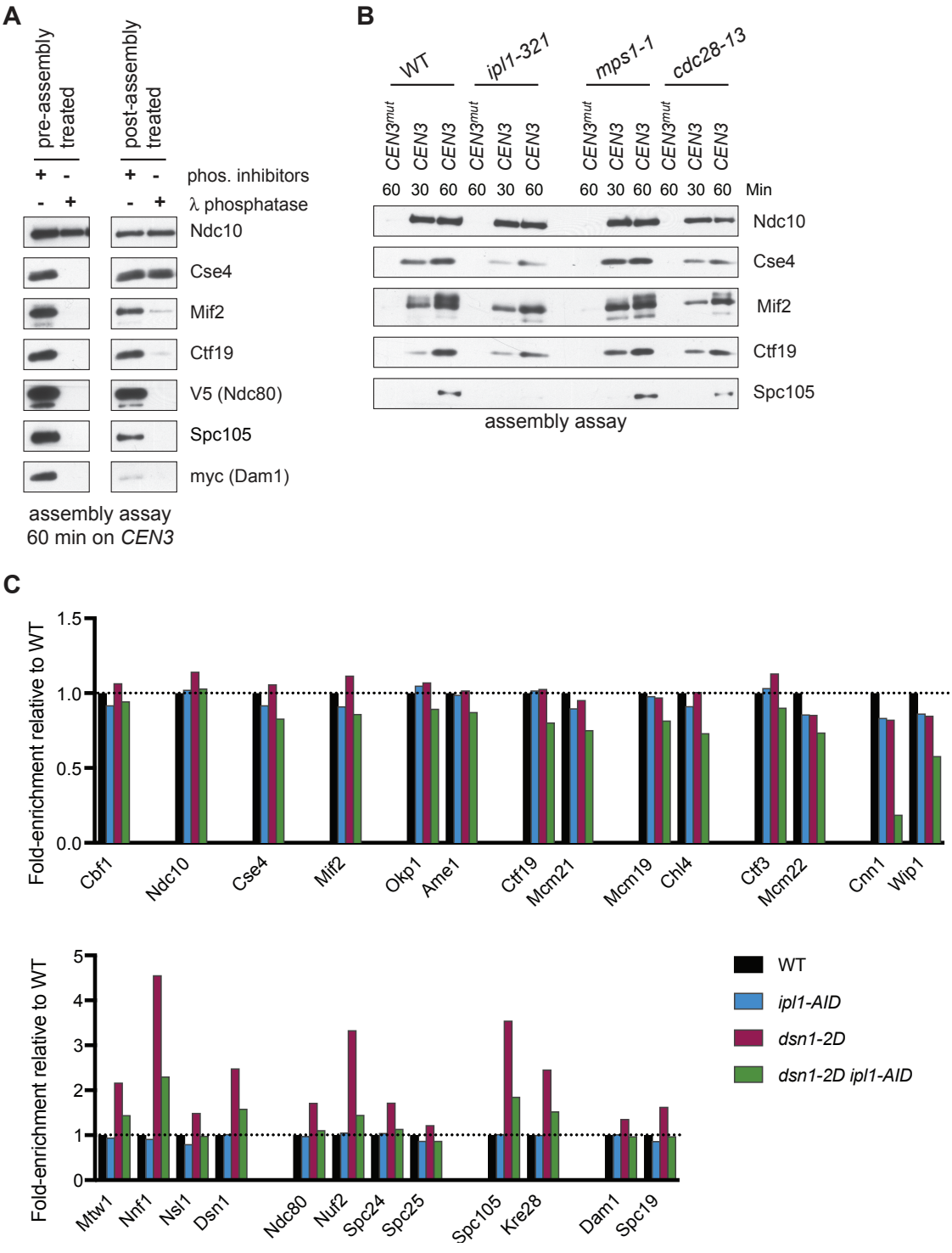


**Figure 3.7. Kinetochore assembly is regulated by phosphorylation**

**(A)** Extract from *dsn1-2D-3Flag dsn1D NDC80-3V5 DAM1-9myc* (SBY14146) was used for assembly assays. Left, extracts were treated with phosphatase inhibitors or lambda phosphatase prior to assembly. Right, assembled kinetochore were washed and incubated with phosphatase inhibitors or lambda phosphatase. Bound proteins were analyzed with the indicated immunoblots. **(B)** Temperature sensitive mutants of mitotic kinases were shifted to the non-permissive temperature and the resulting extracts were

used in assembly and analyzed by immunblotting. The strains used were: *NDC80-13myc* (SBY6992), *ipl1-321 NDC80-13myc* (SBY5426), *mps1-1 DSN1-3Flag NDC80-13myc* (SBY9205), and *cdc28-13* (SBY1891). Extracts in Supplemental Figure 3.2D. **(C)** Assembly assays were performed using extracts from IAA-treated yeast strains: *DSN1-3Flag* (SBY14441), *DSN1-3Flag ipl1-3HA-AID TIR1* (SBY14123), *dsn1-2D-3Flag* (SBY14151), and *dsn1-2D-3Flag ipl1-3HA-AID TIR1* (SBY14142). The assembled kinetochores were labeled with tandem mass tags and analyzed by quantitative mass spectrometry. For each sample, the relative abundance of each protein was divided by the relative abundance in the WT sample to calculate the fold enrichment. The dotted line indicates the level of assembly from WT extracts.

### 3.3.8 Assembled kinetochores are capable of binding microtubules

One of the most fundamental activities of the kinetochore is microtubule binding, so I next tested whether the assembled kinetochores are competent to attach to microtubules. I assembled kinetochores in extracts made from *dsn1-2D* cells, as well as extracts depleted of the major microtubule-binding component Ndc80 as a control [94, 170]. Because the Chromosomal Passenger Complex (CPC) can mediate microtubule binding when bound to centromeric DNA *in vitro* [8], I also performed the experiment in extracts depleted of INCENP$^{Sli15}$, the CPC scaffold protein [171, 172]. Although the AID-tagged proteins were significantly depleted from cells after auxin addition (**Figure 3.8A**), low levels of Ndc80 remained that were capable of assembling *in vitro* (**Figure 3.8B**). However, the residual levels were not sufficient for the proteins to perform their recruitment functions since Dam1 was absent in the *ndc80-AID* assembled kinetochores and Aurora B$^{Ipl1}$ was absent from the *sli15-AID* assembled kinetochores [171, 173, 174]. I incubated the assembled kinetochores with either taxol-stabilized microtubules or free tubulin as a negative control. Microtubules bound much more robustly than free tubulin to the assembled *dsn1-2D* kinetochores (**Figure 3.8B**). Although the single mutants did not significantly alter microtubule binding, the double *ndc80-AID sli15-AID* mutant kinetochores were not able to bind microtubules. Thus, kinetochores assembled *in vitro* are capable of binding to microtubules through the established microtubule-binding interfaces.

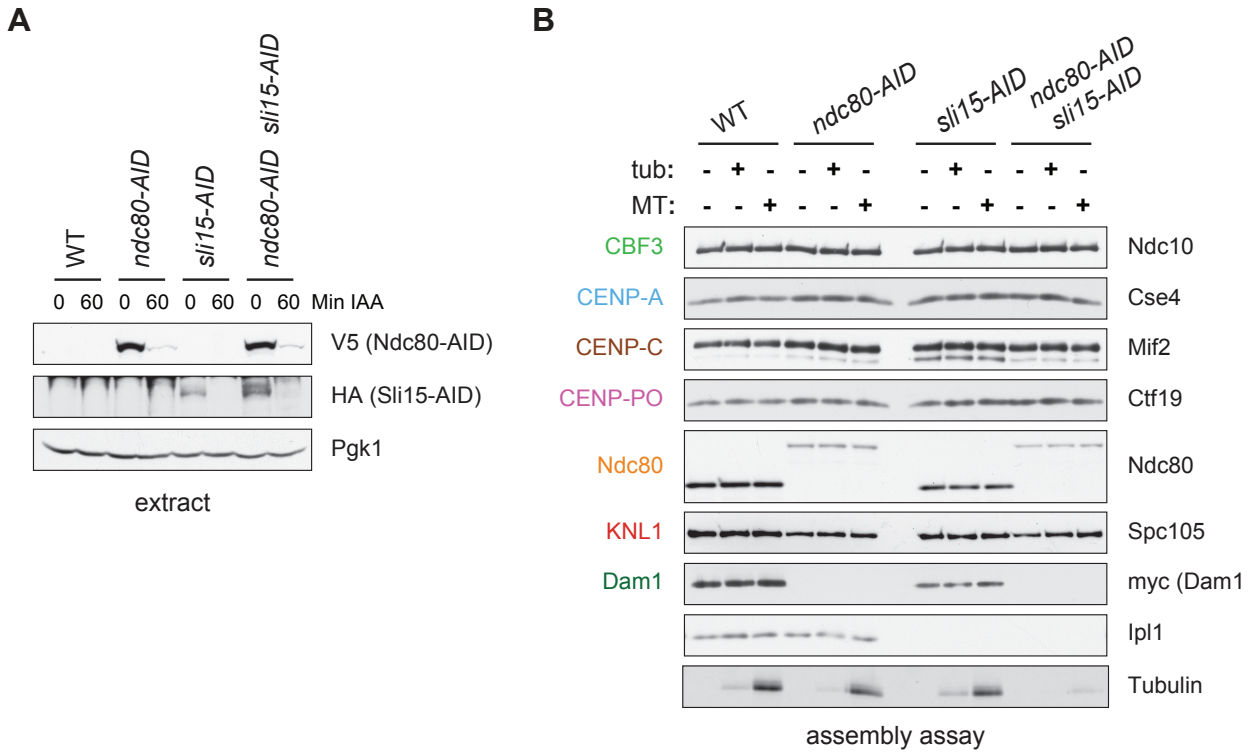


**Figure 3.8. Assembled kinetochore particles bind to microtubules**

**(A)** Samples were taken were taken before and after auxin treatment, and the Ndc80-3V5-AID and Sli15-3HA-AID proteins were analyzed by immunoblotting. **(B)** Assembly assays were performed using extracts from the following strains: *dsn1-2D-3Flag DAM1-9myc OsTIR1* (SBY14343), *dsn1-2D-3Flag DAM1-9myc OsTIR1 ndc80-3V5-AID* (SBY14336), *dsn1-2D-3Flag DAM1-9myc OsTIR1 sli15-3HA-AID* (SBY14890), and *dsn1-2D-3Flag DAM1-9myc OsTIR1 ndc80-3V5-AID sli15-3HA-AID* (SBY17238). All strains were arrested in benomyl and treated with auxin before harvesting. The assembled kinetochores were then incubated with buffer, free tubulin, or taxol-stabilized microtubules. The free tubulin and the microtubules contained alexa-647-labeled tubulin. DNA-bound proteins were analyzed by immunoblotting with the indicated antibodies, and the tubulin and microtubules were analyzed by fluorescence imaging. The Ndc80-3V5-AID protein migrates slower than untagged Ndc80. Extracts and tubulin input in Supplemental Figure 3.2E.

## 3.4 DISCUSSION

### 3.4.1 Kinetochores can be assembled *de novo*

I developed an assay using centromeric DNA and whole cell yeast extracts to assemble kinetochores *de novo*. Although similar assays incubating yeast centromeric DNA in extracts were previously developed, none achieved assembly of the outer kinetochore [8, 138, 139]. By altering the extract conditions, I was able to assemble all known kinetochore subcomplexes on a centromeric DNA template. Outer kinetochore assembly was dramatically enhanced when the extracts were made from cells expressing a conserved phospho-mimetic mutant that promotes kinetochore assembly *in vivo* [82, 83, 154-156]. In addition, the assembly assay utilizes both conserved pathways for Ndc80 recruitment, and the assembled kinetochores are competent to attach to microtubules *in vitro*.

A number of criteria indicate that the assay I developed reflects kinetochore assembly *de novo*. First, the assembly of all kinetochore proteins depends on the CBF3 complex, which is required to initiate assembly *in vivo* [76]. Second, assembly occurs in a hierarchical manner from inner to outer kinetochore [3, 81]. Third, CENP-A association with the template requires its chaperone [46, 47, 159]. Histone H2A, H2B, and H4 are also present, suggesting that a centromeric nucleosome forms on the DNA. Fourth, outer kinetochore protein recruitment depends on the inner kinetochore proteins [158, 175]. Fifth, kinetochore assembly is more efficient in extracts made from cells arrested in S phase or mitosis. Although it was previously shown that yeast kinetochores assemble during S phase, it was not clear if assembly required DNA replication [103, 104]. Because replication cannot occur in extracts without sequential kinase treatment [137], our assay shows that active DNA replication is not a strict requirement for kinetochore assembly.

### 3.4.2 A single CENP-A$^{Cse4}$ nucleosome is sufficient for kinetochore assembly

A single well-positioned CENP-A$^{Cse4}$ nucleosome occupies the CDEII region of the centromere [65, 66, 162, 176], but there are additional CENP-A$^{Cse4}$ molecules in the pericentromeric region [41-43]. This has led to controversy about the number of CENP-A nucleosomes sufficient for kinetochore assembly [177]. Here, I demonstrate that a single centromeric nucleosome is sufficient to assemble a kinetochore capable of binding to microtubules, consistent with recent biochemical reconstitutions that showed a single CENP-A nucleosome is sufficient to link some CCAN components to the KMN complex [141]. The DNA template I used can only assemble one nucleosome, and histones H2A, H2B, H4, and CENP-A are present. Therefore, surrounding pericentromeric chromatin is not required for kinetochore assembly *in vitro*, although it contributes to kinetochore function *in vivo* [178]. In the future, the use of longer DNA templates in our assembly assay will be useful for further exploring the functions of pericentromeric chromatin.

### 3.4.3 Phosphoregulation of kinetochore assembly

I found that phosphorylation plays a key role in the assembly and stability of kinetochores. Several kinases may be responsible for this stabilization, but Aurora B$^{Ipl1}$ appears to have the strongest effect. Aurora B phosphorylation is linked to destabilizing erroneous kinetochore-microtubule attachments. Because Aurora B is active when kinetochores are improperly attached to microtubules, it is intriguing that its phosphorylation can also promote assembly of kinetochore components, which may assist in establishing proper attachments. Our search for additional Aurora B$^{Ipl1}$ targets that regulate kinetochore assembly was inconclusive for a number of potential reasons. Many of these experiments were performed before I appreciated

the impact of cell cycle stage regulation on assembly *in vitro*. Any mutants that have the potential to impact growth rate or checkpoint function should be arrested to ensure that the cell cycle stage is normalized across strains. In the next chapter, I show that the CENP-$T^{Cnn1}$ pathway to Ndc80 recruitment can compensate for perturbations in the Mis12 complex pathway. Deleting *CENP-$T^{Cnn1}$* therefore generates a sensitized background to better detect defects in kinetochore assembly. Although some phosphomutants were assayed in a *cnn1Δ* background with no effect, the remaining mutants should undergo this same test. Additionally, these phosphomimetic proteins may be poor mimics of phosphorylation or the mutations may partially disrupt the proteins' function through an unrelated mechanism.

The phosphoregulation of kinetochore assembly may also be more nuanced and dynamic than I realize. Phosphorylation of Dsn1 strongly enhances assembly, suggesting that it may function as a switch to recruit more outer kinetochore as cells enter mitosis. Other phosphorylated substrates may have more subtle, non-switch-like effects and may require being tested combinatorially to detect their impact. Finally, I consider the possibility that Dsn1 is the only target of Aurora B that promotes assembly of the kinetochore, and is therefore an important regulatory switch in establishing proper microtubule attachments.

### 3.4.4 Future directions, other implications, and conclusions

One clear difference between the assembly assay and assembly *in vivo* is the duration of the process. Yeast kinetochores assemble within approximately five minutes after the replication fork passes through the centromere during S phase [103, 104]. This speed is facilitated in part by the disassembled proteins remaining locally concentrated near the centromere for rapid reassembly of the kinetochore [103]. In our *in vitro* system, not only are kinetochore proteins

dispersed in the extract, but they are also diluted with buffer and with cytoplasmic proteins, as I use whole cell rather than nuclear extracts. In the future, nuclear extracts may improve the efficiency and specificity of the assembly assay.

The development of a kinetochore assembly assay *de novo* has helped to define biochemically active extract conditions. These conditions can be applied to other *in vitro* studies as well. For example, purifying kinetochores from extracts lysed by freezer mill in the assembly buffer helps to remove contaminating spindle pole body components, which has confounded the study of kinetochore-associated motor proteins. Our assay is complementary to a previously developed assembly method using preassembled chromatin templates and frog egg extracts [140], but provides the advantage of using a genetically tractable system. A partial reconstitution system using recombinant human proteins helped define the protein specificity of CENP-A nucleosomes, but was lacking post-translational modifications, such as phosphorylation which I found as a key regulator of kinetochore assembly and stability. In the future, our assembly assay will be useful for directly examining the role of other post-translational modifications in kinetochore assembly. Our assembly assay also builds upon previous work in budding yeast, where a DNA template of a tandem repeats of the centromere was able to assemble the inner kinetochore. By using a single copy of the centromere, our kinetochore assembly assay will allow us to pursue single molecule techniques to study individual kinetochores in the future. Current studies and future prospects that will utilize the kinetochore assembly assay will be discussed in the final chapter.

## 3.5 MATERIALS AND METHODS

### 3.5.1 Yeast strain construction and microbial techniques

The *Saccharomyces cerevisiae* strains used in this study are listed in Supplementary Table 3.1. Integrated plasmids are listed in Supplementary Table 3.2. Standard genetic crosses and media were used to generate and grow yeast [149]. Gene deletions, *AID* alleles, and epitope tagged alleles were constructed at the endogenous loci by standard PCR-based integration as described in [150] and confirmed by PCR. *DSN1-3Flag* and *dsn1-2D-3Flag* were generated by PCR amplification part of the *DSN1* gene, the Flag tags, and *URA3* from plasmids pSB1113 and pSB1115, respectively. The PCR products were transformed into yeast, and the transformants were confirmed by sequencing. Point mutants were made using site-directed mutagenesis and confirmed by sequencing. By Western blot analysis, most mutant proteins were expressed at normal levels.

All liquid cultures were grown in yeast peptone dextrose rich (YPD) media. Cells were arrested in G1 or S phase by adding drug (10 μg/mL α-factor in DMSO or 0.2M hydroxyurea, respectively) to log phase cells in liquid culture for three hours until at least 90% of the cells were shmoos (α-factor) or large-budded (hydroxyurea). To arrest cells in mitosis, log phase cultures were diluted 1:1 with liquid media containing 60 μg/mL benomyl and grown for another three hours until at least 90% of cells were large-budded.

Temperature sensitive alleles (*ndc10-1, ipl1-321*, *mps1-1*, *cdc28-13*) were inactivated by diluting log phase cultures 1:1 with 37 °C liquid media and shifting the cultures to 37 °C for 2 hours.

For strains with auxin inducible degron (*AID*) alleles, all cultures used in the experiment were treated with 500 μM indole-3-acetic acid (IAA, dissolved in DMSO) for the final 60 minutes of growth (*scm3-AID, ndc80-AID,* and *sli15-AID)* or for the final two hours (*ipl1-AID*) as described in [136, 160].

Growth assays were performed by diluting log phase cultures to OD600 ~1.0 from which a 1:5 serial dilution series was made. This series was plated on YPD plates that were top-plated with either DMSO or 500 μM IAA plates and incubated at 23 °C.

### 3.5.2 Protein techniques

Whole cell extracts for immunoblotting were made by freezing cells in liquid nitrogen and resuspending in SDS buffer. Cells were lysed using glass beads and a beadbeater (Biospec Products), then clarified by centrifugation at 16,100 g for 5 minutes at 4 °C.

To test the ATP regenerating system, extracts were incubated at room temperature for 30 minutes with 8 mM ATP, 0.165 μM ATP, [ $\gamma$-$^{32}$P] (Perkin Elmer, Catalog BLU 502A), and either control Buffer L, phosphatase inhibitors (0.1 mM Na-orthovanadate, 0.2 μM microcystin, 2 mM β-glycerophosphate, 1 mM Na pyrophosphate, and 5 mM NaF), or the ATP regenerating system (46 mM creatine phosphate (Roche Catalog #621-714) and 1.6 units of creatine phosphokinase (Sigma C3755). 4x SDS sample buffer was added to the extracts. Samples were run on a NuPAGE 4-12% Bis-Tris protein gel (Invitrogen) that was subsequently dried and used for autoradiography.

### 3.5.3 Preparation of DNA templates, Dynabeads, and competitive DNA

Plasmid pSB963 was used to generate the *ampC* and *CEN3* DNA templates and pSB972 was used to generate the *CEN3*$^{mut}$ template used in this study. DNA templates were generated by PCR using a 5' primer with pericentromeric homology upstream of the centromere and a biotinylated 3' primer with linker DNA, an *EcoRI* restriction site, and pericentromeric homology downstream of the centromere. The latter primer was ordered from Invitrogen with a 5'

biotinylation. Sequences of the primers used to PCR amplify the DNA templates are listed in Supplementary Table 3.3.

The PCR product was purified using the Qiagen PCR Purification Kit and conjugated to Streptadivin-coated Dynabeads (M-280 Streptavidin, Invitrogen) for 2.5 hours at room temperature, using 1 M NaCl, 5 mM Tris-HCl (pH7.5), and 0.5 mM EDTA as the binding and washing buffer. Per 1 mg (100 μL) of beads, I conjugated 1.98 μg/mg of the 180 bp templates, 2.75 μg/mg of the 250 bp centromeric templates, or 5.5 μg/mg of the 500 bp *ampC* template to have equivalent numbers of templates on beads. After washing 3 times, the beads were stored in 10 mM HEPES-KOH and 1 mM EDTA at 4 °C until use. Competitive DNA was made by sonicating 5 μg/mL salmon sperm DNA in $dH_2O$. The sonicated salmon sperm DNA was stored at -20 °C in between uses.

### 3.5.4 Kinetochore assembly assay

For a standard kinetochore assembly *in vitro*, cells were grown in 600 mL of liquid YPD media to log phase and harvested by centrifugation. All subsequent steps were performed on ice with 4 °C buffers. Cells were washed once with $dH_2O$ with 0.2 mM PMSF, then once with Buffer L (25 mM HEPES pH 7.6, 2 mM $MgCl_2$, 0.1mM EDTA pH 7.6, 0.5 mM EGTA pH 7.6, 0.1 % NP-40, 175 mM potassium glutamate, and 15% Glycerol) supplemented with protease inhibitors (10 μg/ml leupeptin, 10 μg/ml pepstatin, 10 μg/ml chymostatin, 0.2 mM PMSF), and 2 mM DTT. Cells were resuspended in Buffer L according to the following calculation: OD of culture x number of mL of culture harvested = number of μL of Buffer L. This suspension was then snap frozen in liquid nitrogen by pipetting drops directly into liquid nitrogen. These dots were then lysed using a Freezer/Mill (SPEX SamplePrep), using 10 rounds that consisted of 2

minutes of bombarding the dots at 10 cycles per second, then cooling for 2 minutes. The subsequent powder was thawed on ice and clarified by centrifugation at 16,100g for 30 minutes at 4 °C. The resulting soluble whole cell extracts (WCE) generally have a concentration of 50-70 mg/mL. The dots, powder, and WCE were stored at -80 °C if needed. 5 μL of WCE were saved in a sodium dodecyl sulfate (SDS) buffer for immunoblot analysis.

Typically, 750 μL of whole cell extract was incubated on ice for 15 minutes with 24.75 μg sonicated salmon sperm DNA (30-fold excess competitive DNA relative to the DNA template on beads). Then, 30 μL of beads pre-conjugated with DNA were added, and the reaction was rotated constantly at room temperature for 30-90 min. The reaction was stopped on ice by addition of 3-5 times the reaction volume of Buffer L. The beads were then washed once with 1 mL Buffer L supplemented with 33 μg/mL of competitive DNA, then 3 more times with 1 mL Buffer L. Bound proteins were eluted by resuspending the beads in 75 μL of SDS buffer, boiling the beads at 100°C for 3 minutes, and collecting the supernatant. Samples were stored at -20 °C. Bound proteins were examined by immunoblotting, described below. All experiments were repeated two or more times to verify reproducibility and a representative result is reported.

### 3.5.5 Changes in earlier versions of the assay

To bind DNA templates to the beads post-assembly (as in Figure 3.1C), extracts were incubated with free DNA templates for one hour at 30 °C. Dynabeads were washed once in lysis buffer and added to the extract for three hours at 4 °C. The beads were washed and proteins were eluted as described above. For the assembly using DNA conjugated to beads, the assembly reaction was carried out at room temperature for 20 minutes.

Early assembly assays were performed using Buffer H (25 mM HEPES pH 8, 2 mM $MgCl_2$, 0.1 mM EDTA pH 8, 0.5 mM EGTA pH 8, 0.1 % NP-40, 150 mM potassium chloride, and 15% Glycerol) [135]. Some early assays also contained phosphatase inhibitors (0.1 mM Na-orthovanadate, 0.2 μM microcystin, 2 mM β-glycerophosphate, 1 mM Na pyrophosphate, and 5 mM NaF) and/or 6.5 mM ATP and the ATP regenerating system (46 mM creatine phosphate (Roche Catalog #621-714) and 1.6 units of creatine phosphokinase (Sigma C3755).

Extracts for the assembly assay were initially generated by lysing cells by bead beating. Cells were resuspended in lysis buffer as described above and lysed using glass beads and a beadbeater (Biospec Products), for 4-8 x 30 second rounds of bead beating, resting on ice for two minutes between rounds. Extracts were clarified by centrifugation at 16,100 g for 30 minutes at 4 °C.

Extracts were phosphatase treated prior to assembly by adding 1 mM $MnCl_2$, 1x Protein Metallophosphatases (PMP) buffer, and either phosphatase inhibitors or 6.6 units/μL lambda phosphatase (New England Biolabs Catalog #P0753L). The mixture was incubated for 45 minutes 30 °C before proceeding with the assembly assay protocol. For post-assembly treatment, assembled kinetochores were resuspended in 1 mM $MnCl_2$, 1x PMP buffer, and either phosphatase inhibitors or 6.6 units/μL lambda phosphatase. The mixture was incubated for 45 minutes 30 °C before washing twice with Buffer L and eluting the DNA-bound proteins in SDS buffer.

### 3.5.6 Immunological methods

Whole cell extract or samples were prepared as described above. Techniques used for SDS-PAGE gels and immunoblotting with primary and secondary antibodies are described in

2.5.5. Primary antibodies were used as follows: α-Flag M2 (Sigma-Aldrich Catalog #F3165) 1:3,000; α-myc (9E10, Covance Catalog #MMS-150R) 1:10,000; α-HA (12AC5, Roche Catalog #1-583-816) 1:10,000; α-V5 (Invitrogen Catalog #R960-25) 1:5,000; α-Pgk1 (Invitrogen Catalog #459250) 1:10,000; α-Ndc10 (OD1) 1:5,000; α-Cse4 (9536) 1:500 [151], α-Mif2 (OD2) 1:6,000; α-Ctf19 (OD10) 1:15,000; α-Ndc80 (OD4) 1:10,000; α-Spc105 (PAC4065) 1:10,000; and α-Ipl1 (OD121) 1:300. The α-Ndc10, α-Mif2, α-Ctf19, α-Ndc80, and α-Ipl1 antibodies were generous gifts from Arshad Desai. HRP conjugated secondary antibodies were detected with Pierce enhanced chemiluminescent (ECL) substrate and SuperSignal West Dura and Femto ECL (ThermoFisher Scientific). Note that the immunoblot exposures vary to best represent differences across extracts or assembly samples. The levels of proteins in input extracts and assembly samples can therefore not be directly compared.

### 3.5.7 Bulk microtubule-binding assay

Microtubules were polymerized at 37 °C for 15 minutes using a 1:50 mixture of Alexa-647-labeled and unlabeled bovine tubulin in polymerization buffer [BRB80 (80 mM PIPES, 1 mM $MgCl_2$, 1 mM EGTA, pH 6.8), 1 mM GTP, 5.7% (v/v) DMSO, and an additional 4 mM $MgCl_2$]. The polymerization was stopped with the addition of BRB80 and 10 mM taxol. Microtubules were sheared by pulling them through a 27 1/2G needle 10 times, and then pelleted by room temperature centrifugation for 10 minutes at 170,000 g. Polymerized microtubules were resuspended in BRB80 with 10 mM taxol to approximately 14.4 mM, based on the initial amount of tubulin. Serial dilutions of both the polymerized microtubules and the equivalent amount of initial tubulin mixture were run on an SDS-PAGE gel and analyzed by fluorescence imaging with a Typhoon Trio (GE Healthcare). The amount of tubulin that successfully polymerized was

estimated to ensure that comparable amounts of free tubulin and microtubules were introduced to the assembled kinetochores. Assembled and washed kinetochores on beads were resuspended in room temperature Buffer L with 0.9 mg/mL K-casein, 20 uM taxol, and either ~5 nM tubulin or polymerized microtubules. This reaction was incubated at room temperature with constant rotation for 45 minutes, then washed twice with room temperature Buffer L, resuspended in SDS buffer, and eluted by boiling. Bound tubulin or microtubules were detected by fluorescence imaging.

### 3.5.8 Mass spectrometry

Following the standard assembly protocol and washes, assembled kinetochores were washed twice with 1 mL of 50 mM HEPES pH 8, then resuspended in ~60 μL of 0.2% RapiGest SF Surfactant (Waters) in 50 mM HEPES pH 8. Proteins were eluted by gentle agitation at room temperature for 30 minutes. A small portion of the eluate was added to SDS buffer and analyzed by SDS-PAGE and immunoblotting and/or silver staining. The remaining sample was snap frozen in liquid nitrogen and sent to the Taplin Mass Spectrometry Facility for LC/MS/MS analysis, or to Thermo Fisher Scientific Center for Multiplexed Proteomics at Harvard Medical School (TCMP@HMS) for TMT labeling and MS3 analysis.

For samples sent to the Fred Hutch Proteomics Facility (**Figure 3.7C**), 5 mM TCEP was added and samples were incubated for 30 minutes at 55 °C. Then, 20 mM Iodoacetamide in 50 mM HEPES pH 8 was added and samples were incubated for 30 minutes in the dark at room temperature. Finally, trypsin was added to an approximately 50:1 protein-to-protease ratio and samples were incubated overnight at 37 °C. To label samples with Tandem Mass Tags (TMT) (Thermo Fisher Catalog #90119), 12.3 μL anhydrous acetonitrile then 8.2 μL of the TMT Label

Reagent were added to each 50 μL sample, such that the final acetonitrile concentration was approximately be 30% (v/v). The reaction was incubated for 1 hour at room temperature. Then 4 μL of 5% hydroxylamine was added to each sample and incubated for 15 minutes at room temperature to quench reaction (calculation based on total volume of reaction, rather than amount of TMT added). The differentially labeled samples were combined at equal volumes and stored at -20 °C before being sent to the Fred Hutch Proteomics Facility for MS3 analysis.

## 3.6 ACKNOWLEDGEMENTS

I am grateful to Arshad Desai for generously sharing many of the antibodies used in this study, and to Erman Akbay for assisting with mass spectrometry data analysis. I thank Phil Gafken and Yuko Ogata from the Fred Hutch Proteomics Facility, Ross Tomaino from the Taplin Mass Spectrometry Facility, and Ryan Kunz from TCMP@HMS for providing experimental advice and performing mass spectrometry. I also thank Alex Chan, a summer undergraduate HHMI EXROP student, for helping to develop the protocol for quantitative mass spectrometry. Thank you to Munira Basrai for providing the CENP-A$^{Cse4}$ phosphomutant strains and Stephan Westermann for providing a plasmid containing the *MIF2* gene. I am grateful to Niel Umbreit for generously sharing recombinant Mis12 complex. Finally, I would like to thank all members of the Biggins lab for strains and insightful discussions.

## 3.7 SUPPLEMENTAL FIGURES

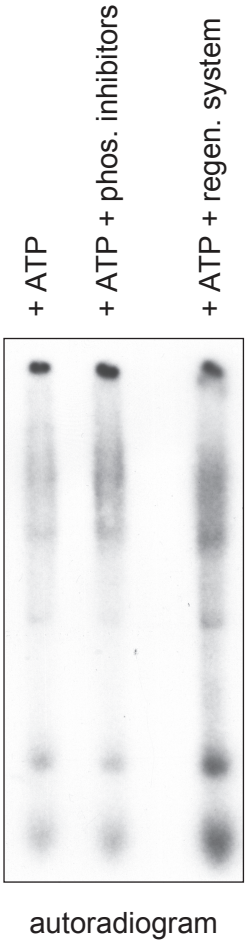


**Supplemental Figure 3.1. Cell extracts have kinase activity**
Extract from *CSE4-3FLAG cse4D OKP1-3HA NDC80-3V5* (SBY12036) was incubated with ATP, [ g-$^{32}$P] and buffer, phosphatase inhibitors, or an ATP regenerating system, as indicated. Extracts were run on an SDS-PAGE gel and analyzed by autoradiography.

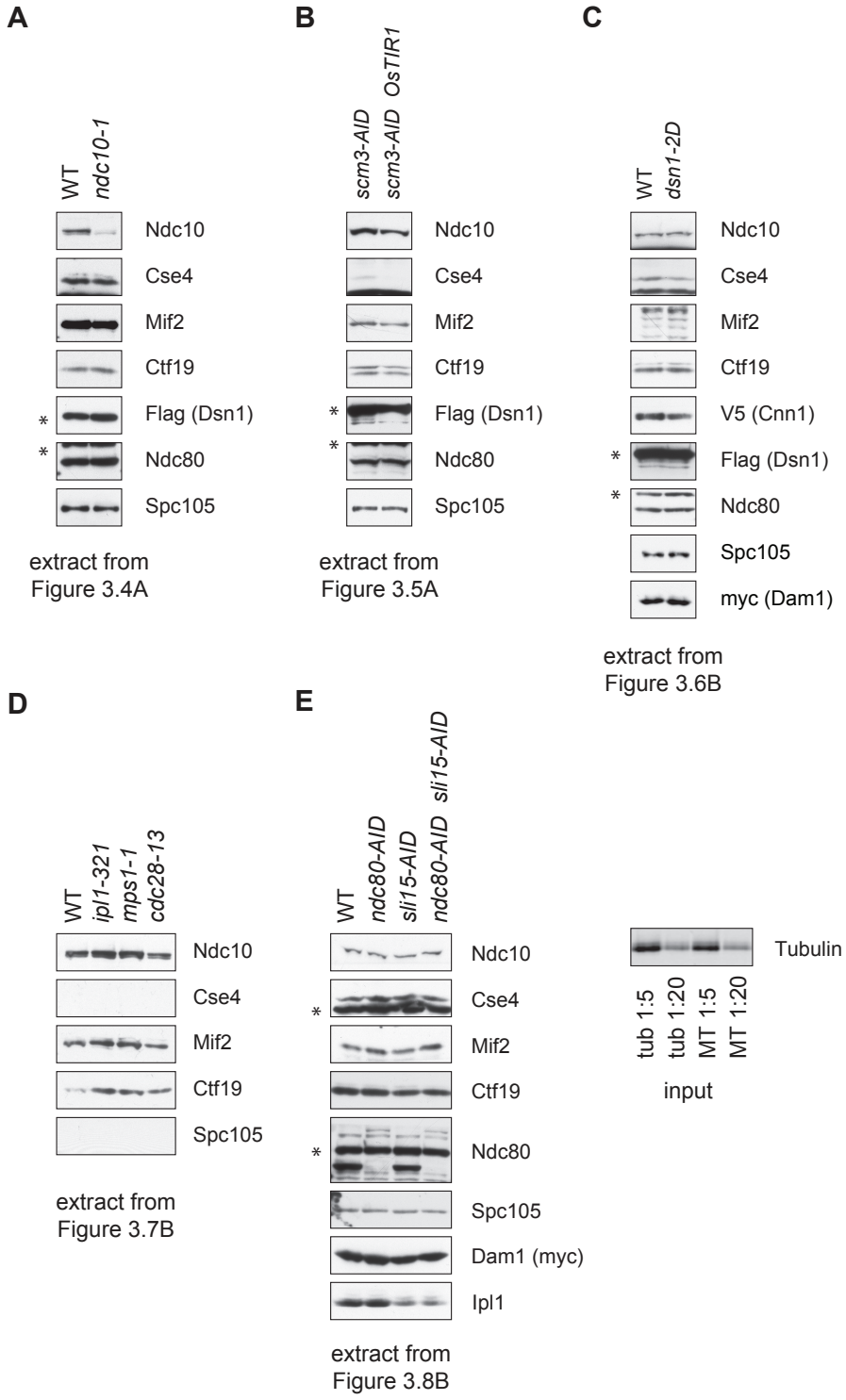


**Supplemental Figure 3.2. Whole cell extracts from selected figures**
Whole cell extracts were immunoblotted with the indicated antibodies from experiments **(A)** Figure 3.4A, **(B)** Figure 3.5A, **(C)** Figure 3.6B, **(D)** Figure 3.7B, and **(E)** Figure 3.8B. In **(E),** free tubulin and microtubule inputs are loaded at 1:5 and 1:20 of the amount introduced to assembled kinetochores.

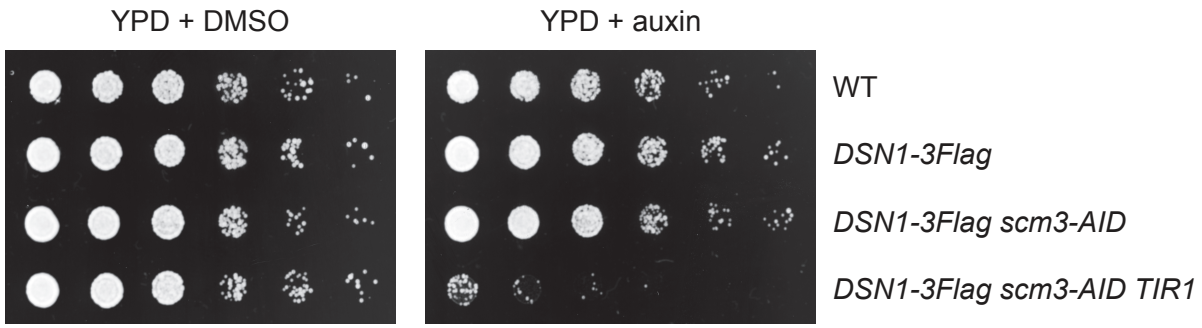


**Supplemental Figure 3.3. Degradation of HJURP$^{Scm3}$ is lethal to cells**
The Scm3-AID protein is degraded in the presence of both auxin and OsTIR1, resulting in lethality. Saturated cultures were serial diluted and plated on the indicated media. The strains used are WT (SBY4), *DSN1-3Flag* (SBY14441), *DSN1-3Flag scm3-EGFP-AID* (SBY16440), and *DSN1-3Flag scm3-EGFP-AID OsTIR1-myc* (SBY16438).

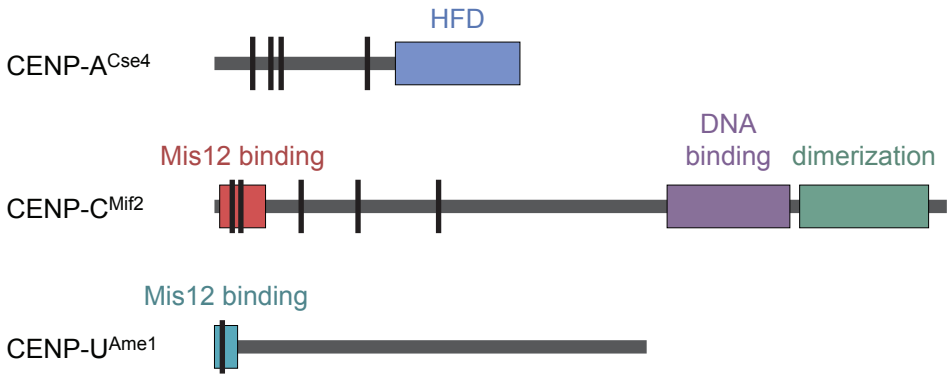


**Supplemental Figure 3.4. Testing other candidates for Aurora B$^{Ipl1}$ phosphorylation**
A schematic of the candidate Aurora B target proteins and their functional domains. The reported or predicted sites of Aurora B phosphorylation that I tested are indicated with black lines.

## 3.8 SUPPLEMENTAL TABLES

**Supplemental Table 3.1. Yeast strains used in this chapter**
Complete genotypes of the *Saccharomyces cerevisiae* strains used are listed along with the strain number to reference. All strains are isogenic with W303.

| Strain | Genotype | Integrated plasmids |
|---|---|---|
| SBY4 | *MATα ura3-1 leu2,3-112 his3-11 trp1-1 ade2-1 LYS2 can1-100 bar1-1* | |
| SBY1891 | *MATα ura3-1 leu2,3-112 his3-11 trp1-1 ade2-1 LYS2 can1-100 bar1-1 cdc28-13* | |
| SBY5426 | *MATa ura3-1 leu2,3-112 his3-11 trp1-1 ade2-1 LYS2 can1-100 bar1-1 NDC80-13myc:KanMX ipl1-321* | |
| SBY6992 | *MATa ura3-1 leu2,3-112 his3-11 trp1-1 ade2-1 LYS2 can1-100 bar1-1 NDC80-13myc:KanMX* | |
| SBY8253 | *MATa ura3-1 leu2,3-112 his3-11 trp1-1 ade2-1 LYS2 can1-100 bar1-1 DSN1-6His-3Flag:URA3* | |
| SBY8361 | *MATa ura3-1 leu2,3-112 his3-11 trp1-1 ade2-1 LYS2 can1-100 bar1-1 DSN1-6His-3Flag:URA3 ndc10-1* | |
| SBY9205 | *MATa ura3-1 leu2,3-112 his3-11 trp1-1 ade2-1 LYS2 can1-100 bar1-1 DSN1-3Flag:KanMX NDC80-13myc:KanMX mps1-1* | |
| SBY11618 | *MATa ura3-1::CSE4-3Flag:URA3 leu2,3-112 his3-11 trp1-1 ade2-1 LYS2 can1-100 bar1-1 cse4D::KanMX NDC10-3HA:URA3 CHL4-13myc:HIS3* | pSB1067 |
| SBY12036 | *MATα ura3-1::CSE4-3Flag:URA3 leu2,3-112 his3-11 trp1-1 ade2-1 LYS2 can1-100 bar1-1 cse4Δ::KanMX OKP1-3HA:HIS3 NDC80-3V5:HIS3* | pSB1067 |
| SBY12178 | *MATa ura3-1::dsn1-2D(S240/250D)-3Flag:URA3 leu2,3-112 his3-11 trp1-1 ade2-1 lys2- can1-100 bar1-1 dsn1D::KanMX NDC80-3V5:HIS3 DAM1-9myc:TRP1* | pSB1115 |
| SBY13958 | *MATα ura3-1 leu2,3-112::pGPD1-TIR1:LEU2 his3-11 trp1-1 ade2-1 LYS2 can1-100 bar1-1 ip1-3HA-IAA17:KanMX* | pSB2271 |
| SBY14086 | *MATα ura3-1 leu2,3-112::pGPD1-TIR1:LEU2 his3-11 trp1-1 ade2-1 LYS2 can1-100 bar1-1* | pSB2271 |
| SBY14093 | *MATα ura3-1 leu2,3-112 his3-11 trp1-1 ade2-1 LYS2 can1-100 bar1-1 ip1-3HA-IAA17:KanMX* | |
| SBY14123 | *MATα ura3-1 leu2,3-112::pGPD1-TIR1:LEU2 his3-11 trp1-1 ade2-1 LYS2 can1-100 bar1-1 DSN1-3Flag:URA3 ip1-3HA-IAA17:KanMX* | pSB2271 |
| SBY14142 | *MATα ura3-1 leu2,3-112::pGPD1-TIR1:LEU2 his3-11 trp1-1 ade2-1 LYS2 can1-100 bar1-1 dsn1-2D(S240/250D)-3Flag:URA3 ip1-3HA-IAA17:KanMX* | pSB2271 |

| | | |
|---|---|---|
| SBY14146 | *MAT**a** ura3-1 leu2,3-112 his3-11 trp1-1 ade2-1 LYS2 can1-100 bar1-1 dsn1-2D(S240/250D)-3Flag:URA3 NDC80-3V5:HIS3 DAM1-9myc:TRP1* | |
| SBY14151 | *MATα ura3-1 leu2,3-112 his3-11 trp1-1 ade2-1 LYS2 can1-100 bar1-1 dsn1-2D(S240/250D)-3Flag:URA3* | |
| SBY14336 | *MAT**a** ura3-1 leu2,3-112::pGPD1-TIR1:LEU2 his3-11 trp1-1 ade2-1 LYS2 can1-100 bar1-1 dsn1-2D(S240/250D)-3Flag:URA3 ndc80-3V5-IAA7:KanMX DAM1-9myc:TRP1* | pSB2271 |
| SBY14343 | *MAT**a** ura3-1 leu2,3-112::pGPD1-TIR1:LEU2 his3-11 trp1-1 ade2-1 LYS2 can1-100 bar1-1 dsn1-2D(S240/250D)-3Flag:URA3 DAM1-9myc:TRP1* | pSB2271 |
| SBY14441 | *MATα ura3-1 leu2,3-112 his3-11 trp1-1 ade2-1 LYS2 can1-100 bar1-1 DSN1-3Flag:URA3* | |
| SBY14890 | *MAT**a** ura3-1 leu2,3-112::pGPD1-TIR1:LEU2 his3-11 trp1-1 ade2-1 LYS2 can1-100 bar1-1 dsn1-2D(S240/250D)-3Flag:URA3 sli15-3HA-IAA17:KanMX DAM1-9myc:TRP1* | pSB2271 |
| SBY16438 | *MAT**a** ura3-1 leu2,3-112 his3-11::TIR1-myc:HIS3 trp1-1 ade2-1 LYS2 can1-100 bar1-1 DSN1-3Flag:URA3 scm3-EGFP-AID:KanMX* | pSB1934 |
| SBY16440 | *MATα ura3-1 leu2,3-112 his3-11 trp1-1 ade2-1 LYS2 can1-100 bar1-1 DSN1-3Flag:URA3 scm3-EGFP-AID:KanMX* | |
| SBY17227 | *MAT**a** ura3-1 leu2,3-112 his3-11 trp1-1 ade2-1 LYS2 can1-100 bar1-1 DSN1-3Flag:URA3 DAM1-9myc:TRP1 CNN1-3V5:KanMX* | |
| SBY17228 | *MATα ura3-1 leu2,3-112 his3-11 trp1-1 ade2-1 LYS2 can1-100 bar1-1 DSN1-3Flag:URA3 DAM1-9myc:TRP1 CNN1-3V5:KanMX* | |
| SBY17234 | *MAT**a** ura3-1 leu2,3-112 his3-11 trp1-1 ade2-1 LYS2 can1-100 bar1-1 dsn1-2D(S240/250D)-3Flag:URA3 DAM1-9myc:TRP1 CNN1-3V5:KanMX* | |
| SBY17238 | *MAT**a** ura3-1 leu2,3-112::pGPD1-OTIR1:LEU2 his3-11 trp1-1 ade2-1 LYS2 can1-100 bar1-1 dsn1-2D(S240/250D)-3Flag:URA3 ndc80-3V5-IAA7:KanMX sli15-3HA-IAA17:KanMX DAM1-9myc:TRP1* | pSB2271 |

**Supplemental Table 3.2. Plasmids used in this chapter**
The relevant genes and markers on each plasmid used are listed.

| Plasmids | Description |
|---|---|
| pSB963 | *WT CEN3, 8LacO, TRP1* |
| pSB972 | *Mutant CEN3 (CCG->AGC CEN mutant), 8 LacO, TRP1* |
| pSB1067 | *CSE4, URA3* |
| pSB1113 | *DSN1-3Flag, URA3* |
| pSB1115 | *dsn1-2D(S240/250D)-3Flag, URA3* |
| pSB1934 | *pADH1-TIR1-9myc, HIS3* (integrating) |
| pSB2271 | *pGPD1-TIR1, LEU2* (integrating) |

**Supplemental Table 3.3. Oligonucleotides used in this chapter**
The sequence and purpose of each primer used to generate DNA templates is listed.

| Primer | Sequence (5' to 3') | Purpose |
|---|---|---|
| SB3882 | biotin-GGTTCTGGTGGTTCTGGTGGTTCTGGTGAATTCAGCAATAAACCAGCCAGCCGGAA | 500 bp *ampC* template |
| SB3883 | TTTTCCAATGATGAGCACTTTTA | 500 bp *ampC* template |
| SB3878 | biotin-GGTTCTGGTGGTTCTGGTGGTTCTGGTGAATTCAAACAACCGCCGGCTTCCACCA | 250 bp *CEN3* or *CEN3mut* template |
| SB3880 | ATCAGCGCCAAACAATATGGAA | 250 bp *CEN3* or *CEN3mut* template |
| SB5521 | biotin-GGTTCTGGTGGTTCTGGTGGTTCTGGTGAATTCCCATTCAATGAAATATATATTTCTTACTATTTCT | 180 bp *CEN3* or *CEN3mut* template |
| SB5522 | GCTATTCATTGAAAAAATAGTACAAATAAG | 180 bp *CEN3* or *CEN3mut* template |

# CHAPTER 4. A kinetochore assembly assay reveals the role of the CENP-T pathway in budding yeast

## 4.1 SUMMARY

Kinetochores use two pathways to recruit the key microtubule-binding Ndc80 complex: the Mis12 complex and CENP-T. Although CENP-T has a histone-fold domain, the mechanism of CENP-T recruitment to the kinetochore and the differential contributions of the Ndc80 recruitment pathways to kinetochore function are unclear. I therefore used the kinetochore assembly assay described in Chapter 3 to address these questions and found that yeast CENP-$T^{Cnn1}$ assembles downstream of all DNA-proximal kinetochore proteins. Furthermore, although the CENP-$T^{Cnn1}$ pathway is non-essential in yeast, it becomes essential for cell viability and Ndc80c recruitment when the Mis12 pathway is crippled by defects in mitotic phosphorylation. These data suggest that CENP-$T^{Cnn1}$ can independently recruit sufficient levels of Ndc80c and ensures maximal kinetochore function at anaphase. Our assembly assay provides a method to elucidate additional regulatory events that control kinetochore assembly.

## 4.2 INTRODUCTION

In order to mediate chromosome segregation, kinetochores must establish force-bearing attachments to the spindle microtubules. The Ndc80 complex is a key microtubule-binding site within the kinetochore, because it directly mediates attachment and recruits additional attachment factors, such as the Ska complex in vertebrates and its functional ortholog Dam1 in fungi [94, 97, 170, 174, 179]. Interestingly, there are two parallel kinetochore receptors for

Ndc80c: the Mis12 complex and CENP-T [90-92, 96, 127, 128]. The Mis12 complex interacts with the KNL1 and Ndc80 complexes to create a larger network called KMN (KNL1-Mis12-Ndc80) [94]. CENP-T, a histone-fold domain containing protein, recruits Ndc80c via the same interaction surface on the Ndc80 complex that binds Mis12c [90-93]. Although Mis12c and CENP-T each contribute to Ndc80c recruitment *in vivo* [92, 127], it has been unclear why cells employ two competing receptors for the Ndc80 complex and whether the CENP-T protein is another histone variant at centromeres. Dual pathways for Ndc80 recruitment are also used in yeast, although the CENP-T ortholog, Cnn1, is not essential for viability [91, 126]. However, CENP-$T^{Cnn1}$ contributes to kinetochore function because mutants display increased chromosome loss, and the tethering of CENP-$T^{Cnn1}$ imparts partial stability to acentric minichromosomes via Ndc80 recruitment [92, 126]. In yeast, CENP-$T^{Cnn1}$ localization to kinetochores peaks in mitosis as a result of phosphoregulation [91, 126], but it is unclear why its recruitment is cell cycle regulated and whether this affects the Mis12 pathway of Ndc80 recruitment.

We have been unable to directly assay the function and regulation of the CENP-$T^{Cnn1}$ pathway, because our previously developed method to purify kinetochores from the Mis12 complex does not contain the CENP-$T^{Cnn1}$ pathway. However, in the previous chapter, I found that the assembled kinetochores include CENP-$T^{Cnn1}$. Furthermore, CENP-$T^{Cnn1}$ assembly on the centromeric template shows the same cell cycle regulation as its assembly *in vivo*, enriching during mitosis [91, 126]. I applied this assay to identify the requirements for CENP-$T^{Cnn1}$ assembly and find that it requires all other inner kinetochore subcomplexes, suggesting it is distal to the DNA. CENP-$T^{Cnn1}$ also has no detectable independent DNA-binding capability, further supporting that it does not function as a novel nucleosome at centromeres. I discovered that the CENP-$T^{Cnn1}$ pathway is required for Ndc80c recruitment and cell viability when the Mis12c

pathway is impaired by defects in conserved mitotic phosphoregulation [154-156]. CENP-T$^{Cnn1}$ is therefore a redundant Ndc80 recruitment pathway that is required to maintain kinetochore integrity throughout dynamic changes in phosphoregulation. Taken together, I have established a kinetochore assembly assay that identifies a critical function for the yeast CENP-T$^{Cnn1}$ pathway and that provides a powerful method to identify other key regulatory events required for kinetochore assembly and function in the future.

## 4.3 RESULTS

### 4.3.1 CENP-T$^{Cnn1}$ kinetochore localization is distal to centromeric DNA

A conserved feature of kinetochore assembly is the recruitment of Ndc80 via two complexes: Mis12c and CENP-T$^{Cnn1}$. The mechanism of CENP-T$^{Cnn1}$ recruitment to the kinetochore has been controversial. CENP-T$^{Cnn1}$ and its partner CENP-W have histone fold domains (HFD) and can tetramerize with two additional HFD proteins, CENP-S/X, to form a nucleosome-like structure *in vitro* [91, 128, 180]. The human proteins require their heterotetramerization and DNA-binding capabilities to assemble a functional kinetochore *in vivo* [128], leading to the model that CENP-T$^{Cnn1}$ forms a unique centromeric chromatin structure. However, CENP-T$^{Cnn1}$ localization to kinetochores requires other CCAN proteins, suggesting it may not directly bind to centromeric DNA [87-89, 129-131].

To address these issues, I used our DNA-based method to analyze the requirements for CENP-T$^{Cnn1}$ recruitment. The CCAN is composed of distinct subcomplexes and the physical interactions between them have been mapped using co-immunoprecipitation experiments [88, 91]. To map the CENP-T$^{Cnn1}$ assembly pathway on centromeric DNA, I performed the assembly assay from cells containing a representative mutant of each conserved CCAN subcomplex that

had been arrested in mitosis. CENP-T$^{Cnn1}$ is absent or severely reduced in all inner kinetochore mutants tested (**Figure 4.1A-C**), indicating that CENP-T$^{Cnn1}$ does not have independent DNA-binding properties in our assay conditions. In addition, CENP-T$^{Cnn1}$ appears to be the most distal component of the CCAN because every other subcomplex is required for its kinetochore localization (**Figure 4.1D**).

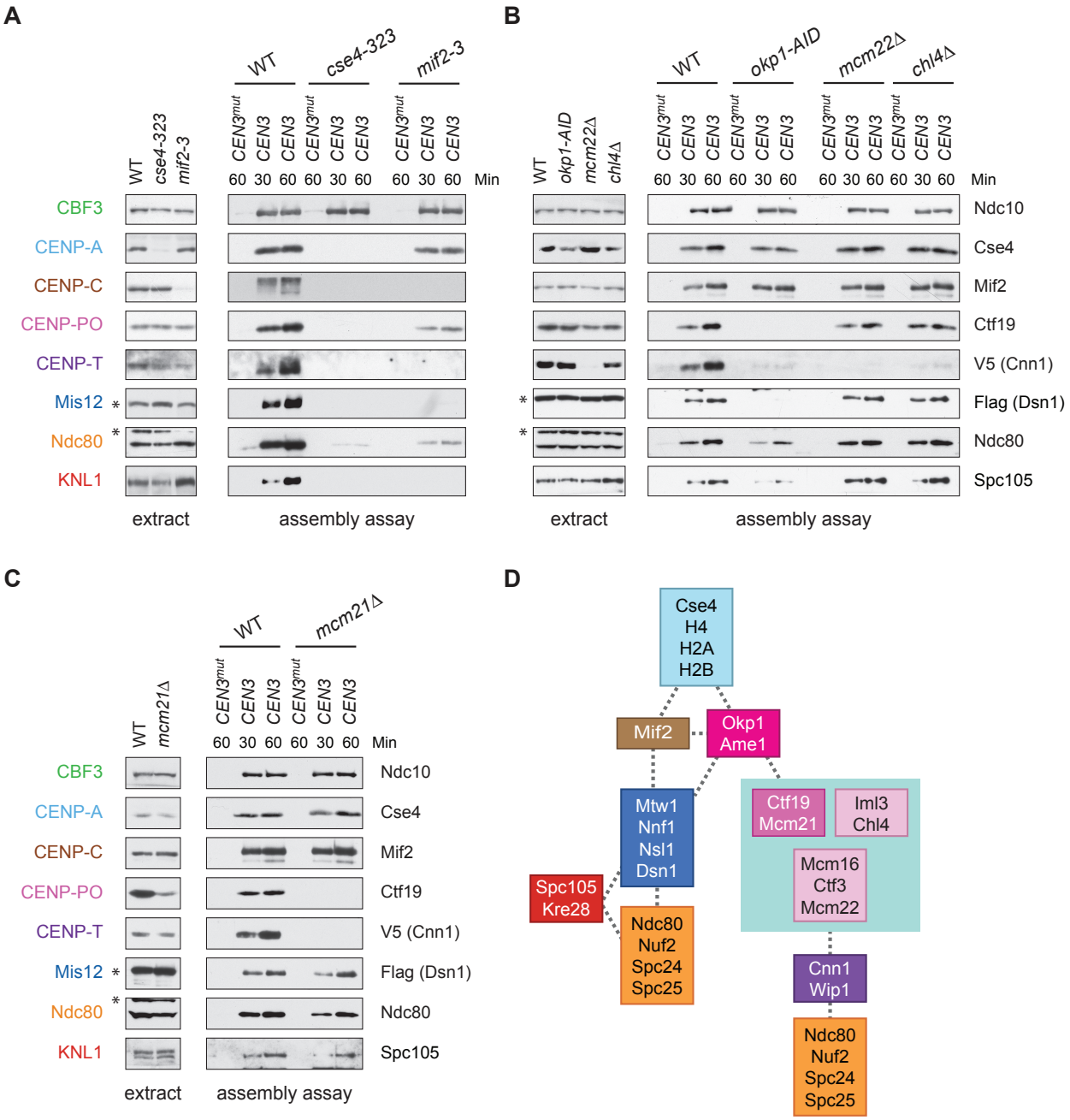


**Figure 4.1. CENP-T$^{Cnn1}$ localization to the kinetochore requires the CCAN**

**(A-C)** Assembly assays were performed on the indicated DNA templates using extracts prepared from cells arrested in benomyl. The strains used in **(A)** were also shifted to the non-permissive temperature for three hours before harvesting: *DSN1-3Flag CNN1-3V5* (SBY17230), *DSN1-3Flag CNN1-3V5 cse4-323* (SBY17770), and *DSN1-3Flag CNN1-3V5 mif2-3* (SBY17603). The strains used in **(B)** were treated with auxin for three hours before harvesting: *DSN1-3Flag CNN1-3V5* (SBY17230), *DSN1-3Flag CNN1-3V5 okp1-3V5-AID OsTIR1* (SBY17764), *DSN1-3Flag CNN1-3V5 mcm22D* (SBY17460), and *DSN1-3Flag CNN1-3V5 chl4D* (SBY17607). The strains used in **(C)** were benomyl treated only: *DSN1-3Flag CNN1-3V5* (SBY17230) and *DSN1-3Flag CNN1-3V5 mcm21D* (SBY18304). **(D)** A schematic distinguishing the proteins involved in the CENP-T$^{Cnn1}$ and Mis12 recruitment pathways.

### 4.3.2 Kinetochore assembly *in vitro* utilizes both pathways to Ndc80 recruitment

It has been unclear how CENP-T$^{Cnn1}$ facilitates kinetochore assembly in yeast, because Ndc80 levels are not noticeably reduced by the loss of CENP-T$^{Cnn1}$ *in vivo* [91, 126]. We therefore performed the assembly assay in a *cnn1Δ* extract and found that Ndc80 levels are slightly reduced, suggesting that CENP-T$^{Cnn1}$ contributes to Ndc80 recruitment (**Figure 4.2**). We next compared this to the role of Mis12c in Ndc80 recruitment by performing the assay in an extract from which *dsn1-AID* had been degraded. Here, Ndc80 assembly is considerably reduced but not absent. To test whether the residual Ndc80 is due to CENP-T$^{Cnn1}$, we analyzed assembly from a *cnn1Δ dsn1-AID* double mutant and found that Ndc80 recruitment is abolished. Together, these data show that the *de novo* assay uses both pathways of assembly and that CENP-T$^{Cnn1}$ contributes to Ndc80 recruitment independently of the Mis12 complex.

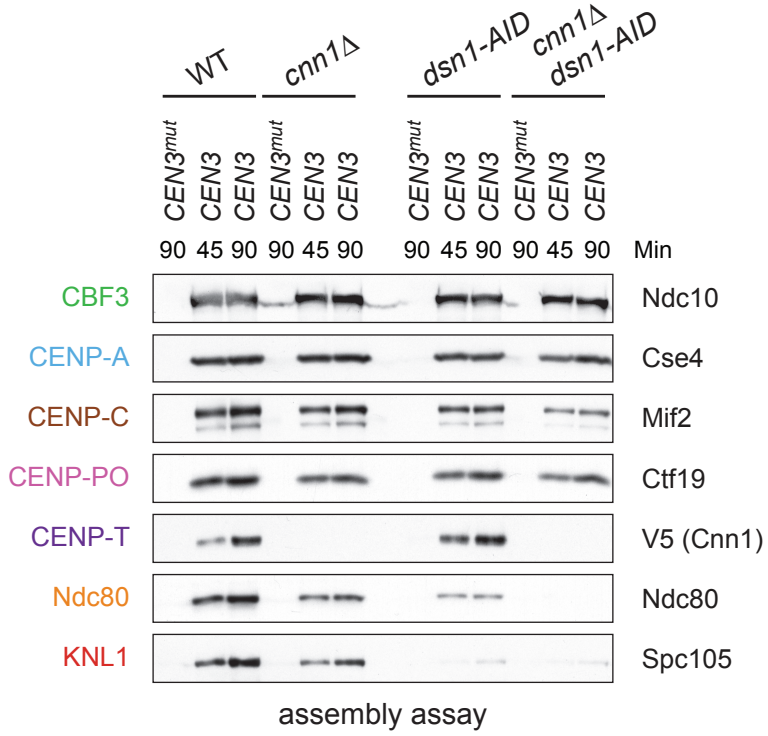


**Figure 4.2. Kinetochore assembly utilizes two pathways for Ndc80 recruitment**
Kinetochores were assembled using extract from WT, *dsn1-AID*, *cnn1D*, or *dsn1-AID cnn1D* double mutant cells that were arrested in benomyl and treated with auxin: *DSN1-3Flag Cnn1-3V5 OsTIR1* (SBY17548), *DSN1-3Flag cnn1D OsTIR1* (SBY17546), *dsn1-3HA-AID Cnn1-3V5 OsTIR1* (SBY17544), and *dsn1-3HA-AID cnn1D OsTIR1* (SBY17380). Extracts in Supplemental Figure 4.1A. *Credit: Adrienne Barber*.

### 4.3.3 CENP-T$^{Cnn1}$ is essential for Ndc80 recruitment when Mis12c lacks mitotic phosphorylation

Although CENP-T$^{Cnn1}$ contributes to Ndc80 recruitment, Mis12c is clearly the major Ndc80 receptor in budding yeast [91, 126]. Consistent with this, Mis12c is essential for viability while CENP-T$^{Cnn1}$ is non-essential, leading to the question of why yeast have retained the CENP-T$^{Cnn1}$ pathway. I hypothesized that CENP-T$^{Cnn1}$ may compensate for downregulation of the Mis12c pathway when the conserved Aurora B sites on Dsn1 are dephosphorylated. Although yeast cells lacking the Aurora B phosphorylation sites (*dsn1-2A*) are inviable due to low Dsn1

protein expression, mutating an additional Cdk1 site (serine 264) restores protein levels and viability (*dsn1-3A*) [154, 181]. Because *dsn1-3A* blocks the interaction between Mis12c and CENP-C$^{Mif2}$, I postulated that this linkage is not essential due to compensation by the CENP-T$^{Cnn1}$ pathway. Consistent with this, I found that *dsn1-3A* and *cnn1Δ* are synthetic lethal (**Figure 4.3A**), indicating that CENP-T$^{Cnn1}$ becomes essential when the Mis12 pathway is misregulated. To confirm this, I crossed *dsn1-3A* to additional mutants in the CENP-T$^{Cnn1}$ pathway (deletions of CENP-K$^{Mcm22}$ and CENP-N$^{Chl4}$). These deletions are also synthetically lethal with *dsn1-3A* (**Figure 4.3A**), indicating that the entire CENP-T$^{Cnn1}$ pathway is essential for viability when the interaction between Dsn1 and CENP-C$^{Mif2}$ is crippled by a lack of Aurora B phosphorylation.

I hypothesized that the synthetic lethality exhibited in the double mutant strain is due to a defect in Ndc80 recruitment. To test this, I attempted to generate a conditional double mutant strain to analyze Ndc80 assembly. However, a *cnn1-AID* allele was hypomorphic and exhibited synthetic lethality with *dsn1-3A* even in the absence of auxin (data not shown). I therefore generated an *mcm22-AID* allele that blocks CENP-T$^{Cnn1}$ assembly (**Supplemental Figure 4.2**). The growth of the *mcm22-AID dsn1-3A* double mutant was slow without auxin and inviable when auxin was added (**Figure 4.3B**) or when CENP-T$^{Cnn1}$ was V5-tagged. To analyze Ndc80 recruitment, I performed the assembly assay from extracts made from the single and the double mutant cells treated with auxin. Because I expected the double mutant to be deficient for Ndc80 recruitment, I reasoned that the mitotic checkpoint might be compromised and therefore arrested cells in S phase rather than mitosis. As expected, the *dsn1-3A* extracts showed a considerable decrease in Ndc80 assembly as well as the other KMN components, Dsn1 and KNL1$^{Spc105}$ (**Figure 4.3C**). Strikingly, Ndc80 recruitment was further reduced in the *dsn1-3A mcm22-AID* double mutant. Despite this reduction in Ndc80, KNL1$^{Spc105}$ assembly appears unaffected by

CENP-K$^{Mcm22}$ degradation, suggesting that the CENP-T$^{Cnn1}$ pathway may specifically recruit Ndc80 and not the full KMN network. Together, our data suggest that the CENP-T$^{Cnn1}$ pathway is required to recruit critical levels of Ndc80 complex to kinetochores when the interaction between the Mis12c and CENP-C$^{Mif2}$ is compromised.

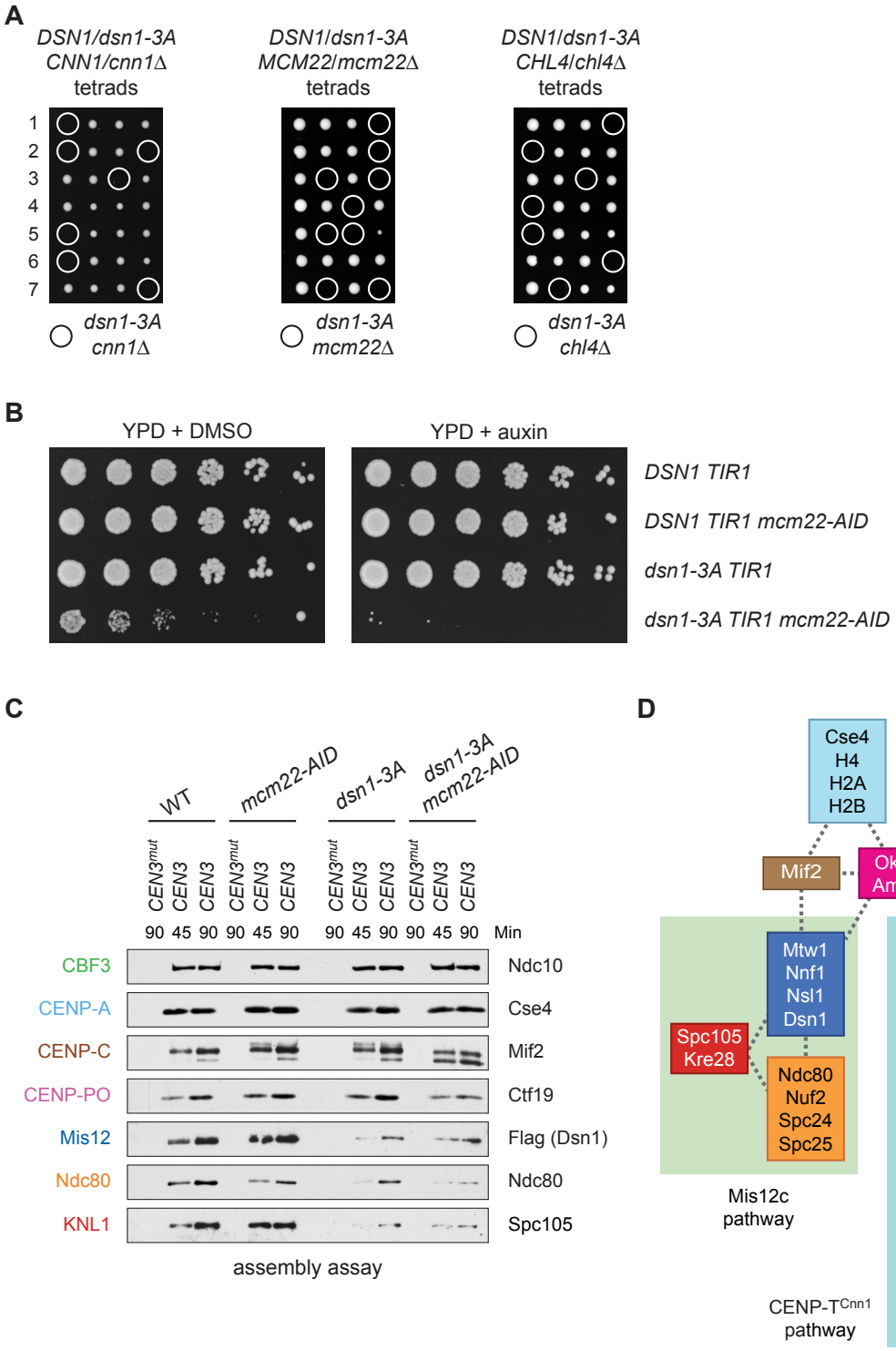


**Figure 4.3. Cells require CENP-T$^{Cnn1}$ when the Mis12 pathway is impaired**
**(A)** A *dsn1-3A* strain (SBY14170) was crossed to *cnn1D* (SBY13386), *mcm22D* (SBY6997), and *chl4D* (SBY8788). The meiotic products (tetrads) of the resulting diploids are oriented left to right, haploid spores were genotyped, and double mutants are indicated with circles. **(B)** A *dsn1-3A mcm22-AID* double mutant is sick but viable until treated with auxin. Serial dilutions of the following yeast strains

were plated on the indicated media: *DSN1-3Flag OsTIR1* (SBY14131), *DSN1-3Flag mcm22-3HA-AID OsTIR1* (SBY18044), *dsn1-3A-3Flag OsTIR1* (SBY14169), and *dsn1-3A-3Flag mcm22-3HA-AID OsTIR1* (SBY18034). **(C)** Assembly was performed with extracts from HU-arrested strains that were treated with auxin: SBY14131, SBY18044, SBY14169, and SBY18034. Extracts in Supplemental Figure 4.1B. **(D)** The sequential order of kinetochore subcomplex recruitment to the DNA, as determined from our data and from (Pekgoz Altunkaya et al., 2016). Dotted lines indicate physical interactions.

## 4.4 DISCUSSION

### 4.4.1 CENP-T$^{Cnn1}$ localization at kinetochores is distal to the centromere

Kinetochores recruit the microtubule-binding complex Ndc80 through both the Mis12 complex and CENP-T$^{Cnn1}$ [90-93]. The position of CENP-T$^{Cnn1}$ within the kinetochore has been unclear because it can form a nucleosome-like structure with CENP-W/S/X *in vitro* [128]. However, the CENP-T$^{Cnn1}$ and CENP-A$^{Cse4}$ DNA-binding sites overlap in yeast [88], suggesting that CENP-T$^{Cnn1}$ may not directly contact the centromere. I found that all CCAN subcomplexes analyzed are required for CENP-T$^{Cnn1}$ kinetochore localization, consistent with work analyzing its localization in human cells [87-89, 129-131]. These data indicate that CENP-T$^{Cnn1}$ is distal to the centromere and does not have intrinsic DNA binding activity under our assay conditions. In addition, I did not detect CENP-S/X$^{Mhf1/2}$ specifically binding to centromeric DNA, suggesting they are not yeast kinetochore components.

I combined our data with known physical interactions of each subcomplex to map the order of the pathway from CENP-A$^{Cse4}$ to CENP-T$^{Cnn1}$ (**Figure 4.3D**) [88]. I propose that the OA complex is the bifurcation point of the Mis12c and CENP-T$^{Cnn1}$ assembly pathways, because the CENP-Q$^{Okp1}$ mutant perturbed the assembly of both KMN and CENP-PO$^{Ctf19\text{-}Mcm21}$, while the other CCAN subcomplexes specifically altered only the CENP-T$^{Cnn1}$ pathway. The CENP-T$^{Cnn1}$ recruitment pathway is therefore comprised of the CENP-PO (CM complex), CENP-HIK, and CENP-LN complexes. I note that all of the non-essential, conserved yeast kinetochore proteins

are specific to the CENP-T pathway, providing an explanation for why the yeast kinetochore contains both essential and non-essential proteins.

### 4.4.2 Functions of the CENP-T$^{Cnn1}$ pathway in budding yeast

In human cells, the CENP-T pathway recruits Ndc80 both directly and indirectly. The CENP-T protein directly binds to two Ndc80 complexes and recruits a third via a phospho-regulated interaction with a Mis12 complex that is also bound to an Ndc80 complex [132, 133]. CENP-T knockdown in human cells results in severely decreased Mis12 and KNL1 complexes at kinetochores and a defect in the spindle checkpoint [127, 155]. In contrast, I did not find evidence for the recruitment of KMN by CENP-T$^{Cnn1}$ in budding yeast, consistent with data showing that CENP-T$^{Cnn1}$ does not interact with the Mis12 complex [91]. The CCAN mutants I assayed that specifically inhibit the CENP-T$^{Cnn1}$ pathway did not alter Mis12 or KNL1$^{Spc105}$ assembly. A lack of linkage between CENP-T$^{Cnn1}$ and the Mis12 complex in yeast may also explain why CENP-T$^{Cnn1}$ is non-essential and does not contribute to spindle checkpoint signaling [91, 126]. It will be important to further analyze the relationship between the yeast Mis12 complex and CENP-T$^{Cnn1}$ in the future.

The Mis12 pathway is responsible for the majority of Ndc80 recruitment in yeast, so it is surprising that yeast cells are viable when the conserved phosphorylation sites that mediate the interaction between Mis12c and CENP-C$^{Mif2}$ are mutated [82, 83, 154-156]. Here, I discovered these cells are viable because they use the CENP-T$^{Cnn1}$ pathway to assemble a functional kinetochore. When the CENP-T$^{Cnn1}$ pathway is eliminated in cells lacking Dsn1 phosphorylation, Ndc80 levels are significantly reduced. A deletion of *CENP-T$^{Cnn1}$* has synthetic phenotypes with two other mutants that cripple Mis12c assembly: a CENP-C$^{Mif2}$ truncation lacking its Mis12c

binding site and a temperature sensitive allele of *NNF1* in the Mis12 complex [126, 182]. Taken together, these data suggest that the CENP-T$^{Cnn1}$ assembly pathway is required to recruit critical levels of Ndc80 when the function of the Mis12 pathway is reduced. This may explain why the highest levels of CENP-T$^{Cnn1}$ at the kinetochore occur at anaphase [126]. In addition to increasing the load-bearing potential of kinetochore-microtubule attachments by recruiting more Ndc80, this may reinforce kinetochore stability when Aurora B-mediated phosphorylation of Dsn1 is removed. In addition, switching to an Ndc80-recruiting pathway that does not recruit KMN may also help silence the spindle assembly checkpoint, as KNL1 is the critical scaffold for the SAC.

The development of a kinetochore assembly assay *de novo* has allowed us to map the remaining unknown hierarchy of CCAN recruitment to the kinetochore. In future work, quantitative mass spectrometry can help us refine this assembly map by analyzing the effect on every protein. I also used the assay to define the two pathways that assemble Ndc80 at kinetochores. Our assembly assay will provide a method to assess the biophysical and structural properties of each Ndc80 recruitment pathway to better understand how cells maintain kinetochore-microtubule attachments to ultimately ensure accurate chromosome segregation.

## 4.5 Materials And Methods

### 4.5.1 Yeast strain construction and microbial techniques

The *Saccharomyces cerevisiae* strains used in this study are listed in Supplementary Table 4.1. Integrated and replicating plasmids are listed in Supplementary Table 4.2. Standard genetic crosses and media were used to generate and grow yeast [149]. Gene deletions, *AID* alleles, and epitope tagged alleles were constructed at the endogenous loci by standard PCR-

based integration as described in [150] and confirmed by PCR. The *dsn1-3A-3Flag* strains were generated the same way as *DSN1-3Flag* and *dsn1-2D-3Flag*, described in 3.5.1 from plasmid pSB1142.

All liquid cultures were grown in yeast peptone dextrose rich (YPD) media. Cells were arrested in S phase by adding 0.2M hydroxyurea to log phase cells in liquid culture for three hours until at least 90% of the cells were large-budded. To arrest cells in mitosis, log phase cultures were diluted 1:1 with liquid media containing 60 μg/mL benomyl and grown for another three hours until at least 90% of cells were large-budded.

Temperature sensitive alleles (*cse4-323 and mif2-3*) were inactivated by diluting log phase cultures 1:1 with 37 °C liquid media supplemented with 60 μg/mL benomyl and shifting the cultures to 37 °C for 3 hours before harvesting.

For strains with auxin inducible degron (*AID*) alleles, all cultures used in the experiment were treated with 500 μM indole-3-acetic acid (IAA, dissolved in DMSO) for the final 60 minutes of growth (*dsn1-AID* and *mcm21-AID*) as described in [136, 160]. For the experiment that included *okp1-AID* (Figure 4.1B), all log phase cultures were diluted 1:1 with media containing benomyl and IAA such that the final concentrations were 30 μg/mL benomyl and 500μM IAA. After two hours, another 150 μM IAA was added, and cultures were harvested after one more hour. For the experiment in Figure 4.3C, 0.2M hydroxyurea and 500μM IAA was added to log phase liquid cultures. After two hours, another 150 μM IAA was added, and cultures were harvested after one more hour.

Growth assays were performed by diluting log phase cultures to OD600 ~1.0 from which a 1:5 serial dilution series was made. This series was plated on YPD plates that were top-plated with either DMSO or 500 μM IAA plates and incubated at 23 °C.

### 4.5.2 Protein techniques

Whole cell extracts for immunoblotting were made by freezing cells in liquid nitrogen and resuspending in SDS buffer. Cells were lysed using glass beads and a beadbeater (Biospec Products), then clarified by centrifugation at 16,100 g for 5 minutes at 4 °C.

### 4.5.3 Kinetochore assembly assay

Preparation of DNA templates, Dynabeads, and competitive DNA and the kinetochore assembly assay were performed at described in sections 3.5.3 and 3.5.4. Sequences of the primers used to PCR amplify the DNA templates are listed in Supplementary Table 4.3. All experiments were repeated two or more times to verify reproducibility and a representative result is reported.

### 4.5.4 Immunological methods

Whole cell extract or samples were prepared as described above. Techniques used for SDS-PAGE gels and immunoblotting with primary and secondary antibodies are described in 2.5.5. Primary antibodies were used as in section 3.5.6. HRP conjugated secondary antibodies were detected with Pierce enhanced chemiluminescent (ECL) substrate and SuperSignal West Dura and Femto ECL (ThermoFisher Scientific). Note that the immunoblot exposures vary to best represent differences across extracts or assembly samples. The levels of proteins in input extracts and assembly samples can therefore not be directly compared.

## 4.6 ACKNOWLEDGEMENTS

I am grateful to Arshad Desai for generously sharing many of the antibodies used in this study. Thank you to Phil Gafken and Yuko Ogata from the Fred Hutch Proteomics Facility for providing experimental advice and performing mass spectrometry. I would also like to thank all members of the Biggins lab for strains and insightful discussions. In particular, I would like to thank Alex Chan, a summer undergraduate student who helped develop the quantitative mass spectrometry protocol, and Adrienne Barber, who contributed to this chapter and has helped to further optimize the kinetochore assembly assay.

## 4.7 SUPPLEMENTAL FIGURES

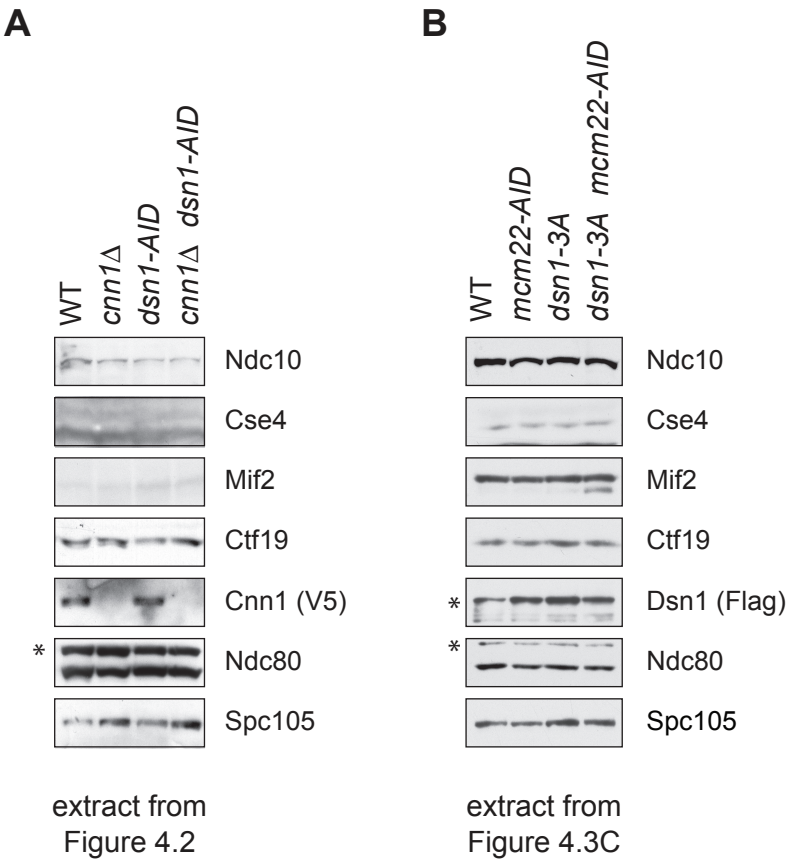


**Supplemental Figure 4.1. Whole cell extracts from selected figures**
Whole cell extracts were immunoblotted with the indicated antibodies from experiments **(A)** Figure 4.2 and **(B)** Figure 4.3C.

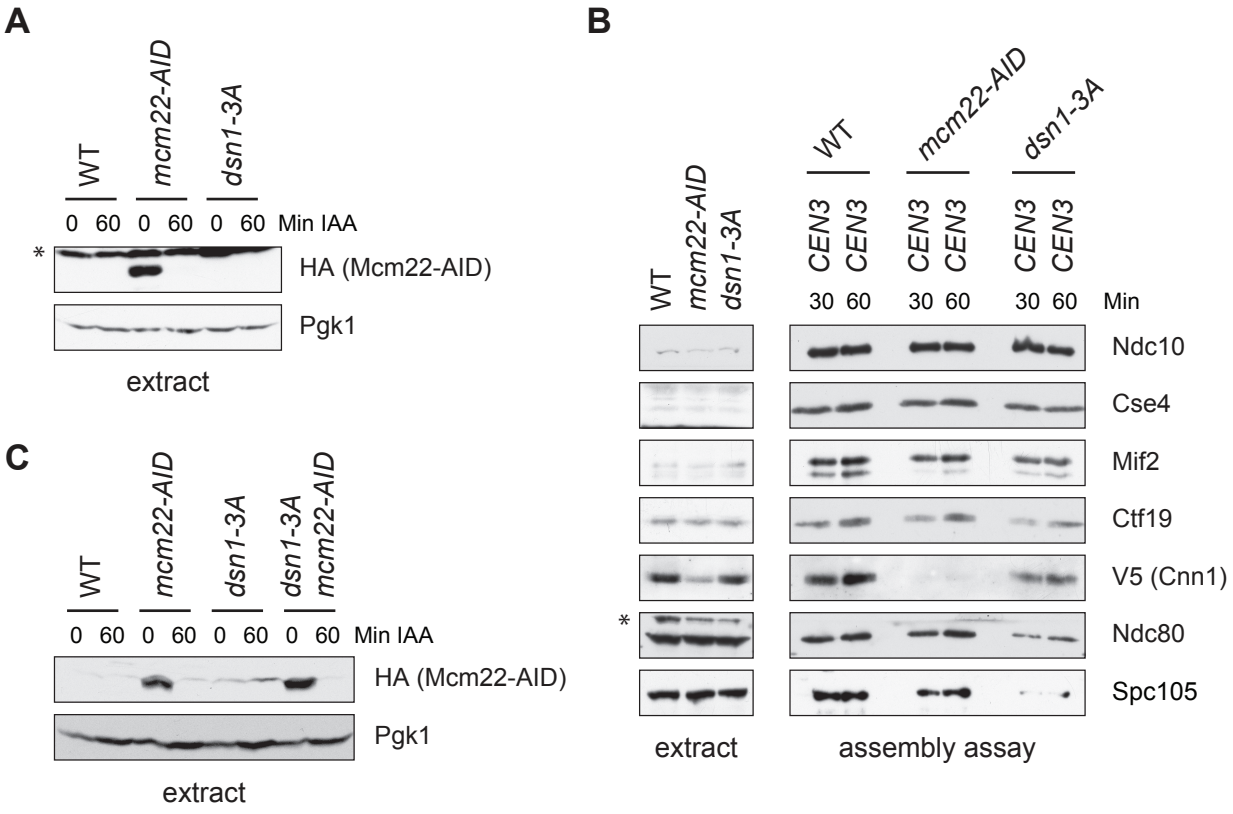


**Supplemental Figure 4.2. Mcm22-AID degradation prevents CENP-T$^{Cnn1}$ assembly**
**(A)** Mcm22-3HA-AID is efficiently degraded after 60 minutes of auxin treatment. The same cells were used to make extract for the assembly assays in **(B)**. The strains are *DSN1-3Flag CNN1-3V5 OsTIR1* (SBY18040), *DSN1-3Flag CNN1-3V5 mcm22-3HA-AID OsTIR1* (SBY18042), and *dsn1-3A-3Flag CNN1-3V5 OsTIR1* (SBY18028). **(C)** Mcm22-3HA-AID degradation for the experiment in Figure 4.3C.

## 4.8 SUPPLEMENTAL TABLES

**Supplemental Table 4.1. Yeast strains used in this chapter**
Complete genotypes of the *Saccharomyces cerevisiae* strains used are listed along with the strain number to reference. All strains are isogenic with W303.

| Strain | Genotype | Integrated and [replicating] plasmids |
|---|---|---|
| SBY6997 | *MATα ura3-1 leu2,3-112 his3-11 TRP1 ade2-1 LYS2 can1-100 BAR1 mcm22Δ::HIS3* | |
| SBY8788 | *MATα ura3-1 leu2,3-112 his3-11 trp1-1 ade2-1 lys2Δ can1-100 bar1-1 chl4Δ::HIS3* | [pRS315] |
| SBY13386 | *MATα ura3-1 leu2,3-112 his3-11 trp1-1 ade2-1 LYS2 can1-100 bar1-1 cnn1Δ::KanMX* | |
| SBY14131 | *MATα ura3-1 leu2,3-112::pGPD1-TIR1:LEU2 his3-11 trp1-1 ade2-1 LYS2 can1-100 bar1-1 DSN1-3Flag:URA3* | pSB2271 |
| SBY14169 | *MATα ura3-1 leu2,3-112::pGPD1-TIR1:LEU2 his3-11 trp1-1 ade2-1 LYS2 can1-100 bar1-1 dsn1-3A(S240/250/264A)-3Flag:URA3* | pSB2271 |
| SBY14170 | *MATa ura3-1 leu2,3-112 his3-11 trp1-1 ade2-1 LYS2 can1-100 bar1-1 dsn1-3A(S240/250/264A)-3Flag:URA3* | |
| SBY17230 | *MATα ura3-1 leu2,3-112 his3-11 trp1-1 ade2-1 LYS2 can1-100 bar1-1 DSN1-3Flag:URA3 CNN1-3V5:KanMX* | |
| SBY17380 | *MATα ura3-1 leu2,3-112::pGPD1-TIR1:LEU2 his3-11 trp1-1 ade2-1 LYS2 can1-100 bar1-1 dsn1-3HA-IAA7:KanMX cnn1Δ::HIS3* | pSB2271 |
| SBY17460 | *MATα ura3-1 leu2,3-112 his3-11 trp1-1 ade2-1 LYS2 can1-100 bar1-1 DSN1-3Flag:URA3 CNN1-3V5:KanMX mcm22Δ::HIS3* | |
| SBY17544 | *MATα ura3-1 leu2,3-112::pGPD1-TIR1:LEU2 his3-11 trp1-1 ade2-1 LYS2 can1-100 bar1-1 dsn1-3HA-IAA7:KanMx CNN1-3V5:KanMX* | pSB2271 |
| SBY17546 | *MATα ura3-1 leu2,3-112::pGPD1-TIR1:LEU2 his3-11 trp1-1 ade2-1 LYS2 can1-100 bar1-1 DSN1-3Flag:URA3 cnn1Δ::HIS3* | pSB2271 |
| SBY17548 | *MATα ura3-1 leu2,3-112::pGPD1-TIR1:LEU2 his3-11 trp1-1 ade2-1 LYS2 can1-100 bar1-1 DSN1-3Flag:URA3 CNN1-3V5:KanMX* | pSB2271 |
| SBY17603 | *MATα ura3-1 leu2,3-112 his3-11 trp1-1 ade2-1 LYS2 can1-100 bar1-1 DSN1-3Flag:URA3 CNN1-3V5:KanMX mif2-3* | |
| SBY17607 | *MATα ura3-1 leu2,3-112 his3-11 trp1-1 ade2-1 LYS2 can1-100 bar1-1 DSN1-3Flag:URA3 CNN1-3V5:KanMX chl4Δ::HIS3* | |
| SBY17764 | *MATα ura3-1 leu2,3-112 his3-11::pGPD1-TIR1:HIS3 trp1-1 ade2-1 LYS2 can1-100 bar1-1 DSN1-3Flag:URA3 CNN1-3V5:KanMX okp1-3V5-IAA7:KanMX* | pSB2273 |

| | | |
|---|---|---|
| SBY17770 | *MATα ura3-1 leu2,3-112 his3-11 trp1-1 ade2-1 LYS2 can1-100 bar1-1 DSN1-3Flag:URA3 CNN1-3V5:KanMX cse4-323* | |
| SBY18028 | *MATα ura3-1 leu2,3-112::pGPD1-TIR1:LEU2 his3-11 trp1-1 ade2-1 can1-100 bar1-1 dsn1-3A(S240/250/264A)-3Flag:URA3 CNN1-3V5:KanMX* | |
| SBY18034 | *MATα ura3-1 leu2,3-112::pGPD1-TIR1:LEU2 his3-11 trp1-1 ade2-1 LYS2 can1-100 bar1-1 dsn1-3A(S240/250/264A)-3Flag:URA3 mcm22-3HA-IAA7(1-125):KanMX* | pSB2271 |
| SBY18040 | *MATa ura3-1 leu2,3-112::pGPD1-TIR1:LEU2 his3-11 trp1-1 ade2-1 LYS2 can1-100 bar1-1 DSN1-3Flag:URA3 CNN1-3V5:KanMX* | |
| SBY18042 | *MATα ura3-1 leu2,3-112::pGPD1-TIR1:LEU2 his3-11 trp1-1 ade2-1 LYS2 can1-100 bar1-1 DSN1-3Flag:URA3 CNN1-3V5:KanMX mcm22-3HA-IAA7(1-125):KanMX* | |
| SBY18044 | *MATα ura3-1 leu2,3-112::pGPD1-TIR1:LEU2 his3-11 trp1-1 ade2-1 LYS2 can1-100 bar1-1 DSN1-3Flag:URA3 mcm22-3HA-IAA7(1-125):KanMX* | pSB2271 |
| SBY18304 | *MATα ura3-1 leu2,3-112 his3-11 trp1-1 ade2-1 LYS2 can1-100 bar1-1 DSN1-3Flag:URA3 CNN1-3V5:KanMX mcm21Δ::HIS3* | |

**Supplemental Table 4.2. Plasmids used in this chapter**
The relevant genes and markers on each plasmid used are listed.

| Plasmids | Description |
|---|---|
| pRS315 | *LEU2, CEN, ARS* [replicating] |
| pSB963 | *WT CEN3, 8LacO, TRP1* |
| pSB972 | *Mutant CEN3 (CCG->AGC CEN mutant), 8 LacO, TRP1* |
| pSB1113 | *DSN1-3Flag, URA3* |
| pSB1115 | *dsn1-2D(S240/250D)-3Flag, URA3* |
| pSB1142 | *dsn1-3A(S240/250/264A)-3Flag, URA3* |
| pSB2271 | *pGPD1-TIR1, LEU2* |
| pSB2273 | *pGPD1-TIR1, HIS3* |

**Supplemental Table 4.3. Oligonucleotides used in this chapter**
The sequence and purpose of each primer used to generate DNA templates is listed.

| Primer | Sequence (5' to 3') | Purpose |
|---|---|---|
| SB3882 | biotin-GGTTCTGGTGGTTCTGGTGGTTCTGGTGAATTCAGCAATAAACCAGCCAGCCGGAA | 500 bp *ampC* template |
| SB3883 | TTTTCCAATGATGAGCACTTTTA | 500 bp *ampC* template |
| SB3878 | biotin-GGTTCTGGTGGTTCTGGTGGTTCTGGTGAATTCAAACAACCGCCGGCTTCCACCA | 250 bp *CEN3* or *CEN3mut* template |
| SB3880 | ATCAGCGCCAAACAATATGGAA | 250 bp *CEN3* or *CEN3mut* template |
| SB5521 | biotin-GGTTCTGGTGGTTCTGGTGGTTCTGGTGAATTCCCATTCAATGAAATATATATTTCTTACTATTTCT | 180 bp *CEN3* or *CEN3mut* template |
| SB5522 | GCTATTCATTGAAAAAATAGTACAAATAAG | 180 bp *CEN3* or *CEN3mut* template |

# CHAPTER 5. Conclusions and Perspectives

In this dissertation I outlined my findings on a novel post-translational modification of the centromeric histone, compared it to studies that have since been published, and presented the most parsimonious model to fit the data provided. Additionally, I have described the development of the first cell-free assay to assemble kinetochores completely *de novo*. I used this assay to investigate numerous aspects of kinetochore assembly: the phosphoregulation of assembly, the order of CCAN recruitment to the centromere, and the role of the CENP-T pathway to Ndc80 localization. Below, I discuss exciting prospective questions we can now address using the kinetochore assembly assay.

## FUTURE PROSPECTS FOR THE KINETOCHORE ASSEMBLY ASSAY

The kinetochore assembly assay developed here will provide the field with a more complete toolkit with which to investigate the biology of centromeres, kinetochores, and the mitotic checkpoint. This is the first method by which to obtain kinetochores that (a) assemble completely *de novo* onto a naked DNA template, (b) span from the DNA to the microtubules, and (c) include native post-translational modifications important for kinetochore assembly and/or stability. Prior to this, the ability to purify intact yeast kinetochores has allowed us to pursue many studies that would have otherwise been impossible. However, the purified kinetochores are generally depleted of inner kinetochore, and therefore do not contain DNA or the mitotic kinase Aurora $B^{Ipl1}$ [135]. Conversely, the assembly assay generates kinetochores that are enriched for inner kinetochore, and is therefore a complementary method. For instance, a colleague studying the mechanism of Aurora $B^{Ipl1}$ function was unable to address some questions using the kinetochore purifications and had to instead use the kinetochore assembly assay, because the

assembled kinetochores contain high levels of endogenous Aurora $B^{Ipl1}$ and its primary recruitment factors.

The assembly assay is also particularly amenable to studying the properties of the centromere and the CENP-A nucleosome. Although the yeast centromere is sequence specific, there is variability in centromeric sequence across the 16 chromosomes. The assembly assay was optimized using the centromere from chromosome III, but a colleague has begun using other centromeres and has found differences in assembly efficiency. One potential reason is that the centromeres have differential binding affinities for the non-essential Cbf1 protein that binds the CDEI region of the centromere [72, 73]. Cbf1 is a transcription factor that is required for transcription of the centromere [138]. My colleague is interested in the role of centromeric transcription and of the transcripts themselves. Although many factors may be involved in this process, it is intriguing that the centromere itself harbors a transcription factor binding site. A detailed analysis of how DNA sequence divergence relates to assembly efficiency *in vitro* can reveal important aspects of centromere function, such as defining a "strong" centromeric sequence that promotes transcription and/or protein binding. This will extend early work that tested the ability of mutated centromeres to impart copy number regulation on centromeric plasmids [183]. Two major advantages of working *in vitro* are that the DNA templates can be easily altered, for instance by mutating the CDEI sequence, and the extracts can be easily manipulated, for example by treatment with RNase to test the role of transcripts. Furthermore, the effects of sequence divergence on kinetochore assembly will not be confounded by the presence of pericentromere, like it would be *in vivo*.

Point centromeres are unique in that CENP-$A^{Cse4}$ deposition occurs through sequence-specificity rather than epigenetic inheritance. The CBF3 complex recruits CENP-$A^{Cse4}$ by

binding the CENP-A$^{Cse4}$ chaperone, but it is unclear whether this is its only role at the centromere. Current work in the lab is testing whether the requirement for the CBF3 complex can be bypassed by performing the assembly assay with pre-formed CENP-A$^{Cse4}$ octamers or CENP-A$^{Cse4}$ nucleosomes. These experiments will address other important questions about centromere biology as well. Is the centromeric DNA sequence required for kinetochore assembly, or can any DNA suffice, such as the 601 DNA used to generate CENP-A$^{Cse4}$ nucleosomes *in vitro* [184]? Is DNA required at all, or is a CENP-A$^{Cse4}$ octamer sufficient? Can a CENP-A$^{Cse4}$ octamer or octameric nucleosome assemble the kinetochore, or must it be a hemisome? We can also learn whether CENP-A$^{Cse4}$ deposition is the key cell cycle regulated event if the temporal regulation of kinetochore assembly is bypassed by using preassembled nucleosomes. The assembly assay provides the most direct method by which to investigate these fundamental queries.

In Chapter 3, I show that assembly *in vitro* is a stepwise process. In Chapter 4, I used the assembly assay to map the hierarchal order of recruitment within the CCAN. Although this bulk assay contributed greatly to our understanding of protein recruitment, adapting the assay to study individual kinetochores will provide greater mechanistic detail. We aim to directly observe the stepwise order of recruitment to individual kinetochores at single molecule resolution using total internal reflection fluorescence (TIRF) microscopy. A member of a collaborating lab (the Asbury lab at the University of Washington) is developing a method to fix the centromeric DNA to glass slides, flow whole extract over it, and visualize the assembly process by TIRF. Centromeres are clustered *in vivo*, so this will provide the first and only way to visualize the assembly of individual kinetochores [102]. This will contribute to my work because it will address which complexes are preassembled prior to binding the centromere as well as allow for the

stoichiometry of components to be measured. It will also serve as the foundation for elucidating the regulation of kinetochore assembly.

The assembled kinetochores will also contribute to structural and biophysical studies. We are now optimizing a method to cleave the DNA from the beads post-assembly, leaving the assembled kinetochores intact on the centromere. We are beginning to use TIRF microscopy to determine the stoichiometry of the assembled kinetochores by analyzing the colocalization and signal intensities of fluorescently labeled DNA and proteins. Eventually, we aim to use the cleaved assembled kinetochores for electron microscopy (EM). Previously, EM of purified kinetochores provided insight into the structure of the outer kinetochore bound to microtubules [134]. The assembled kinetochores are enriched for inner kinetochore and could therefore provide important structural information about the structure of the poorly characterized CCAN bound to the centromeric chromatin. The EM can also be done in a stepwise manner, using inner kinetochore mutants to define the structures and contributions of individual subcomplexes.

Finally, we are working toward testing the biophysical properties of the assembled kinetochores. Using the purified kinetochores, microtubule-binding and force-bearing properties are measured across the outer kinetochore, from the Mis12 complex to the microtubule-binding interface [135]. The assembled kinetochores will allow us to apply tension across the entire length of the kinetochore by conjugating the kinetochores to beads through the DNA. These studies could potentially reveal important differences when complete kinetochores come under tension. Furthermore, the assembled kinetochores contain both pathways to Ndc80 recruitment, while the purified kinetochores contain only the Mis12c pathway. We can now address questions about the differential contributions of the two pathways to the force-bearing properties of kinetochores. The assembled kinetochores also provide the advantage of binding high levels of

the CPC, which harbors the tension sensor, Aurora $B^{Ipl1}$. The kinase activity of Aurora $B^{Ipl1}$ should destabilize microtubule-attachments under low tension, but mechanistically how this works is controversial [166]. The assembled kinetochores provide and easily manipulated *in vitro* system to elucidate how Aurora $B^{Ipl1}$ reaches its substrates.

In summary, the *in vitro* kinetochore assembly assay I developed will serve as a useful biochemical tool to investigate many outstanding questions in the field, and will be a major step toward understanding how the cell regulates assembly of the kinetochore. I am excited to see what the Biggins lab discovers in the coming years using the assay.

# Appendix A: The E3 ubiquitin ligase, Psh1, negatively regulates assembly of the OA/CM complexes

## A.1 Psh1 negatively regulates the binding of OA/CM to DNA

As I tested inner kinetochore mutants in assembly, I included a deletion of *PSH1*, an E3 ubiquitin ligase that regulates CENP-A$^{Cse4}$ levels [52-55]. Although Psh1 targets ectopically incorporated CENP-A$^{Cse4}$, it has also been detected at centromeres by chromatin immunoprecipitation [50, 53]. I postulated that a *psh1Δ* mutant might cause an increase of CENP-A$^{Cse4}$ binding, either to only the *CEN3$^{mut}$* DNA, or to the *CEN3* DNA as well. Surprisingly, CENP-A$^{Cse4}$ binding to either template was unaffected by the deletion of *PSH1* (**Figure A.1A**). However, numerous other kinetochore proteins bound at increased levels to *CEN3* and even more so to *CEN3$^{mut}$* DNA, including CENP-Q$^{Okp1}$, CENP-P$^{Ctf19}$, Ndc80, KNL1$^{Spc105}$, and CENP-T$^{Cnn1}$ (**Figure A.1A** and data not shown). To better define which proteins were affected by *PSH1* deletion, I analyzed the assembled kinetochores by quantitative mass spectrometry. WT and *psh1Δ* assembly assays on the *CEN3* template were analyzed separately from those on the *CEN3$^{mut}$* template. Consistent with immunoblot results, the strongest effect of *PSH1* deletion is enhanced assembly on *CEN3$^{mut}$* template (**Figure A.1B**). CENP-A$^{Cse4}$ and CENP-C$^{Mif2}$ binding levels are largely unchanged in the *psh1Δ* mutant assembly, but the OA and CM complexes are both considerably upregulated. Based on our previous analysis of inner kinetochore recruitment (**Figure 4.3D**), assembly in the *psh1Δ* mutant is upregulated beginning with the OA complex (**Figure A.1B**).

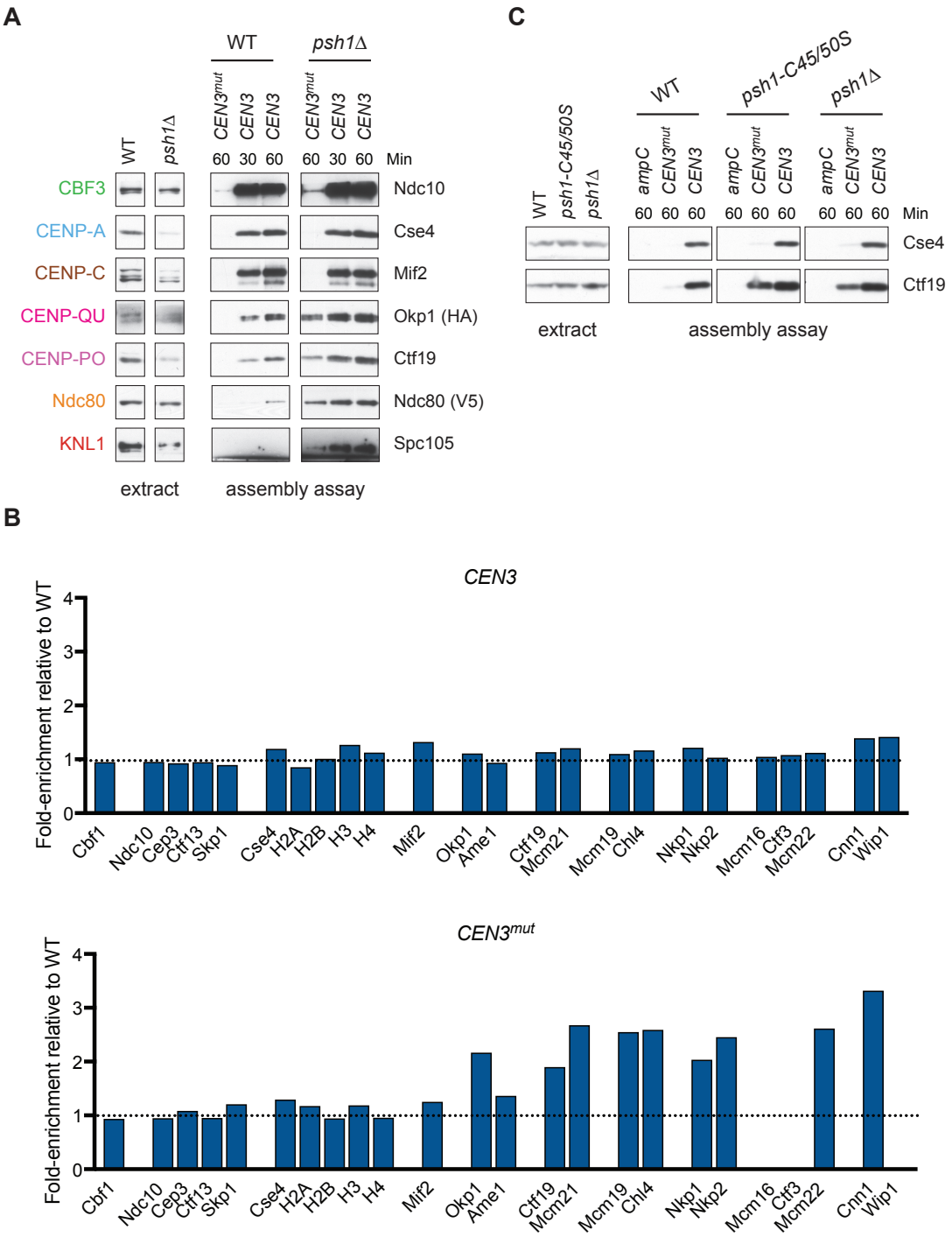


**Figure A.1. Psh1 negatively regulates assembly of the OA/CM complexes**
**(A)** Assembly assays were performed using extracts from *OKP1-3HA NDC80-3V5* (SBY12038) and *OKP1-3HA NDC80-3V5 psh1D* (SBY13116). Whole cell extracts and DNA-bound proteins were analyzed by the indicated immunoblotting. **(B)** Assembly assays from WT (SBY4) and *psh1D* (SBY11473) were labeled with tandem mass tags and compared on *CEN3* DNA or on *CEN3*$^{mut}$ DNA by quantitative mass spectrometry. For each protein, the relative abundance in the *psh1D* mutant assembly was divided by the relative abundance in WT assembly to calculate the fold enrichment. The dotted line

indicates the level of assembly from WT extracts. **(C)** Kinetochores were assembled from extracts *PSH1-13myc psh1D* (SBY10303), *psh1-C45/50S-13myc psh1D* (SBY17020), and *psh1D* (SBY8336) on the indicated DNA templates. Extracts and DNA-bound proteins were analyzed by the indicated immunoblots. *Credit: Adrienne Barber*.

These data explain observations from Chapter 2 that I could not understand at the time. Purified Flag-CENP-A$^{Cse4}$ co-immunoprecipitated significantly more CENP-N$^{Chl4}$ in *psh1Δ* mutants (**Figure 2.5C**). Because I saw this effect whether or not *SIZ1/2* were also deleted, the enhanced interaction is not due to the increased sumoylation in a *psh1Δ* mutant. Taken together, these data suggest that Psh1 negatively regulates an interaction somewhere between CENP-A$^{Cse4}$ and CENP-N$^{Chl4}$, likely at the OA or CM complex.

If OA is upregulated, I would expect to see the upregulation of both Ndc80 pathways, and therefore the entire KMN. Indeed, I saw an increase of both Ndc80 and KNL1$^{Spc105}$, indicating that OA binding is upregulated, and therefore both assembly pathways are enhanced. However, I have not ruled out the possibility that Psh1 regulates CM assembly. Until recently, COMA was considered a single complex with two essential components (OA) and two nonessential components (CM). Our work and other recent studies make it clear that although tightly bind one another they are functionally separable [182]. However, preliminary quantitative mass spectrometry data show that the OA complex is reduced but not absent in a CM mutant assembly. This suggests that although CM assembles downstream of OA, it may help to stabilize OA at the centromere (data not shown). I therefore need to distinguish which of these complexes is negatively regulated by Psh1 by combining *psh1Δ* with a CM mutant (*mcm21Δ*) or an OA mutant (*okp1-AID*) and assaying the assembly of the opposite complex.

## A.2 Psh1 catalytic activity may be required to regulate OA/CM

To better understand mechanistically how Psh1 negatively regulates OA/CM binding, I asked whether Psh1 required its catalytic activity. CENP-A$^{Cse4}$ is the only reported target of Psh1, despite efforts in the lab to find other substrates. I wondered whether the assembly phenotype of the *psh1Δ* mutant was due to loss of Psh1-mediated ubiquitination or loss of a novel Psh1 function, such as directly blocking binding interactions. To test this, I performed the assembly assay from a catalytic-dead Psh1 mutant (*psh1-CD*). Similar to *psh1Δ* mutant assembly, the Psh1 catalytic-dead mutant caused enhanced assembly and aberrant binding to the *CEN3*$^{mut}$ DNA beginning with OA/CM (**Figure A.1C**). This would suggest that the catalytic activity of Psh1 is required to negatively regulate OA/CM binding, but it is unclear whether the Psh1 catalytic-dead mutant has other defects in its structure or function. The mutant protein is stable, since its cellular levels are similar to those of WT Psh1 (data not shown). However, in contrast to studies that have detected Psh1 at centromeres *in vivo*, I have only detected Psh1 binding to the negative control templates, but not to the *CEN3* template [50, 53] (data not shown). I therefore cannot ask whether this localization pattern is perturbed in the mutant. The mutations in *psh1-CD* strongly affect its ability to bind CENP-A$^{Cse4}$ [53, 55]. I therefore cannot distinguish whether the negative regulation of OA/CM requires CENP-A$^{Cse4}$ binding or catalytic activity. It will be important to better characterize the catalytic-dead mutant in order to resolve these two possibilities.

If Psh1 catalytic activity is required to negatively regulate kinetochore assembly, I hypothesized that a member of the OA/CM complexes may be a novel substrate of Psh1 ubiquitination. CENP-P$^{Ctf19}$ consistently shows a slight mobility shift in the *psh1Δ* mutant assembled kinetochores, characteristic of modification with phosphate. Interestingly,

phosphorylation can in some cases help an E3 ubiquitin ligase identify its substrate [51]. To test whether CENP-P$^{Ctf19}$ is a novel target of Psh1 ubiquitination, I analyzed CENP-P$^{Ctf19}$ from the stability assays performed in Chapter 2. Preliminary results showed no difference in CENP-P$^{Ctf19}$ stability in a *psh1Δ* mutant (data not shown). Because changes in CENP-A$^{Cse4}$ stability are more easily detected when CENP-A$^{Cse4}$ is overexpressed, future experiments should consider overexpressing each of the OA/CM complex components to analyze changes in their stability upon *PSH1* deletion.

## A.3 Considering other mechanisms of negative regulation by Psh1

Because the catalytic-dead Psh1 mutant needs to be tested further, I also considered the possibility that Psh1 affects OA/CM binding through an alternative mechanism, such as blocking physical interactions. The OA complex binds has non-specific DNA binding affinity, such that recombinant OA co-purifies with bacterial DNA [182]. Additionally, OA and Psh1 each interact with CENP-A$^{Cse4}$ [52, 53, 182]. I wondered whether Psh1 blocks OA from binding non-centromeric DNA, and if so, whether CENP-A$^{Cse4}$ was required for this inhibition.

I attempted to test several aspects of this model. First, I asked whether Psh1 alters the DNA-binding affinity of OA by incubating recombinant OA complex and Psh1 with centromeric DNA on beads. Unfortunately, OA bound to the negative control beads without DNA (data not shown). Next, I asked whether OA and Psh1 interact, and whether the interaction is dependent upon CENP-A$^{Cse4}$. To test this *in vitro*, I incubated recombinant Psh1 with recombinant OA conjugated to beads, but Psh1 bound to negative control unconjugated beads (data not shown). I also attempted to address the question *in vivo* by purifying CENP-U$^{Ame1}$-V5 ('A' of the OA complex) and looked for the co-immunoprecipitation of Psh1-Flag. Psh1 and CENP-U$^{Ame1}$-V5

interact strongly when extracts are clarified using a low-speed spin, but show no association with a high-speed spin clarification (data not shown). Future experiments will perform the same purification with low speed clarified extracts in both WT and a temperature sensitive CENP-$A^{Cse4}$ mutant (*cse4-323*). These experimental conditions should be optimized in the future, as these are key questions to determine the role of Psh1 in OA/CM complex regulation.

## A.4 Conclusions

After identifying OA as the potential bifurcation point of assembly in Chapter 4, I identified a novel regulator of OA complex assembly, Psh1. The catalytic activity of Psh1 appears to be required to negatively regulate the binding of OA/CM to DNA. Future work should test whether a member of OA/CM are subjected to Psh1-mediated ubiquitination and subsequent proteolysis, which could reveal a novel Psh1 substrate.

The observed interaction between Psh1 and the OA complex should also be further characterized. Does this interaction require CENP-$A^{Cse4}$? Does Psh1 block the ability of OA to bind DNA? Interestingly, preliminary experiments show that in a *psh1Δ* mutant assembly, the OA complex binds aberrantly to the $CEN3^{mut}$ DNA but not to the *ampC* DNA (**Figure A.1C**). One clear difference between these templates is that the $CEN3^{mut}$ DNA contains the binding site for the Cbf1 protein. While attempting to ask whether Cbf1 is required for the aberrant assembly in a *psh1Δ* mutant, we discovered that *psh1Δ* and *cbf1Δ* are synthetic lethal. A colleague is beginning to investigate the role of Cbf1 in kinetochore assembly, and this work should contribute to our understanding of how Psh1 and Cbf1 interact. Furthermore, Psh1 is not evolutionarily conserved, suggesting that this regulation may be specific to point centromeres. This may also explain the difference in aberrant OA binding to the two negative control

templates. Finally, because the OA complex affects both pathways to Ndc80c assembly, it will be interesting to know whether this extra level of regulation contributes to the CENP-T$^{Cnn1}$ pathway of kinetochore assembly being nonessential in yeast.

## A.5 Strains used in Appendix A

**Supplemental Table A.1. Yeast strains used in Appendix A**
Complete genotypes of the *Saccharomyces cerevisiae* strains used are listed along with the strain number to reference. All strains are isogenic with W303.

| Strain | Genotype | Integrated plasmids |
|---|---|---|
| SBY4 | *MATα ura3-1 leu2,3-112 his3-11 trp1-1 ade2-1 LYS2 can1-100 bar1-1* | |
| SBY8336 | *MAT**a** ura3-1 leu2,3-112 his3-11 trp1-1 ade2-1 LYS2 can1-100 bar1-1 psh1Δ::KanMX* | |
| SBY10303 | *MAT**a** ura3-1::pPSH1-PSH1-13myc:URA3 leu2,3-112 his3-11 trp1-1 ade2-1 LYS2 can1-100 bar1-1 psh1Δ::KanMX* | pSB1714 |
| SBY11473 | *MATα ura3-1 leu2,3-112 his3-11 trp1-1 ade2-1 LYS2 can1-100 bar1-1 psh1Δ::KanMX* | |
| SBY12038 | *MAT**a** ura3-1 leu2,3-112 his3-11 TRP1 ade2-1 LYS2 can1-100 BAR1 OKP1-3HA:HIS3 NDC80-3V5:HIS3* | |
| SBY13116 | *MAT**a** ura3-1 leu2,3-112 his3-11 TRP1 ade2-1 LYS2 can1-100 BAR1 OKP1-3HA:HIS3 NDC80-3V5:HIS3 psh1Δ::KanMX* | |
| SBY17020 | *MAT**a** ura3-1::pPSH1-psh1-C45/50S-13myc:URA3 leu2,3-112 his3-11 trp1-1 ade2-1 LYS2 can1-100 bar1-1 psh1Δ::KanMX* | pSB2026 |

**Supplemental Table A.2. Plasmids used in Appendix A**
The relevant genes and markers on each plasmid used are listed.

| Plasmids | Description |
|---|---|
| pSB1714 | *pPSH1-PSH1-13myc, URA3* |
| pSB2026 | *pPSH1-psh1-C45/50S-13myc, URA3* |

# REFERENCES


1. Pfau, S.J. and A. Amon, *Chromosomal instability and aneuploidy in cancer: from yeast to man.* EMBO Rep, 2012. **13**(6): p. 515-27.
2. Yamagishi, Y., et al., *Kinetochore composition and its function: lessons from yeasts.* FEMS Microbiol Rev, 2014. **38**(2): p. 185-200.
3. Musacchio, A. and A. Desai, *A Molecular View of Kinetochore Assembly and Function.* Biology (Basel), 2017. **6**(1).
4. Biggins, S., *The composition, functions, and regulation of the budding yeast kinetochore.* Genetics, 2013. **194**(4): p. 817-46.
5. Joglekar, A.P. and A.A. Kukreja, *How Kinetochore Architecture Shapes the Mechanisms of Its Function.* Curr Biol, 2017. **27**(16): p. R816-R824.
6. Earnshaw, W.C. and N. Rothfield, *Identification of a family of human centromere proteins using autoimmune sera from patients with scleroderma.* Chromosoma, 1985. **91**(3-4): p. 313-21.
7. Salmon, E.D. and K. Bloom, *Tension sensors reveal how the kinetochore shares its load.* Bioessays, 2017. **39**(7).
8. Sandall, S., et al., *A complex of Bir1-Sli15 (Survivin-INCENP) connects centromeres to microtubules and is the likely tension sensor controlling Aurora B activation.* Cell, 2006. **In Press**.
9. Yoon, H.J. and J. Carbon, *Participation of Bir1p, a member of the inhibitor of apoptosis family, in yeast chromosome segregation events.* Proc Natl Acad Sci U S A, 1999. **96**(23): p. 13208-13.
10. Foltz, D.R., et al., *The human CENP-A centromeric nucleosome-associated complex.* Nat Cell Biol, 2006. **8**(5): p. 458-69.
11. Nicklas, R.B., *How cells get the right chromosomes.* Science, 1997. **275**: p. 632-7.
12. Murray, A.W., *A brief history of error.* Nat Cell Biol, 2011. **13**(10): p. 1178-82.
13. Liu, D., et al., *Regulated targeting of protein phosphatase 1 to the outer kinetochore by KNL1 opposes Aurora B kinase.* J Cell Biol, 2010. **188**(6): p. 809-20.
14. Francisco, L., W. Wang, and C.S. Chan, *Type 1 protein phosphatase acts in opposition to Ipl1 protein kinase in regulating yeast chromosome segregation.* Mol Cell Biol, 1994. **14**(7): p. 4731-40.
15. Meadows, J.C., et al., *Spindle checkpoint silencing requires association of PP1 to both Spc7 and kinesin-8 motors.* Dev Cell, 2011. **20**(6): p. 739-50.
16. Rosenberg, J.S., F.R. Cross, and H. Funabiki, *KNL1/Spc105 recruits PP1 to silence the spindle assembly checkpoint.* Curr Biol, 2011. **21**(11): p. 942-7.
17. Espeut, J., et al., *Microtubule binding by KNL-1 contributes to spindle checkpoint silencing at the kinetochore.* J Cell Biol, 2012.
18. Bensasson, D., *Evidence for a high mutation rate at rapidly evolving yeast centromeres.* BMC Evol Biol, 2011. **11**: p. 211.
19. Melters, D.P., et al., *Comparative analysis of tandem repeats from hundreds of species reveals unique insights into centromere evolution.* Genome Biol, 2013. **14**(1): p. R10.
20. Bernad, R., P. Sanchez, and A. Losada, *Epigenetic specification of centromeres by CENP-A.* Exp Cell Res, 2009. **315**(19): p. 3233-41.
21. Blower, M.D., B.A. Sullivan, and G.H. Karpen, *Conserved organization of centromeric chromatin in flies and humans.* Dev Cell, 2002. **2**(3): p. 319-30.

22. Ems-McClung, S.C. and C.E. Walczak, *Kinesin-13s in mitosis: Key players in the spatial and temporal organization of spindle microtubules.* Semin Cell Dev Biol, 2010. **21**(3): p. 276-82.
23. Steiner, F.A. and S. Henikoff, *Holocentromeres are dispersed point centromeres localized at transcription factor hotspots.* Elife, 2014. **3**: p. e02025.
24. Winey, M., et al., *Three-dimensional ultrastructural analysis of the Saccharomyces cerevisiae mitotic spindle.* J Cell Biol, 1995. **129**: p. 1601-15.
25. Clarke, L. and J. Carbon, *The structure and function of yeast centromeres.* Annu Rev Genet, 1985. **19**.
26. Drinnenberg, I.A., et al., *Recurrent loss of CenH3 is associated with independent transitions to holocentricity in insects.* Elife, 2014. **3**.
27. Choo, K.H., *Domain organization at the centromere and neocentromere.* Dev Cell, 2001. **1**(2): p. 165-77.
28. Sullivan, B.A., *Centromere round-up at the heterochromatin corral.* Trends Biotechnol, 2002. **20**(3): p. 89-92.
29. Steiner, F.A. and S. Henikoff, *Diversity in the organization of centromeric chromatin.* Curr Opin Genet Dev, 2015. **31**: p. 28-35.
30. Eckert, C.A., D.J. Gravdahl, and P.C. Megee, *The enhancement of pericentromeric cohesin association by conserved kinetochore components promotes high-fidelity chromosome segregation and is sensitive to microtubule-based tension.* Genes Dev, 2007. **21**(3): p. 278-91.
31. Ng, T.M., et al., *Pericentromeric sister chromatid cohesion promotes kinetochore biorientation.* Mol Biol Cell, 2009. **20**(17): p. 3818-27.
32. Fernius, J. and A.L. Marston, *Establishment of cohesion at the pericentromere by the Ctf19 kinetochore subcomplex and the replication fork-associated factor, Csm3.* PLoS Genet, 2009. **5**(9): p. e1000629.
33. Tanaka, T., et al., *Identification of cohesin association sites at centromeres and along chromosome arms.* Cell, 1999. **98**(6): p. 847-58.
34. Weber, S.A., et al., *The kinetochore is an enhancer of pericentric cohesin binding.* PLoS Biol, 2004. **2**(9): p. E260.
35. Kawashima, S.A., et al., *Phosphorylation of H2A by Bub1 prevents chromosomal instability through localizing shugoshin.* Science, 2010. **327**(5962): p. 172-7.
36. Fernius, J. and K.G. Hardwick, *Bub1 kinase targets Sgo1 to ensure efficient chromosome biorientation in budding yeast mitosis.* PLoS Genet, 2007. **3**(11): p. e213.
37. Kitajima, T.S., et al., *Human Bub1 defines the persistent cohesion site along the mitotic chromosome by affecting Shugoshin localization.* Curr Biol, 2005. **15**(4): p. 353-9.
38. Indjeian, V.B., B.M. Stern, and A.W. Murray, *The centromeric protein Sgo1 is required to sense lack of tension on mitotic chromosomes.* Science, 2005. **307**(5706): p. 130-3.
39. Kiburz, B.M., et al., *The core centromere and Sgo1 establish a 50-kb cohesin-protected domain around centromeres during meiosis I.* Genes Dev, 2005. **19**(24): p. 3017-30.
40. Peplowska, K., A.U. Wallek, and Z. Storchova, *Sgo1 regulates both condensin and Ipl1/Aurora B to promote chromosome biorientation.* PLoS Genet, 2014. **10**(6): p. e1004411.
41. Coffman, V.C., et al., *CENP-A exceeds microtubule attachment sites in centromere clusters of both budding and fission yeast.* J Cell Biol, 2011. **195**(4): p. 563-72.

42. Lawrimore, J., K.S. Bloom, and E.D. Salmon, *Point centromeres contain more than a single centromere-specific Cse4 (CENP-A) nucleosome.* J Cell Biol, 2011. **195**(4): p. 573-82.
43. Wisniewski, J., et al., *Imaging the fate of histone Cse4 reveals de novo replacement in S phase and subsequent stable residence at centromeres.* Elife, 2014. **3**: p. e02203.
44. Black, B.E., et al., *Structural determinants for generating centromeric chromatin.* Nature, 2004. **430**(6999): p. 578-82.
45. Cho, U.S. and S.C. Harrison, *Recognition of the centromere-specific histone Cse4 by the chaperone Scm3.* Proc Natl Acad Sci U S A, 2011. **108**(23): p. 9367-71.
46. Camahort, R., et al., *Scm3 is essential to recruit the histone h3 variant cse4 to centromeres and to maintain a functional kinetochore.* Mol Cell, 2007. **26**(6): p. 853-65.
47. Shivaraju, M., et al., *Scm3 is a centromeric nucleosome assembly factor.* J Biol Chem, 2011. **286**(14): p. 12016-23.
48. Zhou, Z., et al., *Structural basis for recognition of centromere histone variant CenH3 by the chaperone Scm3.* Nature, 2011. **472**(7342): p. 234-7.
49. Xiao, H., et al., *Nonhistone Scm3 binds to AT-rich DNA to organize atypical centromeric nucleosome of budding yeast.* Mol Cell, 2011. **43**(3): p. 369-80.
50. Collins, K.A., S. Furuyama, and S. Biggins, *Proteolysis contributes to the exclusive centromere localization of the yeast Cse4/CENP-A histone H3 variant.* Curr Biol, 2004. **14**(21): p. 1968-72.
51. Finley, D., et al., *The ubiquitin-proteasome system of Saccharomyces cerevisiae.* Genetics, 2012. **192**(2): p. 319-60.
52. Ranjitkar, P., Press, M. O., Yi, X., Baker, R., MacCoss, M. J, Biggins, S, *An E3 ubiquitin ligase prevents ectopic localization of the centromeric histone H3 variant via the centromere targeting domain.* Mol Cell, 2010. **40**(3): p. 455-64.
53. Hewawasam, G., et al., *Psh1 is an E3 ubiquitin ligase that targets the centromeric histone variant Cse4.* Mol Cell, 2010. **40**(3): p. 444-54.
54. Hildebrand, E.M. and S. Biggins, *Regulation of Budding Yeast CENP-A levels Prevents Misincorporation at Promoter Nucleosomes and Transcriptional Defects.* PLoS Genet, 2016. **12**(3): p. e1005930.
55. Deyter, G.M. and S. Biggins, *The FACT complex interacts with the E3 ubiquitin ligase Psh1 to prevent ectopic localization of CENP-A.* Genes Dev, 2014. **28**(16): p. 1815-26.
56. Au, W.C., et al., *A novel role of the N terminus of budding yeast histone H3 variant Cse4 in ubiquitin-mediated proteolysis.* Genetics, 2013. **194**(2): p. 513-8.
57. Cheng, H., X. Bao, and H. Rao, *The F-box Protein Rcy1 Is Involved in the Degradation of Histone H3 Variant Cse4 and Genome Maintenance.* J Biol Chem, 2016. **291**(19): p. 10372-7.
58. Ohkuni, K., et al., *SUMO-Targeted Ubiquitin Ligase (STUbL) Slx5 regulates proteolysis of centromeric histone H3 variant Cse4 and prevents its mislocalization to euchromatin.* Mol Biol Cell, 2016.
59. Cheng, H., et al., *Multiple E3s promote the degradation of histone H3 variant Cse4.* Sci Rep, 2017. **7**(1): p. 8565.
60. Henikoff, S. and T. Furuyama, *The unconventional structure of centromeric nucleosomes.* Chromosoma, 2012. **121**(4): p. 341-52.
61. Furuyama, T., C.A. Codomo, and S. Henikoff, *Reconstitution of hemisomes on budding yeast centromeric DNA.* Nucleic Acids Res, 2013.

62. Dimitriadis, E.K., et al., *Tetrameric organization of vertebrate centromeric nucleosomes.* Proc Natl Acad Sci U S A, 2010. **107**(47): p. 20317-22.
63. Dalal, Y., et al., *Tetrameric structure of centromeric nucleosomes in interphase Drosophila cells.* PLoS Biol, 2007. **5**(8): p. e218.
64. Shivaraju, M., et al., *Cell-cycle-coupled structural oscillation of centromeric nucleosomes in yeast.* Cell, 2012. **150**(2): p. 304-16.
65. Cole, H.A., B.H. Howard, and D.J. Clark, *The centromeric nucleosome of budding yeast is perfectly positioned and covers the entire centromere.* Proc Natl Acad Sci U S A, 2011. **108**(31): p. 12687-92.
66. Krassovsky, K., J.G. Henikoff, and S. Henikoff, *Tripartite organization of centromeric chromatin in budding yeast.* Proc Natl Acad Sci U S A, 2012. **109**(1): p. 243-8.
67. Furuyama, T. and S. Henikoff, *Centromeric nucleosomes induce positive DNA supercoils.* Cell, 2009. **138**(1): p. 104-13.
68. Musgrave, D.R., K.M. Sandman, and J.N. Reeve, *DNA binding by the archaeal histone HMf results in positive supercoiling.* Proc Natl Acad Sci U S A, 1991. **88**(23): p. 10397-401.
69. Pereira, S.L. and J.N. Reeve, *Histones and nucleosomes in Archaea and Eukarya: a comparative analysis.* Extremophiles, 1998. **2**(3): p. 141-8.
70. Palmer, D.K., et al., *A 17-kD centromere protein (CENP-A) copurifies with nucleosome core particles and with histones.* J Cell Biol, 1987. **104**(4): p. 805-15.
71. Clarke, L., *Centromeres: proteins, protein complexes, and repeated domains at centromeres of simple eukaryotes.* Curr Opin Genet Dev, 1998. **8**(2): p. 212-8.
72. Hegemann, J.H. and U.N. Fleig, *The centromere of budding yeast.* Bioessays, 1993. **15**(7): p. 451-60.
73. Mellor, J., et al., *CPF1, a yeast protein which functions in centromeres and promoters.* EMBO J, 1990. **9**(12): p. 4017-26.
74. Baker, R.E. and D.C. Masison, *Isolation of the gene encoding the Saccharomyces cerevisiae centromere-binding protein CP1.* Mol Cell Biol, 1990. **10**(6): p. 2458-67.
75. Lechner, J. and J. Carbon, *A 240 kd multisubunit protein complex, CBF3, is a major component of the budding yeast centromere.* Cell, 1991. **64**(4): p. 717-25.
76. Poddar, A., et al., *Differential kinetochore requirements for establishment and maintenance of the spindle checkpoint are dependent on the mechanism of checkpoint activation in Saccharomyces cerevisiae.* Cell Cycle, 2004. **3**(2): p. 197-204.
77. Cho, U.S. and S.C. Harrison, *Ndc10 is a platform for inner kinetochore assembly in budding yeast.* Nat Struct Mol Biol, 2011. **19**(1): p. 48-55.
78. Milks, K.J., B. Moree, and A.F. Straight, *Dissection of CENP-C-directed centromere and kinetochore assembly.* Mol Biol Cell, 2009. **20**(19): p. 4246-55.
79. Cohen, R.L., et al., *Structural and functional dissection of Mif2p, a conserved DNA-binding kinetochore protein.* Mol Biol Cell, 2008. **19**(10): p. 4480-91.
80. Meluh, P.B. and D. Koshland, *Budding yeast centromere composition and assembly as revealed by in vivo cross-linking.* Genes Dev, 1997. **11**: p. 3401-12.
81. De Wulf, P., A.D. McAinsh, and P.K. Sorger, *Hierarchical assembly of the budding yeast kinetochore from multiple subcomplexes.* Genes Dev, 2003. **17**(23): p. 2902-21.
82. Dimitrova, Y.N., et al., *Structure of the MIND Complex Defines a Regulatory Focus for Yeast Kinetochore Assembly.* Cell, 2016. **167**(4): p. 1014-1027 e12.

83. Petrovic, A., et al., *Structure of the MIS12 Complex and Molecular Basis of Its Interaction with CENP-C at Human Kinetochores.* Cell, 2016. **167**(4): p. 1028-1040 e15.
84. Schmitzberger, F., et al., *Molecular basis for inner kinetochore configuration through RWD domain-peptide interactions.* EMBO J, 2017. **36**(23): p. 3458-3482.
85. Pentakota, S., et al., *Decoding the centromeric nucleosome through CENP-N.* Elife, 2017. **6**.
86. Thakur, J. and S. Henikoff, *CENPT bridges adjacent CENPA nucleosomes on young human alpha-satellite dimers.* Genome Res, 2016. **26**(9): p. 1178-87.
87. Basilico, F., et al., *The pseudo GTPase CENP-M drives human kinetochore assembly.* Elife, 2014. **3**: p. e02978.
88. Pekgoz Altunkaya, G., et al., *CCAN Assembly Configures Composite Binding Interfaces to Promote Cross-Linking of Ndc80 Complexes at the Kinetochore.* Curr Biol, 2016. **26**(17): p. 2370-8.
89. Samejima, I., et al., *Whole-proteome genetic analysis of dependencies in assembly of a vertebrate kinetochore.* J Cell Biol, 2015. **211**(6): p. 1141-56.
90. Nishino, T., et al., *CENP-T provides a structural platform for outer kinetochore assembly.* EMBO J, 2013. **32**(3): p. 424-36.
91. Schleiffer, A., et al., *CENP-T proteins are conserved centromere receptors of the Ndc80 complex.* Nat Cell Biol, 2012. **14**(6): p. 604-13.
92. Malvezzi, F., et al., *A structural basis for kinetochore recruitment of the Ndc80 complex via two distinct centromere receptors.* EMBO J, 2013. **32**(3): p. 409-23.
93. Hori, T., et al., *CCAN makes multiple contacts with centromeric DNA to provide distinct pathways to the outer kinetochore.* Cell, 2008. **135**(6): p. 1039-52.
94. Cheeseman, I.M., et al., *The conserved KMN network constitutes the core microtubule-binding site of the kinetochore.* Cell, 2006. **127**(5): p. 983-97.
95. Screpanti, E., et al., *Direct binding of Cenp-C to the Mis12 complex joins the inner and outer kinetochore.* Curr Biol, 2011. **21**(5): p. 391-8.
96. Maskell, D.P., X.W. Hu, and M.R. Singleton, *Molecular architecture and assembly of the yeast kinetochore MIND complex.* J Cell Biol, 2010. **190**(5): p. 823-34.
97. Maure, J.F., et al., *The Ndc80 loop region facilitates formation of kinetochore attachment to the dynamic microtubule plus end.* Curr Biol, 2011. **21**(3): p. 207-13.
98. Miranda, J.J., et al., *The yeast DASH complex forms closed rings on microtubules.* Nat Struct Mol Biol, 2005. **12**(2): p. 138-43.
99. Tanaka, K., et al., *Molecular mechanisms of kinetochore capture by spindle microtubules.* Nature, 2005. **434**(7036): p. 987-94.
100. Lampert, F. and S. Westermann, *A blueprint for kinetochores - new insights into the molecular mechanics of cell division.* Nat Rev Mol Cell Biol, 2011. **12**(7): p. 407-12.
101. Cheeseman, I.M., et al., *KNL1 and the CENP-H/I/K complex coordinately direct kinetochore assembly in vertebrates.* Mol Biol Cell, 2008. **19**(2): p. 587-94.
102. Jin, Q.W., J. Fuchs, and J. Loidl, *Centromere clustering is a major determinant of yeast interphase nuclear organization.* J Cell Sci, 2000. **113 ( Pt 11)**: p. 1903-12.
103. Kitamura, E., et al., *Kinetochore microtubule interaction during S phase in Saccharomyces cerevisiae.* Genes Dev, 2007. **21**(24): p. 3319-30.
104. Pearson, C.G., et al., *Stable kinetochore-microtubule attachment constrains centromere positioning in metaphase.* Curr Biol, 2004. **14**(21): p. 1962-7.

105. Arnone, J.T., A.D. Walters, and O. Cohen-Fix, *The dynamic nature of the nuclear envelope: lessons from closed mitosis.* Nucleus, 2013. **4**(4): p. 261-6.
106. Gascoigne, K.E. and I.M. Cheeseman, *CDK-dependent phosphorylation and nuclear exclusion coordinately control kinetochore assembly state.* J Cell Biol, 2013. **201**(1): p. 23-32.
107. Xu, Y.M., J.Y. Du, and A.T. Lau, *Posttranslational modifications of human histone H3: an update.* Proteomics, 2014. **14**(17-18): p. 2047-60.
108. Srivastava, S. and D.R. Foltz, *Posttranslational modifications of CENP-A: marks of distinction.* Chromosoma, 2018.
109. Boeckmann, L., et al., *Phosphorylation of centromeric histone H3 variant regulates chromosome segregation in Saccharomyces cerevisiae.* Mol Biol Cell, 2013. **24**(12): p. 2034-44.
110. Samel, A., et al., *Methylation of CenH3 arginine 37 regulates kinetochore integrity and chromosome segregation.* Proc Natl Acad Sci U S A, 2012. **109**(23): p. 9029-34.
111. Ohkuni, K., et al., *N-terminal Sumoylation of Centromeric Histone H3 Variant Cse4 Regulates Its Proteolysis To Prevent Mislocalization to Non-centromeric Chromatin.* G3 (Bethesda), 2018. **8**(4): p. 1215-1223.
112. Wan, J., D. Subramonian, and X.D. Zhang, *SUMOylation in control of accurate chromosome segregation during mitosis.* Curr Protein Pept Sci, 2012. **13**(5): p. 467-81.
113. Johnson, E.S., *Protein modification by SUMO.* Annu Rev Biochem, 2004. **73**: p. 355-82.
114. Kim, K.I., S.H. Baek, and C.H. Chung, *Versatile protein tag, SUMO: its enzymology and biological function.* J Cell Physiol, 2002. **191**(3): p. 257-68.
115. Dasso, M., *Emerging roles of the SUMO pathway in mitosis.* Cell Div, 2008. **3**: p. 5.
116. Geoffroy, M.C. and R.T. Hay, *An additional role for SUMO in ubiquitin-mediated proteolysis.* Nat Rev Mol Cell Biol, 2009. **10**(8): p. 564-8.
117. Meluh, P.B. and D. Koshland, *Evidence that the MIF2 gene of Saccharomyces cerevisiae encodes a centromere protein with homology to the mammalian centromere protein CENP-C.* Mol Biol Cell, 1995. **6**: p. 793-807.
118. Biggins, S., et al., *Genes Involved in Sister Chromatid Separation and Segregation in the Budding Yeast Saccharomyces cerevisiae.* Genetics, 2001. **159**: p. 453-470.
119. Dieckhoff, P., et al., *Smt3/SUMO and Ubc9 are required for efficient APC/C-mediated proteolysis in budding yeast.* Mol Microbiol, 2004. **51**(5): p. 1375-87.
120. Zhang, X.D., et al., *SUMO-2/3 modification and binding regulate the association of CENP-E with kinetochores and progression through mitosis.* Mol Cell, 2008. **29**(6): p. 729-41.
121. Azuma, Y., et al., *PIASy mediates SUMO-2 conjugation of Topoisomerase-II on mitotic chromosomes.* EMBO J, 2005. **24**(12): p. 2172-82.
122. Nie, M., et al., *Genetic and proteomic evidence for roles of Drosophila SUMO in cell cycle control, Ras signaling, and early pattern formation.* PLoS One, 2009. **4**(6): p. e5905.
123. Denison, C., et al., *A proteomic strategy for gaining insights into protein sumoylation in yeast.* Mol Cell Proteomics, 2005. **4**(3): p. 246-54.
124. Wohlschlegel, J.A., et al., *Global analysis of protein sumoylation in Saccharomyces cerevisiae.* J Biol Chem, 2004. **279**(44): p. 45662-8.

125. Montpetit, B., et al., *Sumoylation of the budding yeast kinetochore protein Ndc10 is required for Ndc10 spindle localization and regulation of anaphase spindle elongation.* J Cell Biol, 2006. **174**(5): p. 653-63.
126. Bock, L.J., et al., *Cnn1 inhibits the interactions between the KMN complexes of the yeast kinetochore.* Nat Cell Biol, 2012. **14**(6): p. 614-24.
127. Gascoigne, K.E., et al., *Induced ectopic kinetochore assembly bypasses the requirement for CENP-A nucleosomes.* Cell, 2011. **145**(3): p. 410-22.
128. Nishino, T., et al., *CENP-T-W-S-X forms a unique centromeric chromatin structure with a histone-like fold.* Cell, 2012. **148**(3): p. 487-501.
129. Carroll, C.W., K.J. Milks, and A.F. Straight, *Dual recognition of CENP-A nucleosomes is required for centromere assembly.* J Cell Biol, 2010. **189**(7): p. 1143-55.
130. Suzuki, A., B.L. Badger, and E.D. Salmon, *A quantitative description of Ndc80 complex linkage to human kinetochores.* Nat Commun, 2015. **6**: p. 8161.
131. Logsdon, G.A., et al., *Both tails and the centromere targeting domain of CENP-A are required for centromere establishment.* J Cell Biol, 2015. **208**(5): p. 521-31.
132. Huis In 't Veld, P.J., et al., *Molecular basis of outer kinetochore assembly on CENP-T.* Elife, 2016. **5**.
133. Rago, F., K.E. Gascoigne, and I.M. Cheeseman, *Distinct organization and regulation of the outer kinetochore KMN network downstream of CENP-C and CENP-T.* Curr Biol, 2015. **25**(5): p. 671-7.
134. Gonen, S., et al., *The structure of purified kinetochores reveals multiple microtubule-attachment sites.* Nat Struct Mol Biol, 2012. **19**(9): p. 925-9.
135. Akiyoshi, B., et al., *Tension directly stabilizes reconstituted kinetochore-microtubule attachments.* Nature, 2010. **468**(7323): p. 576-9.
136. Miller, M.P., C.L. Asbury, and S. Biggins, *A TOG Protein Confers Tension Sensitivity to Kinetochore-Microtubule Attachments.* Cell, 2016. **165**(6): p. 1428-1439.
137. Heller, R.C., et al., *Eukaryotic origin-dependent DNA replication in vitro reveals sequential action of DDK and S-CDK kinases.* Cell, 2011. **146**(1): p. 80-91.
138. Ohkuni, K. and K. Kitagawa, *Endogenous transcription at the centromere facilitates centromere activity in budding yeast.* Curr Biol, 2011. **21**(20): p. 1695-703.
139. Sorger, P.K., F.F. Severin, and A.A. Hyman, *Factors required for the binding of reassembled yeast kinetochores to microtubules in vitro.* J Cell Biol, 1994. **127**(4): p. 995-1008.
140. Guse, A., et al., *In vitro centromere and kinetochore assembly on defined chromatin templates.* Nature, 2011. **477**(7364): p. 354-8.
141. Weir, J.R., et al., *Insights from biochemical reconstitution into the architecture of human kinetochores.* Nature, 2016. **537**(7619): p. 249-253.
142. Jalal, D., J. Chalissery, and A.H. Hassan, *Genome maintenance in Saccharomyces cerevisiae: the role of SUMO and SUMO-targeted ubiquitin ligases.* Nucleic Acids Res, 2017. **45**(5): p. 2242-2261.
143. Sampson, D.A., M. Wang, and M.J. Matunis, *The small ubiquitin-like modifier-1 (SUMO-1) consensus sequence mediates Ubc9 binding and is essential for SUMO-1 modification.* J Biol Chem, 2001. **276**(24): p. 21664-9.
144. Rodriguez, M.S., C. Dargemont, and R.T. Hay, *SUMO-1 conjugation in vivo requires both a consensus modification motif and nuclear targeting.* J Biol Chem, 2001. **276**(16): p. 12654-9.

145. Bernier-Villamor, V., et al., *Structural basis for E2-mediated SUMO conjugation revealed by a complex between ubiquitin-conjugating enzyme Ubc9 and RanGAP1.* Cell, 2002. **108**(3): p. 345-56.
146. Chung, T.L., et al., *In vitro modification of human centromere protein CENP-C fragments by small ubiquitin-like modifier (SUMO) protein: definitive identification of the modification sites by tandem mass spectrometry analysis of the isopeptides.* J Biol Chem, 2004. **279**(38): p. 39653-62.
147. Chen, X.L., A. Reindle, and E.S. Johnson, *Misregulation of 2 microm circle copy number in a SUMO pathway mutant.* Mol Cell Biol, 2005. **25**(10): p. 4311-20.
148. Mullen, J.R. and S.J. Brill, *Activation of the Slx5-Slx8 ubiquitin ligase by poly-small ubiquitin-like modifier conjugates.* J Biol Chem, 2008. **283**(29): p. 19912-21.
149. Sherman, F., G. Fink, and C. Lawrence, *Methods in Yeast Genetics*. 1974, Cold Spring Harbor, New York: Cold Spring Harbor Laboratory Press.
150. Longtine, M.S., et al., *Additional modules for versatile and economical PCR-based gene deletion and modification in Saccharomyces cerevisiae.* Yeast, 1998. **14**(10): p. 953-61.
151. Pinsky, B.A., et al., *An Mtw1 complex promotes kinetochore biorientation that is monitored by the Ipl1/Aurora protein kinase.* Dev Cell, 2003. **5**(5): p. 735-45.
152. Sorger, P.K., et al., *Two genes required for the binding of an essential Saccharomyces cerevisiae kinetochore complex to DNA.* Proc Natl Acad Sci U S A, 1995. **92**(26): p. 12026-30.
153. Seki, T. and J.F. Diffley, *Stepwise assembly of initiation proteins at budding yeast replication origins in vitro.* Proc Natl Acad Sci U S A, 2000. **97**(26): p. 14115-20.
154. Akiyoshi, B., C.R. Nelson, and S. Biggins, *The aurora B kinase promotes inner and outer kinetochore interactions in budding yeast.* Genetics, 2013. **194**(3): p. 785-9.
155. Kim, S. and H. Yu, *Multiple assembly mechanisms anchor the KMN spindle checkpoint platform at human mitotic kinetochores.* J Cell Biol, 2015. **208**(2): p. 181-96.
156. Yang, Y., et al., *Phosphorylation of HsMis13 by Aurora B kinase is essential for assembly of functional kinetochore.* J Biol Chem, 2008. **283**(39): p. 26726-36.
157. He, X., S. Asthana, and P.K. Sorger, *Transient sister chromatid separation and elastic deformation of chromosomes during mitosis in budding yeast.* Cell, 2000. **101**(7): p. 763-75.
158. Gascoigne, K.E. and I.M. Cheeseman, *Kinetochore assembly: if you build it, they will come.* Curr Opin Cell Biol, 2011. **23**(1): p. 102-8.
159. Stoler, S., et al., *Scm3, an essential Saccharomyces cerevisiae centromere protein required for G2/M progression and Cse4 localization.* Proc Natl Acad Sci U S A, 2007. **104**(25): p. 10571-6.
160. Nishimura, K., et al., *An auxin-based degron system for the rapid depletion of proteins in nonplant cells.* Nat Methods, 2009. **6**(12): p. 917-22.
161. Aravamudhan, P., I. Felzer-Kim, and A.P. Joglekar, *The budding yeast point centromere associates with two Cse4 molecules during mitosis.* Curr Biol, 2013. **23**(9): p. 770-4.
162. Furuyama, S. and S. Biggins, *Centromere identity is specified by a single centromeric nucleosome in budding yeast.* Proc Natl Acad Sci U S A, 2007. **104**(37): p. 14706-11.
163. McAlister, G.C., et al., *MultiNotch MS3 enables accurate, sensitive, and multiplexed detection of differential expression across cancer cell line proteomes.* Anal Chem, 2014. **86**(14): p. 7150-8.

164. Swaney, D.L., et al., *Global analysis of phosphorylation and ubiquitylation cross-talk in protein degradation.* Nat Methods, 2013. **10**(7): p. 676-82.
165. Westermann, S., et al., *Architecture of the budding yeast kinetochore reveals a conserved molecular core.* J Cell Biol, 2003. **163**(2): p. 215-22.
166. Krenn, V. and A. Musacchio, *The Aurora B Kinase in Chromosome Bi-Orientation and Spindle Checkpoint Signaling.* Front Oncol, 2015. **5**: p. 225.
167. Welburn, J.P., et al., *Aurora B phosphorylates spatially distinct targets to differentially regulate the kinetochore-microtubule interface.* Mol Cell, 2010. **38**(3): p. 383-92.
168. Lampson, M.A. and I.M. Cheeseman, *Sensing centromere tension: Aurora B and the regulation of kinetochore function.* Trends Cell Biol, 2011. **21**(3): p. 133-40.
169. Cheeseman, I.M., et al., *Phospho-Regulation of Kinetochore-Microtubule Attachments by the Aurora Kinase Ipl1p.* Cell, 2002. **111**(2): p. 163-172.
170. DeLuca, J.G., et al., *Hec1 and nuf2 are core components of the kinetochore outer plate essential for organizing microtubule attachment sites.* Mol Biol Cell, 2005. **16**(2): p. 519-31.
171. Jeyaprakash, A.A., et al., *Structure of a Survivin-Borealin-INCENP core complex reveals how chromosomal passengers travel together.* Cell, 2007. **131**(2): p. 271-85.
172. Carmena, M., et al., *The chromosomal passenger complex (CPC): from easy rider to the godfather of mitosis.* Nat Rev Mol Cell Biol, 2012. **13**(12): p. 789-803.
173. Klein, U.R., E.A. Nigg, and U. Gruneberg, *Centromere targeting of the chromosomal passenger complex requires a ternary subcomplex of Borealin, Survivin, and the N-terminal domain of INCENP.* Mol Biol Cell, 2006. **17**(6): p. 2547-58.
174. Lampert, F., et al., *Molecular requirements for the formation of a kinetochore-microtubule interface by Dam1 and Ndc80 complexes.* J Cell Biol, 2013. **200**(1): p. 21-30.
175. Hara, M. and T. Fukagawa, *Kinetochore assembly and disassembly during mitotic entry and exit.* Curr Opin Cell Biol, 2018. **52**: p. 73-81.
176. Henikoff, S. and J.G. Henikoff, *"Point" centromeres of Saccharomyces harbor single centromere-specific nucleosomes.* Genetics, 2012. **190**(4): p. 1575-7.
177. Padeganeh, A., V. De Rop, and P.S. Maddox, *Nucleosomal composition at the centromere: a numbers game.* Chromosome Res, 2013. **21**(1): p. 27-36.
178. Bloom, K.S., *Centromeric heterochromatin: the primordial segregation machine.* Annu Rev Genet, 2014. **48**: p. 457-84.
179. Zhang, Q., et al., *Ska3 Phosphorylated by Cdk1 Binds Ndc80 and Recruits Ska to Kinetochores to Promote Mitotic Progression.* Curr Biol, 2017. **27**(10): p. 1477-1484 e4.
180. Takeuchi, K., et al., *The centromeric nucleosome-like CENP-T-W-S-X complex induces positive supercoils into DNA.* Nucleic Acids Res, 2013.
181. Akiyoshi, B., et al., *The Mub1/Ubr2 ubiquitin ligase complex regulates the conserved Dsn1 kinetochore protein.* PLoS Genet, 2013. **9**(2): p. e1003216.
182. Hornung, P., et al., *A cooperative mechanism drives budding yeast kinetochore assembly downstream of CENP-A.* J Cell Biol, 2014. **206**(4): p. 509-24.
183. Schulman, I.G. and K. Bloom, *Genetic dissection of centromere function.* Mol Cell Biol, 1993. **13**(6): p. 3156-66.
184. Anderson, J.D. and J. Widom, *Sequence and position-dependence of the equilibrium accessibility of nucleosomal DNA target sites.* J Mol Biol, 2000. **296**(4): p. 979-87.

**Jackie Lang**
8929 121st Ave SE
Newcastle, WA 98056
408.355.3554
jmlang11@gmail.com

## OBJECTIVE

After receiving my B.S. in Genetics from UC Davis in 2009, I worked as a research technician in the laboratory of Dr. Susan Strome at UC Santa Cruz. In 2011, I commenced in the Molecular and Cellular Biology Ph.D. program at the University of Washington, where I joined the laboratory of Dr. Sue Biggins at the Fred Hutchinson Cancer Research Center. My ultimate goal is to pursue a scientific research position in an industry where my work can impact and improve patients' lives.

## EDUCATION

*2011-Spring 2018* **University of Washington, Medical School**
Molecular and Cellular Biology, Ph.D. Program

*June 2009* **University of California, Davis**
**Bachelor of Science, Genetics** **[**Graduated with Honors, Dean's list]

## RESEARCH EXPERIENCE

*June 2012-present* **Graduate Research Assistant**
Sue Biggins, Ph.D.; FHCRC, Basic Sciences Division
Developed a novel *in vitro* method to assemble the kinetochore, a macromolecular protein structure. Gained extensive experience with protein biochemistry, genetics, and assay development.

*Aug 2009-July 2011* **Research Technician and Lab Manager**
Susan Strome, Ph.D.; UC Santa Cruz, Molecular, Cell & Dev. Biology
Collaborated with other modENCODE labs to investigate the role of histone modifications in specifying germline versus somatic cell fate. Gained experience with immunostaining and high-resolution microscopy.

*Sept 2008-June 2009* **Undergraduate Research Internship**
Sean Burgess, Ph.D.; UC Davis, Molecular and Cellular Biology
Examined the effect of chromosome motion on the pairing of homologous chromosomes during meiosis. Gained experience with live cell imaging and molecular biology techniques.

## TECHNICAL SKILLS

· Protein biochemistry: immunoprecipitation, ChIP, Western blotting, mass spectrometry
· High-resolution fluorescence microscopy, immunostaining, live cell imaging, antibody characterization
· Electrophoresis, qPCR, Southern blotting
· Genetic manipulation in E. coli and S. cerevisiae, RNA*i* in C. elegans and human stem cells
· Novel assay development, troubleshooting, independent judgement in experimental design

**MENTORING EXPERIENCE**

| | |
|---|---|
| *Summer 2016* | **Mentored an HHMI EXROP undergraduate researcher** |
| *Spring 2013* | **Teaching Assistant** for Molecular and Cellular Biology undergraduate course |
| *July 2012* | Mentored High School students at **BioQuest Academy** (Seattle BioMed) |
| *Spring 2009* | **Undergraduate peer-tutor** for Advanced Eukaryotic Genetics |

**LEADERSHIP**

| | |
|---|---|
| *Dec 2015 - Present* | **Co-chair of Hutch United**, a grassroots organization aimed at promoting the success of underrepresented minority scientists at the Fred Hutch |
| *Spring 2016* | Organized **MCB Symposium** |
| *Oct 2015 - Present* | **Hutch United Core Board Member** |
| *April 2015 - Present* | **Hutch United Liaison** for partnership with the Association for Women in Science |
| *Fall 2015* | Served on **Weintraub Award Review Committee** |
| *Spring 2013* | Organized **MCB Annual Retreat** |
| *Fall 2013* | Served on **Weintraub Award Review Committee** |
| *Winter 2012* | Organized **MCB Recruitment** |
| *April 2010* | **Strome Lab Manager and Lab Safety Representative** |

**AWARDS & FELLOWSHIPS**

| | |
|---|---|
| *March 2017* | Named one of **2017's Husky 100 –** University of Washington |
| *June 2015* | **1st place poster presentation -** Seattle Genetic Instability Symposium |
| *May 2015* | **1st place poster presentation -** EMBO Workshop: The Dynamic Kinetochore |
| *Dec 2014* | **1st place Ph.D. oral presentation -** American Indians in Science and Engineering Society (AISES) National Conference 2014 |
| *Sept 2014* | **Best poster -** Fred Hutchinson Basic Sciences Retreat |
| *Sept 2013* | **Chromosome Metabolism and Cancer Training Grant** |
| *Nov 2012* | **1st place Ph.D. poster presentation** - AISES National Conference 2012 |
| *Spring 2012* | **NSF GRFP Honorable Mention** |
| *Dec 2008* | **Awarded the President's Undergraduate Fellowship** - UC Davis Undergraduate Research Center |

**PUBLICATIONS**

Ding Y, Herman JA, Toledo CM, **Lang J**, Corrin P, Girard EJ, Basom R, Delrow JJ, Olson JM, Paddison PJ. ZNF131 suppresses centrosome fragmentation in glioblastoma stem-like cells through regulation of HAUS5. Oncotarget, July 2017.

Vielle A*, **Lang J***, Dong Y, Ercan S, Kotwaliwale C, et al. H4K20me1 Contributes to Downregulation of X-Linked Genes for *C. elegans* Dosage Compensation. PLOS Genetics, Sept 2012. **Authors contributed equally*

**REFERENCES**

A full list of references is available upon request. You may also see my LinkedIn for more details.
https://www.linkedin.com/in/jackie-lang-7ba35a118/